GEOLOGICAL SURVEY OF CANADA
BULLETIN 582

QUATERNARY GEOLOGY OF WESTERN META INCOGNITA PENINSULA AND IQALUIT AREA, BAFFIN ISLAND, NUNAVUT

D.A. Hodgson

2005

Natural Resources Canada Ressources naturelles Canada

Canada

The CD-ROM accompanying this publication contains the full report, including any oversized figures and/or A-series maps, in Portable Document Format (PDF). Oversized items may be purchased separately as paper plots from any of the following locations.

Geological Survey of Canada Bookstore (Ottawa)
601 Booth Street
Ottawa, Ontario
K1A 0E8
Tel.: (613) 995-4342
Tel.: (888) 252-4301 (toll-free)
Fax: (613) 943-0646
E-mail: gscbookstore@nrcan.gc.ca
Web: http://gsc.nrcan.gc.ca/bookstore/index_e.php

Geological Survey of Canada Bookstore (Calgary)
3303-33rd Street, N.W.
Calgary, Alberta
T2L 2A7
Tel.: (403) 292-7030
Fax.: (403) 299-3542
E-mail: gsc_calgary@nrcan.gc.ca
Web: http://www.nrcan.gc.ca/gsc/calgary/products/index_e.html

Geological Survey of Canada Bookstore (Vancouver)
101-605 Robson Street
Vancouver, B.C.
V6B 5J3
Tel.: (604) 666-0271
FAX: (604) 666-1337
E-mail: gscvan@gsc.nrcan.gc.ca
Web: http://gsc.nrcan.gc.ca/org/vancouver/index_e.php

Le CD-ROM qui accompagne cette publication renferme le rapport au complet, y compris les figures surdimensionnées ou les cartes de série A, en format PDF. On peut acheter séparément dans les endroits suivants des copies papier des éléments surdimensionnés :

Librairie de la Commission géologique du Canada (Ottawa)
601, rue Booth
Ottawa (Ontario)
K1A 0E8
Tél. : (613) 995-4342
Tél. : (888) 252-4301 (sans frais)
Télécopieur : (613) 943-0646
Courriel : librairiecgc@nrcan.gc.ca
Web : http://cgc.rncan.gc.ca/librairie/index_f.php

Librairie de la Commission géologique du Canada (Calgary)
3303-33rd Street, N.W.
Calgary (Alberta)
T2L 2A7
Tél. : (403) 292-7030
Télécopieur : (403) 299-3542
Courriel : gsc_calgary@gsc.nrcan.gc.ca
Web : http://www.rncan.gc.ca/cgc/calgary/products/index_f.html

Librairie de la Commission géologique du Canada (Vancouver)
101-605 Robson Street
Vancouver (C.-B.)
V6B 5J3
Tél. : (604) 666-0271
Télécopieur : (604) 666-1337
Courriel : gscvan@gsc.nrcan.gc.ca
Web : http://cgc.rncan.gc.ca/org/vancouver/index_f.php

GEOLOGICAL SURVEY OF CANADA
BULLETIN 582

QUATERNARY GEOLOGY OF WESTERN META INCOGNITA PENINSULA AND IQALUIT AREA, BAFFIN ISLAND, NUNAVUT

D.A. Hodgson

2005

Catalogue No. M42-582E
ISBN 0-660-19369-8

Available in Canada from
Geological Survey of Canada offices:

601 Booth Street
Ottawa, Ontario K1A 0E8

3303-33rd Street N.W.
Calgary, Alberta T2L 2A7

101-605 Robson Street
Vancouver, B.C. V6B 5J3

A copy of this publication is also available for reference by depository
libraries across Canada through access to the Depository Services Program's
website at http://dsp-psd.pwgsc.gc.ca

A free digital download of this publication is available from the Geological Survey of
Canada Bookstore Web site:

http://gsc.nrcan.gc.ca/bookstore/

Click on "Free Download".

Toll-free (Canada and U.S.A.): 1-888-252-4301

Cover illustration

One of a number of major river valleys dissecting the south-tilted plateau surface of Meta Incognita Peninsula, southern Baffin Island. This unnamed river, incised 300 m, drains south to Shaftesbury Inlet on Hudson Strait. The gravelly silt and sand valley train deposits flooring the valley were laid as ice retreated north to the divide on the western portion of the peninsula, where an early Holocene stand or readvance redoubled outwash production. The GSC camp is shown in July, 1997. GSC 2004-148

Author's address
D.A. Hodgson
Geological Survey of Canada
601 Booth Street
Ottawa, Ontario
K1A 0E8

Original manuscript submitted: 2002–05–04
Final version approved for publication: 2003–05–20

CONTENTS

Tables

Illustrations

QUATERNARY GEOLOGY OF WESTERN META INCOGNITA PENINSULA AND IQALUIT AREA, BAFFIN ISLAND, NUNAVUT

Abstract

Surficial materials mapping has enlarged on previous Quaternary topical and areal studies in an area that includes the largest community in Nunavut. Till, which is uniformly sandy and clast-supported, covers a minority of the varied metamorphic and igneous bedrock. A strongly developed end-moraine belt, the Frobisher Bay Moraine System and associated outwash valley trains are the only extensive depositional landforms. Till geochemistry shows no significant anomalies.

There is no terrestrial record of the pre-Late Wisconsin Glaciation other than cirques. Last glacial ice flowing from local, Foxe Ice Dome, down Hudson Strait, and cross-strait sources is recorded by scarce striations. The chronology of the flows is partially known: by 8.9 ka, local ice retreated onshore in Frobisher Bay; and by 8.4 ka local and Labrador (Noble Inlet) ice left the Hudson Strait shore. The physical relationships of local and offshore (Hudson Strait) ice remain poorly understood. The latter peripheral ice flows had minor impact on the landscape.

Local and Amadjuak ice divides underwent phases of warm and cold-based flow reflected in, respectively, thick till and till veneer–bedrock. The peninsula topographic and ice divides corresponded in the south, but diverged in the north, where the Foxe Ice Dome topography became dominant. The asymmetric cross-peninsula ice profile was buttressed by the marine-based Frobisher Bay glacier. In a climate-controlled readvance phase, this glacier fluctuated while depositing a belt of terminal moraines between 9–7 ka. Meanwhile, the land-based belt of the Frobisher Bay Moraine System remained more stable. In the final phase of deglaciation, the ice divide entirely corresponded with the terrestrial divide. Local ice centres explain much of the emergence pattern.

Résumé

La cartographie des matériaux superficiels vient ici s'ajouter aux autres études quaternaires, à base thématique ou géographique, déjà publiées sur une région qui comprend la plus grande agglomération du Nunavut. Le till, qui est uniformément sableux et à texture jointive, ne couvre qu'une faible proportion des roches métamorphiques et ignées diverses qui constituent le substratum rocheux. Le complexe morainique de Frobisher Bay, ceinture bien développée de moraines frontales, ainsi que les traînées fluvioglaciaires qui lui sont associées, sont les seules formes de dépôts de grande étendue. L'analyse géochimique des échantillons de till n'a relevé aucune anomalie significative.

Mis à part les cirques, aucune trace de glaciations antérieures au Wisconsinien tardif n'a été relevée en milieu continental. Les dernières glaces en provenance de sources locales, du dôme de Foxe, et de glaciers traversant ou descendant le détroit d'Hudson n'ont laissé que de rares stries. La chronologie des écoulements est partiellement connue : avant 8,9 ka, les glaces locales avaient reculé au-dessus du littoral de la baie Frobisher, et avant 8,4 ka, les glaces locales et celles du secteur du Labrador (avancée de Noble Inlet) avaient quitté le rivage du détroit d'Hudson. Les relations physiques entre les glaces locales et celles venant du large (détroit d'Hudson) sont encore mal élucidées. Ces dernières, situées à la périphérie de la région, ont eu peu d'impact sur le paysage.

Comme en témoignent respectivement un till épais et un placage de till sur le substratum rocheux, des glaciers à base tempérée et à base froide se sont écoulés depuis les lignes de partage glaciaire locales et la ligne de partage glaciaire d'Amadjuak. Les lignes de partage topographique et de partage glaciaire de la péninsule coïncidaient dans le sud, mais elles divergeaient dans le nord, où la topographie du dôme glaciaire de Foxe s'imposait. Le profil glaciaire de la péninsule était asymétrique en coupe transversale, appuyé d'un côté sur le front de marée du glacier de Frobisher Bay. Pendant une réavancée contrôlée par le climat, entre 9 et 7 ka, cette marge glaciaire a fluctué, déposant une ceinture de moraines frontales. Pendant ce temps, en milieu continental, un autre front de ce glacier demeurait plus stable tandis qu'il déposait le complexe morainique de Frobisher Bay. Durant la phase finale de la déglaciation, la ligne de partage glaciaire coïncidait entièrement avec la ligne de partage topographique. La configuration de l'émersion de la région reflèterait surtout l'influence des centres glaciaires locaux.

SUMMARY

Surficial materials of the terrestrial area of central-southernmost Baffin Island (NTS 25 K, L, M, N) were mapped and described in an analysis that also provides a framework for a range of environmental and paleoclimate studies, for mineral indicator surveys, and for physical development of the two local communities (Iqaluit and Kimmirut). The report draws extensively from a number of topical and areal Quaternary studies carried out by others in and adjacent to the map area.

Western Meta Incognita Peninsula, which is the bulk of the map area, has a rift-determined asymmetric cross-profile, peaking in the east at 800 m as little as 10 km from the Frobisher Bay shore, and 500 m in the north. Weathered to unaltered rock is the most extensive surficial material; it is divided on the basis of decreasing susceptibility to weathering into five units: limestone, clastic and metasedimentary rocks, marble, tonalite and monzogranite gneiss, and monzogranite, of which the clastic and metasedimentary rocks, marble, and monzogranite are dominant. Limestone has very minor outcrop at the head of Frobisher Bay, but is widespread in the Arctic Platform from 50 km beyond the map area to the northwest; it also underlies adjacent Hudson Strait.

Mappable till covers a minority of the map area; elsewhere, pockets of thin till overlie bedrock. The single till unit is clast supported with an acidic silty sand matrix, though a silty matrix-supported till is discontinuously present on the southeast coast. Clasts are boulder and cobble shield rocks of local origin. Till samples do not show anomalies for 34 elements analyzed. Thickest till is in the Frobisher Bay Moraine System, which is composed of multiple end-moraine ridges on the flanks of Frobisher Bay (linear on the north side, where ice pushed upslope; convoluted on the south side in ridges and valleys) and a thick till belt farther west (looping down the regional slope).

Subglacial and proglacial aqueous deposits and landforms are prominent locally. The most common are sand and gravel subaerial glaciofluvial deposits concentrated in the Frobisher Bay Moraine System adjacent to Frobisher Bay; farther west, distal valley trains follow preglacial valleys to Hudson Strait. Raised glacial marine deposits in the form of proglacial deltas are present where Frobisher Bay Moraine System intersects coasts (Frobisher and Markham bays) and where valley trains terminate. Thick, silty marine deposits are patchy around Frobisher Bay; on the southeast Hudson Strait coast, calcareous silty till indicates source ice was in the strait. An elevation difference of more than 10 m between deltas and prominent washing limits records a large tidal range in the early Holocene, similar to that at present.

SOMMAIRE

Ce volume présente les résultats d'une étude au cours de laquelle les matériaux superficiels des terres de l'extrême centre sud de l'île de Baffin (SNRC 25 K, L, M, N) ont été décrits et cartographiés. L'information présentée ici pourra servir de cadre pour un éventail d'études environnementales et paléoclimatiques, pour des levés de minéraux indicateurs et pour l'aménagement des deux agglomérations locales (Iqaluit et Kimmirut). Ce rapport renferme une quantité considérable d'information empruntée à des études quaternaires, à base thématique ou géographique, effectuées par d'autres chercheurs dans la même région et les environs.

La partie occidentale de la péninsule Meta Incognita, qui occupe presque toute la région étudiée, présente un profil transversal asymétrique, résultant de la formation d'un rift, qui s'élève jusqu'à 800 m dans l'est — à 10 km à peine du rivage de la baie Frobisher — et jusqu'à 500 m dans le nord. Le matériau superficiel le plus répandu est la roche affleurante, dont le degré d'altération varie. Nous avons divisé les affleurements en cinq unités selon leur susceptibilité à l'altération météorique, soit, en ordre décroissant de susceptibilité, le calcaire, les roches clastiques et métasédimentaires, le marbre, le gneiss tonalitique et monzogranitique, et le monzogranite. Parmi ces unités, les plus abondantes sont les roches clastiques et métasédimentaires, le marbre et le monzogranite. Le calcaire n'est présent que dans un très petit affleurement au fond de la baie Frobisher, mais il est très répandu dans la plate-forme de l'Arctique, à partir d'une distance de 50 km au nord-ouest de la région cartographique, et il s'étend également au fond du détroit d'Hudson voisin.

Les étendues cartographiables de till ne couvrent qu'une petite portion de la région étudiée; ailleurs, une mince couche de till recouvre ici et là le substratum rocheux. L'unique unité de till possède une texture jointive et une matrice de sable silteux acide, quoiqu'une couche discontinue de till silteux à texture non jointive s'étende sur la côte sud-est. Les clastes sont des blocs et des cailloux provenant d'affleurements locaux du Bouclier canadien. Des analyses de till n'ont relevé aucune anomalie pour 34 éléments mesurés. Les dépôts de till les plus épais se trouvent dans le complexe morainique de Frobisher Bay, constitué de multiples crêtes de moraine frontale qui s'étalent sur les pentes du littoral de la baie Frobisher (en formes linéaires du côté nord, où la glace a escaladé les pentes; en volutes sur les crêtes et dans les vallées du côté sud), ainsi que dans une épaisse ceinture de till, située plus à l'ouest, qui louvoie en descendant la pente régionale.

Des dépôts et des modelés sous-glaciaires et proglaciaires d'origine aquatique sont en évidence par endroits. Les plus communs sont des dépôts fluvioglaciaires subaériens de sable et de gravier, qui sont concentrés dans le complexe morainique de Frobisher Bay, près de la baie Frobisher; plus à l'ouest, des traînées fluvioglaciaires distales suivent des vallées préglaciaires jusqu'au détroit d'Hudson. Là où le complexe morainique de Frobisher Bay rejoint les côtes (baies Frobisher et Markham) et où les traînées fluvioglaciaires se terminent, on retrouve les dépôts glaciomarins soulevés des deltas proglaciaires. D'épais dépôts marins silteux sont présents çà et là dans la région de la baie Frobisher; sur la côte sud-est du détroit d'Hudson, la présence de till silteux calcareux indique qu'une source de glace se trouvait dans le détroit. Une différence d'altitude de plus de 10 m entre le sommet des deltas et la limite d'action des vagues indique qu'à l'Holocène précoce, l'amplitude des marées était aussi importante qu'aujourd'hui.

Cirques concentrated on the height of land and along the Hudson Strait shore do not contain moraines, thus are likely pre-Late Wisconsinan, however, all other glacial landforms and deposits are believed to be Late Wisconsinan. Striations (which are uncommonly exposed) on regional topographic highs record Laurentide Ice Sheet flow directions, divided here by style and chronology into domains. Firstly, Laurentide ice flowed southeast down Hudson Strait (domain 1) and retreated (<11 ka) before the 8.9 ka Noble Inlet advance of Labrador ice across the strait and onto southeast Meta Incognita Peninsula (domain 2). The dominant ice flow in the map area (domain 3) was from the local Meta Incognita Ice Divide down the asymmetric peninsula limbs to cover much of the map area (possibly including at times domain 2). In the north, the ice divide diverged from the topographic divide to connect with the Late Wisconsinan Amadjuak Ice Divide which extended southeast from the Foxe Ice Dome. At the fork of the Amadjuak Ice Divide into Meta Incognita and Hall Peninsula ice divides, a lobe or glacier filled inner Frobisher Bay, buttressing the north side of the Meta Incognita Peninsula ice. Retreat of the Frobisher Bay glacier in the map area was underway by 8.9 ka, though the oldest evidence of postglacial marine overlap on the Hudson Strait coast is 8.3 ka. A readvance and subsequent fluctuation of ice margins within domain 4 formed the Frobisher Bay Moraine System between 8.9 ka and 7 ka. Final drawdown to the head of Frobisher Bay was directed mainly from the Meta Incognita Ice Divide, creating domain 5. In domain 6, residual bodies of ice retreated in deeper valleys.

The long-term alignment of Amadjuak and local ice divides separated the Arctic Platform and the map area precluding transport of carbonate rocks into the area from the north. For Hudson Strait, the restriction of downstrait ice to the channel centre prevented direct deposition of carbonate rocks onshore; in the southeast, carbonate rocks were deposited where cross-strait glaciers came onshore. Whatever the cause of the Frobisher Bay Moraine System readvance, and climatic control seems the most reasonable explanation, the fluctuations of ice fronts adjacent to Frobisher Bay probably resulted from instability of the tidewater-based glacier during the high sea levels at the time of deglaciation.

The pattern of glacially induced isostatic uplift in the area as outlined by marine limit isolines is controlled by the former local (Meta Incognita Peninsula) ice load rather than by Laurentide ice in Hudson Strait. This inference is reinforced by the straightforward patterns of the two available postglacial emergence curves.

Les cirques concentrés sur les hauteurs et le long du rivage du détroit d'Hudson ne contiennent pas de moraines; ils sont donc probablement antérieurs au Wisconsinien tardif. Par contre, tous les autres dépôts et modelés glaciaires remonteraient au Wisconsinien tardif. Les stries sont peu exposées en général, mais sur les hauteurs régionales elles révèlent des directions d'écoulement glaciaire de l'Inlandsis laurentidien, que nous avons classées en domaines d'après le style et la chronologie de l'écoulement. Les glaces de l'Inlandsis laurentidien se sont d'abord écoulées vers le sud-est dans le détroit d'Hudson (domaine 1); elles ont reculé (<11 ka) avant l'avancée de Noble Inlet (8,9 ka), au cours de laquelle les glaces du Labrador ont traversé le détroit pour occuper la partie sud-est de la péninsule Meta Incognita (domaine 2). L'écoulement glaciaire principal dans la région étudiée (domaine 3) descendait les flancs asymétriques de la péninsule depuis la ligne de partage glaciaire locale de Meta Incognita, couvrant une grande partie de la région étudiée (dont peut-être à l'occasion le domaine 2). Dans le nord, la ligne de partage glaciaire divergeait de la ligne de partage topographique pour rejoindre la ligne de partage glaciaire d'Amadjuak du Wisconsinien tardif, qui s'allongeait en direction sud-est à partir du dôme glaciaire de Foxe. Là où la ligne de partage glaciaire d'Amadjuak bifurquait pour former les lignes de partage glaciaire de Meta Incognita et de Hall, un lobe ou un glacier comblait le fond de la baie Frobisher et servait d'appui au côté nord des glaces de la péninsule Meta Incognita. Le retrait de ce glacier (le glacier de Frobisher Bay) dans la région étudiée avait déjà commencé avant 8,9 ka, quoique l'indice le plus ancien d'une transgression marine postglaciaire sur la côte du détroit d'Hudson ne remonte qu'à 8,3 ka. Une réavancée et une fluctuation subséquente des marges glaciaires dans le domaine 4 ont entraîné la formation du complexe morainique de Frobisher Bay entre 8,9 ka et 7 ka. Le retrait final des glaces vers le fond de la baie Frobisher a suivi l'axe de partage glaciaire de Meta Incognita, créant le domaine 5. Dans le domaine 6, les masses de glace résiduelles ont reculé dans les vallées plus profondes.

La position des lignes de partage glaciaire locales dans le prolongement de la ligne de partage glaciaire d'Amadjuak a donné lieu à une séparation de longue durée entre la plate-forme de l'Arctique et la région étudiée, empêchant le transport de roches carbonatées jusqu'à cette région à partir du nord. Les glaces qui empruntaient le détroit d'Hudson n'ont pu déposer des roches carbonatées directement sur le rivage, puisqu'elles étaient confinées au centre du chenal; dans le sud-est, toutefois, des roches carbonatées ont été déposées par des glaciers ayant traversé le détroit. Quelle qu'ait été la cause de la réavancée qui a donné lieu au complexe morainique de Frobisher Bay (le contrôle climatique semble l'explication la plus plausible), les fluctuations des fronts glaciaires près de la baie Frobisher ont probablement été provoquées par l'instabilité du glacier de marée à l'époque de la déglaciation, alors que le niveau de la mer était élevé.

La configuration du soulèvement glacio-isostatique dans la région, révélée par les anciennes limites marines, serait régie par l'ancienne surcharge glaciaire locale (péninsule Meta Incognita) plutôt que par la surcharge associée aux glaces de l'Inlandsis laurentidien dans le détroit d'Hudson. Cette déduction est confortée par les configurations simples des deux courbes d'émersion postglaciaire dont nous disposons.

INTRODUCTION

The impetus for mapping surficial materials and examining the Quaternary history of this part of southern Baffin Island was the need for glacial drift-based mineral-indicator studies to complement a regional bedrock mapping program (St-Onge et al., 1999b, c, d, e, f, g, h). Arctic Quaternary geology also is crucial in studies of vegetation, soil, and wildlife; natural hazards; engineering performance of material; and climate change studies from local to global scale. The surficial geology maps will assist community development — for this area contains 21% of the population of Nunavut (Statistics Canada 2002: Census - Release 1 - March 12, 2002; http://www12.statcan.ca/english/census01/release/index.cfm), including the largest community, Iqaluit (pop. 5236; formerly Frobisher Bay), and Kimmirut (population 433; formerly Lake Harbour).

Some geographical names that appear in this bulletin, but are not included in the federal government's list of formal geographical names, are included in the report, but are offset by single quotation marks.

Map area

The area covers four 1:250 000 NTS sheets (25 K, L, M, N) between 62°N and 64°N and 68°W and 72°W (Fig. 1), with a land area of 26 838 km^2 (41% of the NTS maps is sea; Sebert and Munro (1972)). The majority of the land is part of Meta Incognita Peninsula of Baffin Island, i.e. the southeastern-most projection of Baffin Island, bounded by Frobisher Bay, Hudson Strait, and informally, a line joining the head of Frobisher Bay and Markham Bay (Fig. 2). To complete the NTS map sheets, an area northwest of Meta Incognita Peninsula is included in the report. Similarly, the small area northeast of the head of Frobisher Bay, including the community of Iqaluit, is described, though it is part of Hall Peninsula (between Frobisher Bay and Cumberland Sound).

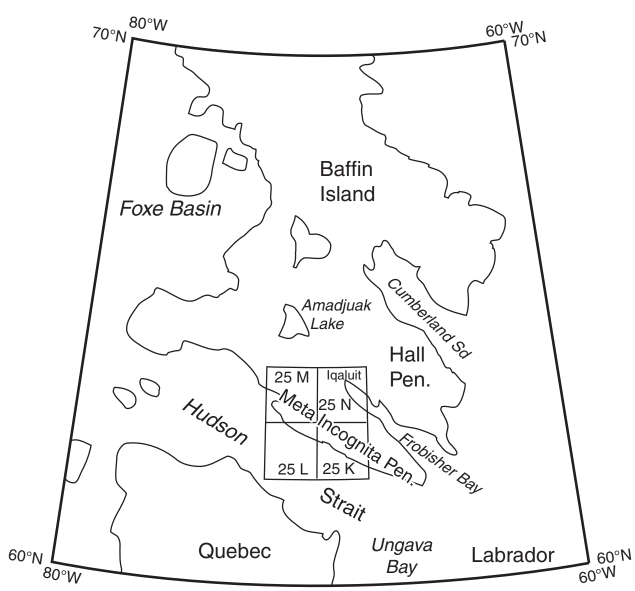

Figure 1. *Location of map area in southeast Arctic.*

Access

The area is normally entered via the large (originally military) airport at Iqaluit or the short airstrip at Kimmirut. Both ports are accessible to moderate-size ocean-going vessels. Coastal water travel in small craft can be hazardous due to the rugged shoreline (over 2000 km long in the map area), very large tides, and frequent strong winds. Gravel roads extend a maximum of 10 km from the centre of Iqaluit and 5 km from Kimmirut. The 120 km 'Itijjagiaq Trail' traverses the Meta Incognita Peninsula from Bay of Two Rivers to Kimmirut through the Katannilik Territorial Park Reserve (Fig. 2). Bay of Two Rivers is reached from Iqaluit either across seasonal sea ice by dog teams or snowmobiles, or by boat (for hiking).

Pre-Quaternary geology and physiography

Recent bedrock geology studies have reorganized the Precambrian geology of southern Baffin Island from a diverse metamorphic terrane included in the Churchill Province (Blackadar, 1967) to a segment of the Trans-Hudson Orogeny formed during a major Early Proterozoic episode of North American Plate convergence and continental accretion (St-Onge et al., 1999h). The area is underlain by the Superior Province of the Archean craton, which outcrops on Big Island. Supracrustal units accumulated in the Paleoproterozoic while plutonic rocks intruded the craton. Contemporary Paleoproterozoic metamorphism and deformation left distinct northwest-southeast and northeast-southwest structural grains (Fig. 3); but by the end of the Precambrian, the shield was largely reduced to a paleoplain (Ambrose, 1964). There is no further geological record until mid-Paleozoic marine transgressions over the denuded craton deposited mainly carbonate (now limestone and dolostone) sediments (Bolton et al., 1976; Sanford and Grant, 2000). Large erosional remnants of this cratonic cover remain in Foxe Basin, Hudson Strait, outer Frobisher Bay, and on the southeast Baffin Island shelf (Fig. 4).

The cover presumably still was extensive in the Cretaceous, when tectonic events associated with initial opening of the North Atlantic Ocean and Baffin Bay induced rifting which led later to preservation of downdropped Paleozoic deposits in Frobisher Bay (MacLean et al., 1990). The fault line for the Frobisher Bay half graben runs along the southwest shore (Fig. 3). Hudson Strait, already a depocentre in the mid-Paleozoic (Bolton et al., 1976), was also downdropped on the south side. In the Cretaceous, passive plate-margin tectonics associated with opening of the North Atlantic Ocean caused 500–800 m uplift of the main Baffin Island rift flank (Keen and Beaumont, 1990), resulting in the present high elevations of eastern Baffin Island, including Meta Incognita Peninsula (Fig. 5). Cretaceous and Tertiary syn- and post-rift sediments underlie Davis Strait and Labrador Sea, but no trace of these has been found onshore on southern Baffin Island (MacLean et al., 1990, p. 330), and possibly they never overlapped present land.

Bird (1958, 1967) suggested that the extensive areas of upland in the eastern Arctic with concordant elevations are elevated surfaces originally eroded anywhere between the Precambrian and Cretaceous. The most widespread element described by Bird (1967) is the 'Baffin Surface', composed of high-level plains and rolling upland, and represented on Meta Incognita Peninsula by plateau remnants and concordant summits on the peninsula height of land at 700 m elevation ('Frobisher Upland' of Bird (1958)). Mainly using radar altimetry, Bird (1958) identified raised surfaces east of the height of land ('Frobisher Benches') at about 500 m and 350 m, separated by fault-line scarps. West of the height of land and 700 m Baffin Surface, Bird found surfaces at about 550 m and 500 m, above a conspicuous slope to the dissected coastal zone; i.e. the levels, scarps, and slopes noted by Soper (1936); however, Bird (1967) preferred to describe all the southwest side of Meta Incognita Peninsula as a southwest-tilted block. Bird (1967) observed that the major rivers south of the divide flow south (Fig. 5), rather than aligning with the southwest decline in topography or the southwest- and southeast-trending deformation structures, and thus are likely superimposed on the Precambrian terrain. This supports the existence of a

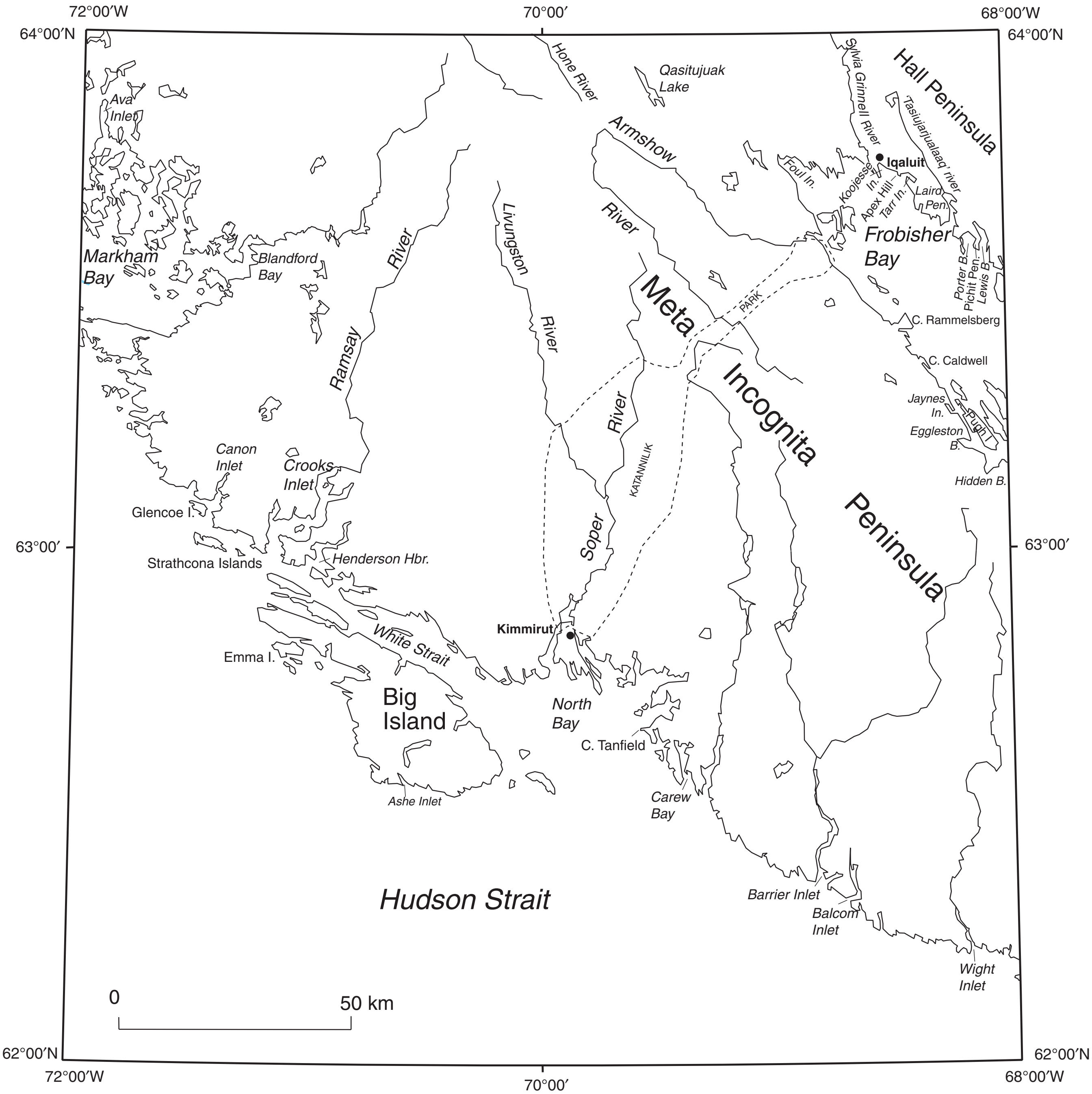

Figure 2. *Location of place names referred to in this study.*

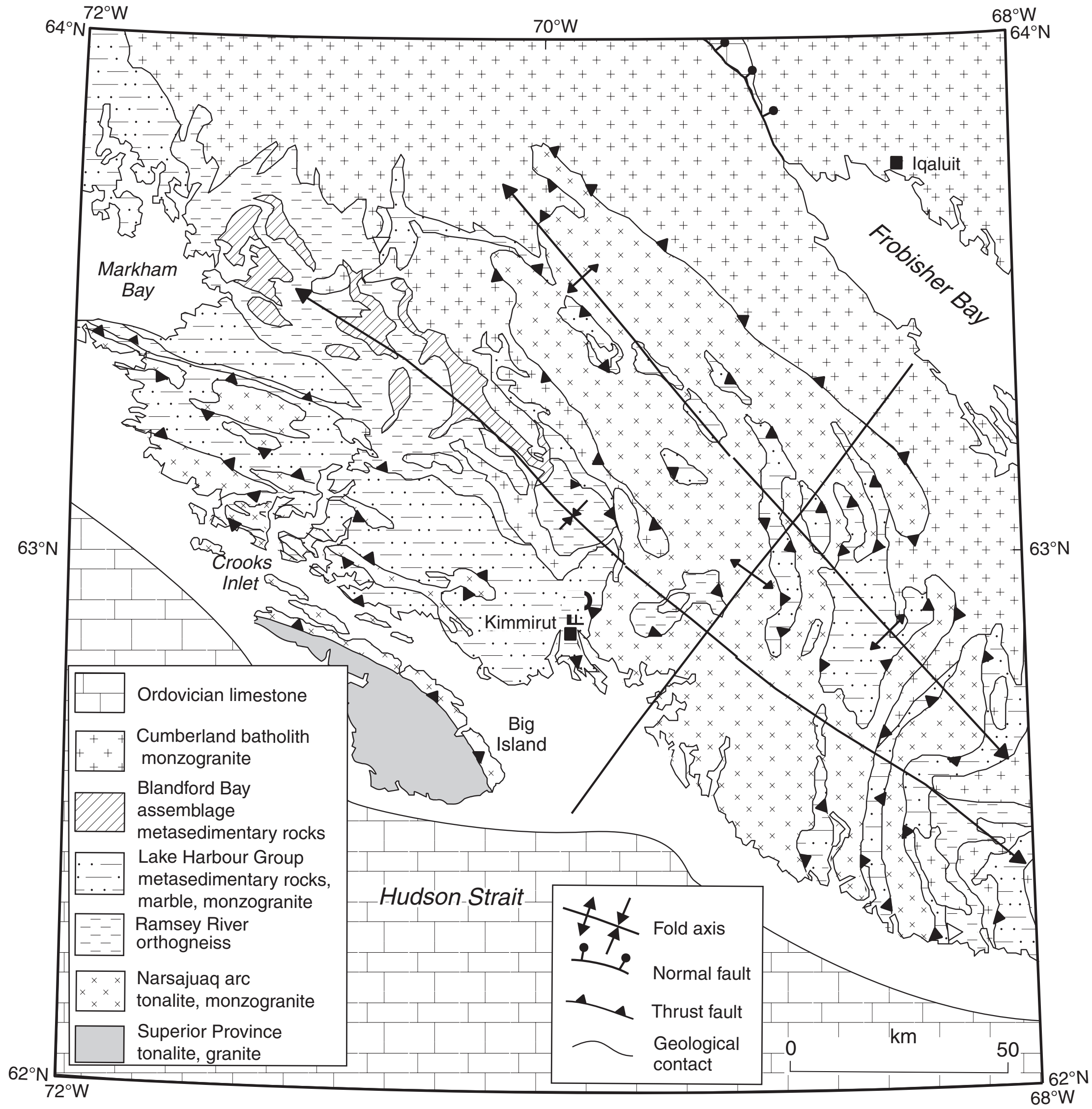

Figure 3. *Generalized bedrock geology of map area. Terrestrial geology* after *St-Onge and Scott (1999b, c, d, e, f, g, h); marine geology* after *MacLean et al. (1986).*

complete Paleozoic sediment cover, bearing a river-system tributary to Hudson Strait, until at least the Cretaceous when rifting was complete. The rectilinear drainage patterns within the map area north of the peninsula divide must postdate the Cretaceous rifting.

There are smaller elements of possibly tectonic relief within the broad pattern of Hudson Strait trough–Meta Incognita Peninsula–Frobisher Bay trough. For example, both Big Island and the upland between Crooks Inlet and Markham Bay are edged by steep bluffs to the northeast, though no faults have been detected. No evidence of postglacial (Holocene) faulting was observed.

Quaternary landscape

As a result of pre-Quaternary tectonics and erosion, Meta Incognita Peninsula has an asymmetric southwest-northeast cross-section, where, over a distance of 80–100 km from Hudson Strait to the height of land, elevations rise to 800 m in the east and 500 m in the west. In contrast, a distance of only 10–30 km separates Frobisher Bay from the height of land (Fig. 5). Drainage generally accords with the structural pattern, but south of the Meta Incognita Peninsula divide, as described above, major rivers flow south in deep valleys, crossing known structure obliquely. Most rivers drain to sea inlets, particularly on Hudson Strait coast where the fretted coast supports the concept of a tilted and partially drowned peneplain. Numerous lake-filled rock basins and scattered cliffy valley walls indicate glacial erosion. The only obvious fiord system is Crooks Inlet, which likely follows a

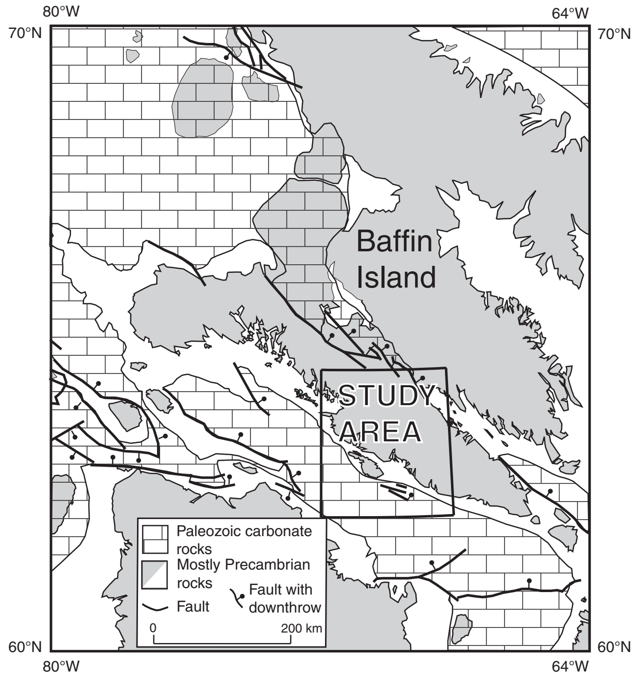

Figure 4 (left).

Regional bedrock geology: distribution of Paleozoic sediments overlying Precambrian metamorphic and igneous rocks (after Sanford and Grant, 2000 and MacLean et al., 1986). Symbols on faults are on downthrown side.

Figure 5 (below).

Physiography (contours at 100 m intervals) showing asymmetric cross-section of Meta Incognita Peninsula.

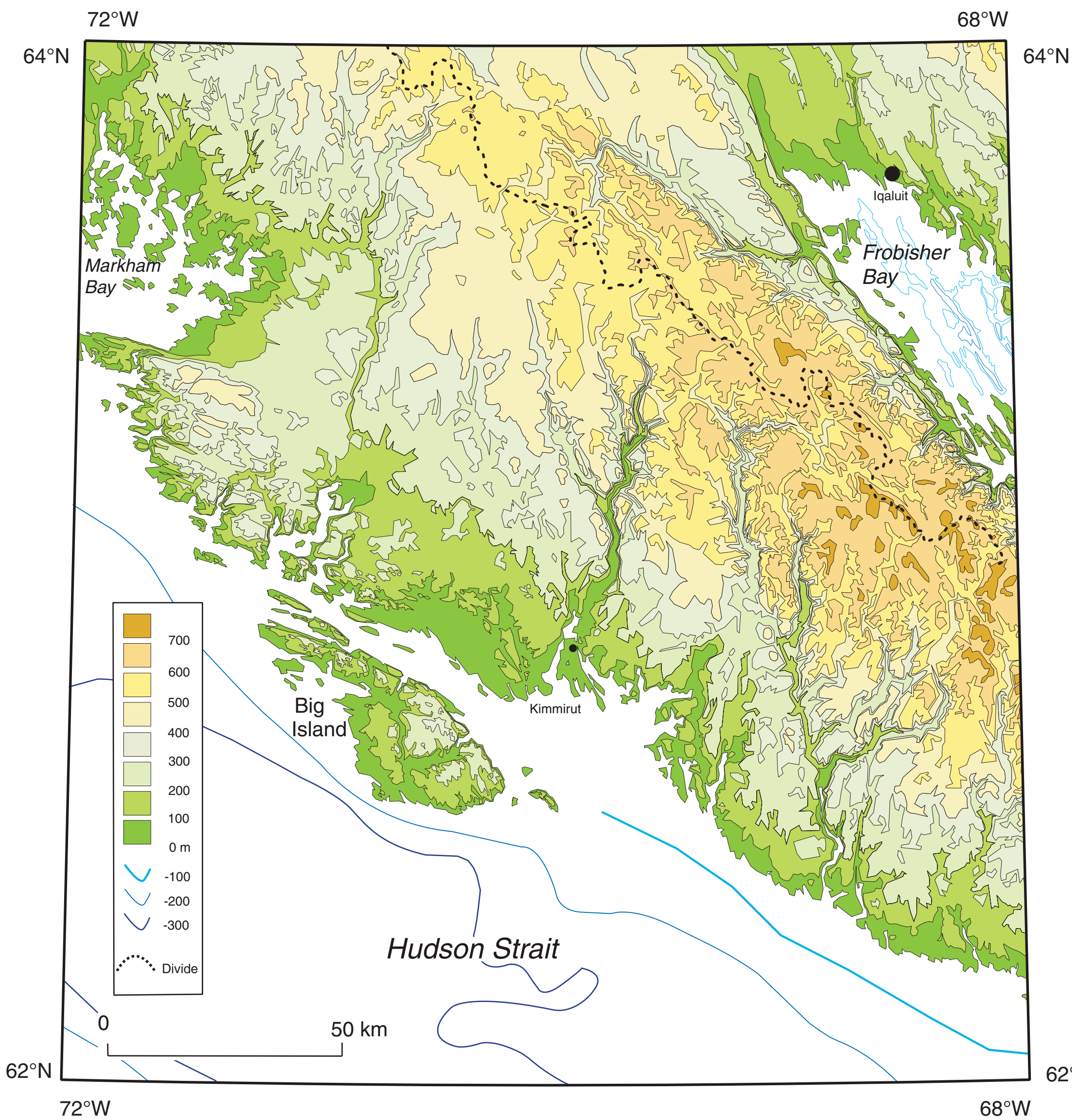

proto-Ramsay River superimposed on coastal upland, even though it aligns with a southwesterly Precambrian structural trend. Part of the south-flowing upper headwaters of the Ramsay River drainage have been captured by a glacially induced diversion to Blandford Bay. The upper, beaded reach of the Armshow River, flowing northwest, may be a recent glacial modification of drainage resulting from deposition of the Frobisher Bay Moraine System and proximal, thick till blocking the 'normal' southwestward consequent drainage from the highest land, which lies to the east of the Armshow River headwaters. For this reason, the crest of the peninsula is generally referred to here as the height of land rather than the topographic divide. The crest and flanks of Meta Incognita Peninsula tend to a broad rolling landscape, whereas towards the coast there is more irregularity. Thick till deposits, where present, smooth the topography.

Frobisher Bay is a Cretaceous tectonic depression apparently modified by later fluvial processes that produced narrow channels on the bay floor, and Quaternary glacial scouring that created small basins. Inner Frobisher Bay within the map area has a maximum recorded depth of 272 m. The lowland at the head of Frobisher Bay connects to Foxe Basin at an elevation of only 150 m, whereas to the east of Frobisher Bay, the Hall Peninsula rises to 500 m in the 35 km to the edge of the map area. Main rivers flow southeast on the bay-head lowland and flanking sections of Meta Incognita and Hall peninsulas, controlled by the structural grain. Hudson Strait is a Paleozoic or older depression enlarged by Cretaceous tectonism and Quaternary glacial scouring (the latter eroding the large basins). The Western basin of Hudson Strait is over 300 m deep off the coast of Big Island.

Quaternary nomenclature

The last glacial stage on Baffin Island commonly has been referred to as the Foxe Glaciation, because of the dominance over the eastern Arctic of an ice dome centred over Foxe Basin, within the Laurentide Ice Sheet. The Late Foxe Glaciation substage continued up to 6–5 ka (*see* discussion *in* Andrews and Miller (1984)) and so is not entirely correlative with the Late Wisconsin Glaciation, which terminated at 10 ka (Fulton, 1989). In this report, the last glaciation is referred to as the Wisconsin Glaciation; it occurred during the Wisconsinan stage (80–10 ka) of the Late Pleistocene (final substage: Late Wisconsinan (23–10 ka)), and the subsequent, continuing epoch is the Holocene (<10 ka).

Climate, permafrost, soils, and vegetation

The map area was divided down the axis of Meta Incognita Peninsula into two climatic subregions by Maxwell (1981). The northern unit (Frobisher Bay and Hall Peninsula) has an annual temperature range 5–6°C larger than to the south (Hudson Strait), where summers are cooler and winters warmer. The only long-term climate data in the map area is from a site at Iqaluit, 1 km inland and 34 m a.s.l. Here, daily mean air temperature is -9.5°C, ranging between a daily mean of 7.7°C in July and -26.8°C in February (Environment Canada 2000/5/19: Canadian Climate Normals 1961–1990, Iqaluit A.; http://www.cmc.ec.gc.ca/climate/normals/NWTI002.HTM ©1998). The envelope enclosing mean daily maximum and minimum temperatures (Fig. 6) indicates that freeze-thaw cycles are limited to two months per year above the ground surface at the height of air-temperature-recording instruments. Total annual precipitation is 424.1 mm: 192.9 mm rain, 95% in June–September; 256.8 cm snow, 90% in October–April. A short-term climate record from interior Baffin Island, 150 km northwest of Iqaluit and 150 m a.s.l., showed winter temperatures 2–3°C lower than at Iqaluit and about 1°C higher in summer; precipitation amounted to 92% of the annual average amount recorded at Iqaluit for the same period (Jacobs et al., 1997). A 10 year record from Kimmirut (Lake Harbour) through the 1930s compared to the more recent 30 year average for Iqaluit indicated mean winter temperatures 2°C higher in Kimmirut, mean summer temperatures 1°C higher, and precipitation 30% lower (Bradley, 1973). On the south side of Hudson Strait, in northernmost Quebec, mean annual air temperatures of -7.4° to -8.9°C are recorded, and total precipitation and rainfall are lower than at Iqaluit (Allard et al., 1995). Summer temperatures at Iqaluit are anomalously low for the latitude and precipitation is relatively high for the Arctic, due to frequent cyclonic activity between the North Atlantic Ocean and Baffin Bay, the cool water of western Davis Strait and Labrador Sea, and the year-round open water of the Labrador Sea (Williams and Bradley, 1985).

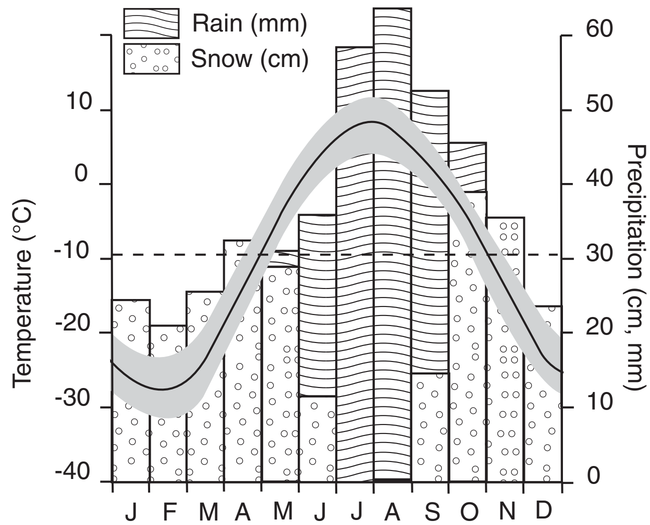

Figure 6. *Iqaluit climate: daily mean temperature is contained within the envelope of daily maximum to daily minimum. Mean annual temperature is dashed line. Data* after *Environment Canada 2000/5/19: Canadian Climate Normals 1961-1990, Iqaluit A.; http://www.cmc.ec.gc.ca/climate/normals/NWTI002.HTM ©1998.*

Maximum winter sea-ice conditions are a complete cover of first-year ice — mostly moving, but landfast on some coasts. Summer seas are completely open, other than scattered icebergs in the westerly current on the north side of Hudson Strait. Glaciation threshold is 1000 m a.s.l. in a zone connecting Iqaluit and Kimmirut (Andrews and Miller, 1972), declining to the west and to the east, where, beyond the map area, the Grinnell Glacier and Terra Nivea ice cap persist above 600 m.

The only known ground temperature data from the map area is from a shallow borehole in gneiss at Iqaluit. Sporadic measurements (Sharon Smith, pers. comm., 2001) indicate an active layer 1.5 m thick, which is similar to observations in a few pits dug in glaciofluvial, gravelly sand deposits. There is a relative abundance of information from northern Quebec, including records from a number of deep monitored boreholes inland from Hudson Strait, in igneous and metamorphic rocks similar to those north of the strait. These sites, at elevations around 500 m, are underlain by permafrost over 500–600 m thick (Taylor and Judge, 1979; Judge et al., 1981). They probably had similar last-glacial and Holocene conditions to higher elevations of southernmost Baffin Island. Taylor and Judge (1979) calculated a 300 m maximum depth of permafrost near the coast. Shallow boreholes near the Ungava Peninsula coast showed maximum active-layer thicknesses of 1.5–4 m in gneiss and sandy till over gneiss (Allard et al., 1995). No excess ice was observed in till at Ungava Peninsula locations, though 65% ice by volume was found in marine silt under peat.

Soils of the map area are broadly described by Tarnocai and Kroetsch (1994) as regosolic static cryosols (i.e. no B horizon, no cryotubation, permafrost at 1–2 m depth) developed on sandy morainal material; however frost boils and other sorted microlandforms are common on till, so it is assumed here that turbic cryosols are widespread. Probably half of the map area is lithosol, comprising bedrock outcrop or block fields. Organic cryosols are rare; little wetland has more than a few centimetres of peat.

Most investigators place the map area near the northern limit of low-arctic tundra, the richest of the circumpolar floristic zones (Polunin, 1951; Porsild, 1958; Young, 1971; Jacobs et al., 1997). Young (1971) quantified arctic vegetation distribution (identified zones by summer warmth), using summer warmth as the chief parameter. Vegetation of the Low Arctic is characteristically a nearly continuous cover of sedges, grasses, forbs, heath, and dwarf shrubs. Porsild (1958) and Porsild and Cody (1980) showed distribution of these vascular plants in the Canadian Arctic. Short and Jacobs (1982) observed the dominant vegetation for the Iqaluit area to be *Salix* (willow) and *Ericaceae* (heath), with extensive areas of grasses, sedges, and mosses especially in low, wet areas and on moist (till or marine deposit) slopes. Polunin (1948) described the variety of plant communities around Kimmirut (Lake Harbour), including hill summits and slopes, lowlands, marshes, and freshwater and marine shores; however, topography is sufficient to raise large areas of the map area into the Middle Arctic zone, which includes much lichen-covered rock and block fields. Using a dwarf birch species (*Betula glandulosa)* as an indicator of low-arctic tundra, Jacobs et al. (1985a) placed the zone limit at an elevation of 300 m around inner Frobisher Bay. It is likely that the highest altitudes (maximum 800 m) fall in the high-arctic zone because the glaciation limit is only 200 m higher. Specialized habitats include the poorly vegetated pea-gravel residuum on marble and the stands of erect willows (*Salix planifolia*) reported to 3.5 m high by Soper (1936) in some sheltered tributaries of the Soper River.

Previous Quaternary geomorphology studies

There have been three phases in Quaternary geology studies of the area: late 19th century exploratory observations that noted widespread evidence of glaciation and raised marine deposits; 1950–1970 reconnaissance surveys that established the framework of last glaciation and of physiography; and post-1970 systematic (topical and areal) studies of Pleistocene and Holocene landforms, environments, and processes, many of them doctoral or masters theses at the Institute of Arctic and Alpine Research, University of Colorado.

Bell (1885) found evidence of ice flow down Hudson Strait with 115° striations at the southwest corner of Big Island, the closest land to the centre-line of the strait, which is oriented at 120°. Later, Bell (1901b) recorded 165° striations on the west side of Big Island, and he (Bell, 1901a) observed that everywhere on the Baffin Island coast of Hudson Strait striations ran southwest (even though "distinct glacial striae [were] seldom seen"), indicating to him tributary flow to the strait. Watson (1897) recognized on southern Big Island that a clear break, measured 90 m a.s.l., between large loose, angular rocks (above) and extensive bare rock with scattered beach ridges and marine shells (below) was a washing limit marking the height of recent uplift, and was coextensive with uplift recorded farther west by Bell (1896). Possibly this marine limit is what Barton (1899) identified as a moraine.

Wengerd (1951) provided a good description of the modern shoreline of inner Frobisher Bay, and recognized recent uplift due to "elastic and plastic glacial rebound", but his claim that raised marine strandlines were present to 270 m a.s.l., and possibly even 420 m a.s.l. was disputed by Ward (1952), who suggested they record water levels held up by glacial ice dams in fiords and bays. Mercer (1956) supported Wengerd's (1951) marine origin for high apparent strandlines. He also suggested that the presence of cirques along Frobisher Bay, east of the map area indicated that area was not covered by continental ice in the last glaciation, whereas the apparent absence of cirques to the west indicated an ice sheet was present there; however, the large volume of ice necessary to depress the crust and raise relative sea level greater than 400 m perplexed him; he placed much of this ice in Hudson Strait. He also concluded that after initial deglaciation of Hudson Strait, Quebec–Labrador ice dammed a lake in Hudson Strait, for which the 'York gorges', transecting Meta Incognita Peninsula east of the map area, were outlets (cf. Stravers, 1986). Ives and Andrews (1963) showed Late Wisconsinan ice flowing from a Foxe Basin centre into the map area, and later dispersing from Amadjuak Lake at the southern end of a Baffin Island ice divide. Both Ives and Andrews (1963) and Falconer et al. (1965) hinted that a segment of a Holocene ice front, recorded elsewhere by the Cockburn Moraines, lay in the map area. In the course of outlining the late Pleistocene and early Holocene history of southern Baffin Island, Blake (1966) was the first to show that a major end moraine coeval with Cockburn Moraines crossed the map area, including inner Frobisher Bay. This moraine, not named by Blake (1966), was named the Frobisher Bay moraine by Miller (1980), and has been variously referred to as "Frobisher Bay Moraine" (Colvill, 1982; Lind, 1983; Mode and Jacobs, 1987) and the "Frobisher Bay

Moraine System" (Manley and Moore, 1995). It is referred to in this report as the Frobisher Bay Moraine System. Blake (1966) concluded that it was landforms of the Frobisher Bay Moraine System adjacent to Frobisher Bay that were identified by Wengerd (1951) and others as strandlines. Blake (1966) provided a framework of Late Quaternary ice flows on southern Baffin Island (unpublished map manuscripts summarized *in* Prest et al. (1968)) and a chronology for the area that remains broadly intact (though significant additional events are described below): ice flowing down Hudson Strait until 9–8 ka barely brushed shores of Big and Baffin islands, but deposited Paleozoic erratics and interstadial marine shells, and diverted meltwater through the 'York gorges'; ice lay at the Frobisher Bay Moraine System at 8.2 ka and did not leave the head of the bay until ca. 6.8 ka. (In the radiocarbon time scale used here, ka = thousands of years before present (BP), i.e. 1950, and marine shells are corrected by 400 years for marine reservoir effect — *see* 'Age estimates of sediments and landforms', below.)

Surficial materials, landforms, late-glacial stratigraphy and chronology around inner Frobisher Bay were mapped and discussed by Colvill (1982), Lind (1983), Squires (1984), and Manley and Moore (1995) (Fig. 7). Clark (1985) constructed the first emergence curve within the map area (in the vicinity of Kimmirut (then known as Lake Harbour)). Most of the late Holocene dates (Table 1) that Clark used came from archeological investigations in the Cape Tanfield area (Maxwell, 1973). Manley (1995, 1996) has produced the most comprehensive survey to date of the last glaciation of all Meta Incognita Peninsula, based on observations from coastal areas. The map of glacial landforms of Kleman and Jansson (1996) adds more detail to Blake's (1966) and Prest et al.'s (1968) maps. Late-glacial and Holocene terrestrial, lacustrine, and marine environments of inner Frobisher Bay were examined by Matthews (1967), Short and Jacobs (1982), Jacobs et al. (1985b), and Abbott (1991). The glacial history of adjacent (outer) Frobisher Bay and Meta Incognita Peninsula was described by Miller (1980), Muller (1980), Osterman (1982), Osterman and Andrews (1983), Dowdeswell (1984), Stravers (1986), and Duvall (1993). No Quaternary studies since Blake's (1966) have been carried out on the Baffin Island shore of Hudson Strait west of the map area, though Laymon (1988, 1992) examined the islands at the western end of the strait. Reviews of late-glacial events on southeastern Baffin Island have been presented by Miller (1980, 1985), Andrews et al. (1985), Osterman et al. (1985), Miller et al. (1988), Stravers et al. (1992), Kaufman et al. (1993a), and Manley and Miller (2001).

The generally accepted model, after Mercer's (1956) study, for the Late Wisconsin Glaciation of Meta Incognita Peninsula and inner Frobisher Bay has been one of an ice cap lying along the axis of Meta Incognita Peninsula withstanding or merging with southeast-streaming Laurentide ice (summarized *in* Dyke and Prest (1987a)). Ice from this local centre flowed southwest into Hudson Strait, joining a Hudson Strait glacier until the latter retreated out of the strait prior to general retreat of ice from Meta Incognita Peninsula. Retreat of the glacier from the eastern end of the strait commenced ca. 14 ka (Andrews et al., 1995) and the ice front left the west end of the strait before 8.1 ka (Laymon, 1988). Meta Incognita Peninsula ice also flowed northeast into Frobisher Bay, where it merged with a glacier fed by the Foxe Ice Dome and subsequently an "Amadjuak ice centre" (Falconer et al., 1965; Blake, 1966). The Frobisher Bay glacier commenced retreat by 10.5 ka (Stravers, 1986). Blake (1966) recognized that a late-glacial ice margin stood at the head of the bay from at least 8.2 ka to not later than 6.7 ka, depositing moraines (Frobisher Bay Moraine System) of the Cockburn Substage (9–8 ka) (Andrews and Ives, 1978).

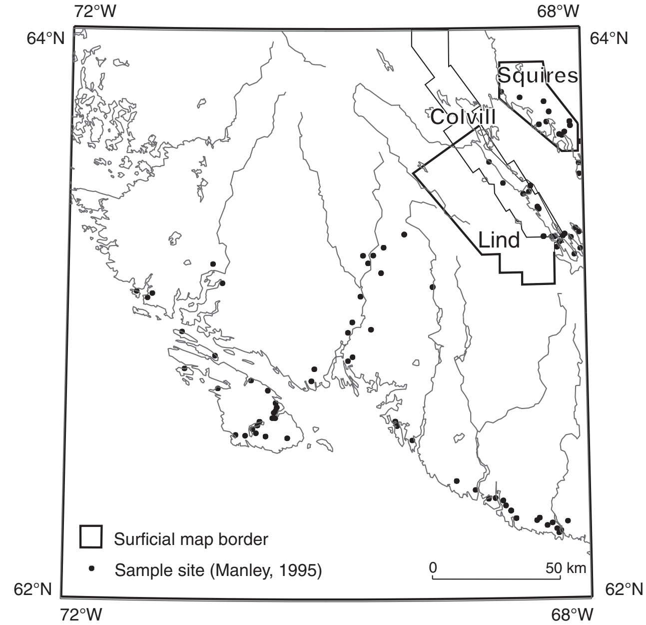

Figure 7. *Previous surficial materials studies: location of surficial materials maps of Colvill (1982), Lind (1983), and Squires (1984); till and radiocarbon sample locations of Manley (1995).*

Modifications to this general pattern include:

1) The high southern mid-bay rim of Frobisher Bay (Everett Mountains) remained unglaciated during the Late Wisconsinan, based on the presence of cirques (Mercer, 1956) and associated moraines dated greater than late Foxe age by lichenometry and weathering pits (Dowdeswell, 1984); and based on the presence of a pre-Wisconsinan weathering zone, differentiated by the degree of boulder weathering and the absence of indicators of glacierization (Mercer, 1956; Muller, 1980; Stravers, 1986).

2) The Frobisher Bay glacier did not extend beyond the mid-bay area in the Late Wisconsinan (Duvall, 1993), based on provenance of ice-proximal sediments in marine cores (Osterman and Andrews, 1983). Possibly this limit correlates with end moraines on Hall Peninsula 50 km distal to the Frobisher Bay Moraine System mapped by Blake (1966). Miller (1980) named these the Hall Moraine which he initially incorrectly correlated with moraines on the north side of outer Frobisher Bay (*see* Gold Cove advance, in this section, below).

3) The Frobisher Bay Moraine System was nearly 1 ka older than previous age estimates, based on 8.9 ka proximal and distal sediments at Cape Rammelsberg (Manley *in* Manley and Jennings (1996))

A more fundamental divergence from a pattern of local ice merging with mid-continent ice outflow is that of Labrador Sector ice crossing the deglaciated eastern end of Hudson Strait to invade eastern Meta Incognita Peninsula during the Late Wisconsinan, as first suggested by Mercer (1956) to explain the "York canyons". Stravers (1986) and Miller et al. (1988) provided the first direct evidence of a trans-Hudson Strait ice flow crossing the eastern peninsula into outer Frobisher Bay (though Blake (1966) had noted appropriate striations). Three Late Wisconsinan advances of Labrador ice have been proposed, based on glacial striations, carbonate till provenance, and radiocarbon ages of marine shells within and between till sheets (Miller and Kaufman, 1990). All require a mainly ice-free eastern Meta Incognita Peninsula. A pre-Gold Cove advance (Miller and Kaufman, 1990; the "Beare Sound advance" of Kaufman et al. (1992)), at ca. 11.5 ka, maintained for 1 ka, crossed eastern Meta Incognita Peninsula and outer Frobisher Bay to Hall Peninsula, but was restricted by Pfeffer et al. (1997) to an early Younger Dryas (ca. 11 ka) advance only to Meta Incognita Peninsula, and referred to by them as the DC-0 or H-0 advance. The Gold Cove advance — a readvance between 9.9 ka and 9.6 ka (Stravers et al., 1992; Kaufman et al., 1993a, b), or a culmination of the DC-0 advance under increased precipitation (Pfeffer et al., 1997) — crossed Frobisher Bay to southeast Hall Peninsula, and was followed by a retreat of the ice margin at least as far south as Hudson Strait. The Noble Inlet advance terminated on Meta Incognita Peninsula between 8.9 ka and 8.4 ka (Stravers, 1986; Dyke and Prest, 1987a; Miller et al., 1988; Stravers et al., 1992; Manley, 1995, 1996; Jennings et al., 1998). Duvall (1993) more specifically suggested that Gold Cove (Labrador) ice blocked a Hudson Strait glacier, causing it to overtop the central peninsula, leaving the high-elevation carbonate erratics in Everett Mountains and creating a mid-Frobisher Bay lake, though Muller (1980) had measured a definite upper limit of carbonate erratics (<600 m) and believed that this indicated last ice overlapped only from Frobisher Bay. England and Smith (1993), summarized by Gray (2001), argued for down-Hudson Strait flow only, but the weight of evidence from the north side of the strait continues to favour ice advances across the strait (e.g. Jennings et al., 1998; Manley and Miller, 2001).

Work methods and acknowledgments

Fieldwork in 1995, 1996, and 1997 was carried out largely from base camps organized by Continental Geoscience Division, South Baffin Project (M.R. St-Onge, leader), supported by aircraft contracted by Polar Continental Shelf Project (80 hours of helicopter flying was used in the Quaternary component). Observations of surficial materials and landforms were made on foot traverses (set-outs by helicopter); some striation measurements and representative till samples were collected during several helicopter traverses (Fig. 8). Geologists and assistants in the concurrent bedrock mapping project contributed a number of striation measurements. Erica Kotler assisted Quaternary field studies in 1995. In 1999 Tommy Papatsie assisted during a two-week camp at Wight Inlet (NTS 25 K) that was set out by boat from Kimmirut. Lynda Dredge and Arthur Dyke, Terrain Sciences Division, GSC provided careful and helpful critical reviews.

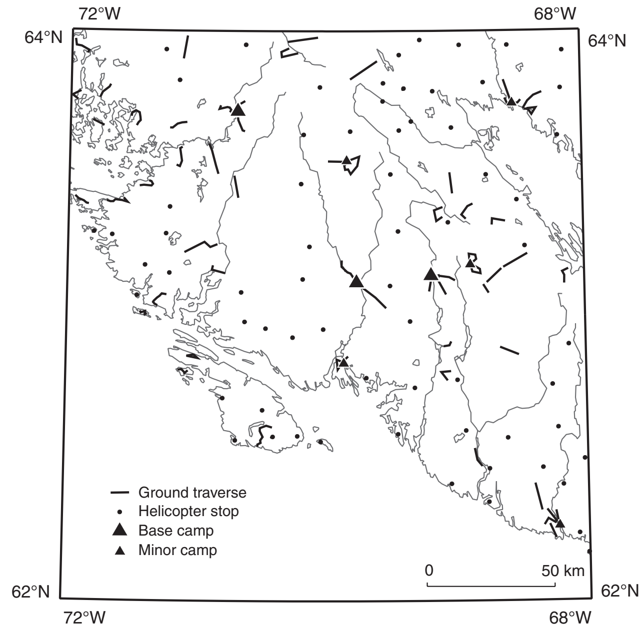

Figure 8. *Traverse map: location within the map area of field studies and camps.*

The accompanying surficial materials maps are based on field observations and interpretation recorded on 1:60 000 airphotos. Maps were compiled by the author digitizing from airphotos onto a digital topographic base (1:250 000) using the MapInfo desktop mapping system. There is partial 1:50 000 map/photomap coverage of the map area.

Till grain size, pH, and carbonate-content analyses, and initial preparation of samples for base-metal and trace-element analysis were performed by the Quaternary Services Laboratory, Terrain Sciences Division, and GSC radiocarbon age estimates were provided by the Geochronology Laboratory, Terrain Sciences Division.

The pattern of field traverses (Fig. 8) shows that the objective of investigating areas of geological significance was tempered by logistical constraints, especially distance from base camps. Given the limitations, little work was done wherever a body of field observations already existed; i.e. surrounds of Frobisher Bay, examined by Colvill (1982), Lind (1983), and Squires (1984), and the shores of Hudson Strait, especially from Big Island southeastwards (Blake, 1966; Manley, 1995, 1996), including the Kimmirut area (Clark, 1985).

Table 1. Radiocarbon dates

Lab. Id.[1]	Method[2]	Uncorrected age[3]	$\delta^{13}C$[4]	Corrected age (GSC)[5]	Corrected age (INSTAAR)[6]	Normalized age[7]	Lat. ′W[8]	Long. ′E[8]	Easting	Northing	Elev. (m a.s.l.)
HUDSON STRAIT											
AA-7901	AMS			>43 500		>43 900	62°23′	69°01′	499500	6917000	-5
AA-7897	AMS			>43 300		>43 700	62°37′	69°30′	476300	6942800	0.3
AA-12605	AMS			43 350 ± 2100	43 300 ± 2100	43750 ± 2100	62°36′	70°32.2′	420700	6942500	114
AA-11453	AMS			40 360 ± 1450	40 310 ± 1450	40 760 ± 1450	62°14.5′	68°19.5′	535000	6901000	65
AA-11452	AMS			38 745 ± 1180	38 695 ± 1180	39 145 ± 1180	62°15.5′	68°23.0′	531000	6903000	74
AA-12606	AMS			37 360 ± 1050	37 310 ± 1050	37 760 ± 1050	62°36′	70°32.3′	420400	6942500	114
AA-11451	AMS			34 880 ± 760	34 830 ± 760	35 280 ± 760	62°14′	68°13.5′	541000	6900000	83
AA-7899	AMS			34 390 ± 710	34 340 ± 710	34 790 ± 710	62°38′	70°29′	429300	6947300	15
AA-10252	AMS			30 390 ± 450	30 340 ± 450	30 790 ± 450	62°19.5′	68°39.5′	518000	6911000	56
GSC-414	C	30 200 ± 1500					62°22.5′	68°58′	501725	6915757	66-72
CAMS-22022	AMS			27 270 ± 440	27 220 ± 440	27 670 ± 440	62°37.28′	71°35.68′	366907	6945883	-347
AA-13175	AMS			8725 ± 65	8675 ± 65	9125 ± 65	62°37.28′	71°35.68′	366907	6945883	-339
CAMS-22023	AMS			8590 ± 80	8540 ± 80	8990 ± 80	62°37.28′	71°35.68′	366907	6945883	-342
AA-10645	AMS			8360 ± 65	8310 ± 65	8760 ± 65	62°17.7′	68°35.5′	521000	6907000	19
AA-12609	AMS			8155 ± 95	8105 ± 95	8555 ± 95	62°33.5′	70°16.4′	434400	6937100	55
AA-10251	AMS			8045 ± 55	7995 ± 55	8445 ± 55	62°58.1′	69°47.3′	459700	6982000	35
GSC-425	C	7980 ± 220					62°36′	70°40′	414430	6941929	75
AA-7893	AMS			7960 ± 60	7910 ± 60	8360 ± 60	62°47′	69°50′	456600	6968300	73
GSC-433	C	7880 ± 140					62°53.5′	69°50.5′	457209	6973600	64
QC-1137	C	7865 ± 250					62°51′	69°54′	454178	6968998	75
AA-13050	AMS			7845 ± 75	7795 ± 75	8245 ± 75	62°37.8′	70°23.7′	428700	6945200	34
AA-12607	AMS			7775 ± 95	7725 ± 95	8175 ± 95	62°36′	70°30.1′	422900	6942400	58
AA-12610	AMS			7730 ± 65	7680 ± 65	8130 ± 65	63°04.5′	71°21′	381287	6995918	63
GSC-5699	C	7680 ± 190	2.22	7710 ± 190	7670 ± 95	8110 ± 190	62°37.8′	70°22.4′	429800	6945100	49
GSC-5526	C	7670 ± 90	1.4	7690 ± 90	7650 ± 45	7690 ± 90	62°17.7′	68°35.5′	521000	6907000	12
AA-10649	AMS			7645 ± 60	7595 ± 60	8045 ± 60	62°14′	68°14′	540000	6901000	16
AA-7892	AMS			7595 ± 65	7545 ± 65	7995 ± 65	62°47′	69°50′	456600	6968700	57
GSC-504	C	7490 ± 160					62°53.5′	69°51′	456785	6973605	43
GSC-5677	C	7490 ± 130	3.07	7540 ± 130	7500 ± 65	7940 ± 130	62°37.2′	70°29.3′	423700	6943900	45
AA-7900	AMS			7410 ± 70	7360 ± 70	7810 ± 70	62°41′	70°27′	430400	6949300	-11
GSC-5688	C	7350 ± 200	1.63	7380 ± 200	7340 ± 100	7780 ± 200	62°46.4′	70°06.1′	443800	6959300	39
QC-1138	C	7185 ± 120					62°51′	69°53.5′	454320	6968996	45
AA-7898	AMS			6255 ± 65	6205 ± 65	6655 ± 65	62°40′	70°28′	430000	6948000	-4
GSC-1382	C	4620 ± 380	-20.1			4690 ± 380	62°39.2′	69°34.9′	470200	6947200	14
GaK-1281	C	4460 ± 100	-23e			4480 ± 105e	62°39.2′	69°34.9′	470200	6947200	14
P-707	C	4067 ± 73	-23e			4087 ± 81e	62°39.2′	69°34.9′	470200	6947200	12
M-1532a*	C	3880 ± 150	-23e			3900 ± 155e	62°39.4′	69°34.4′	470570	6947300	8
M-1532b*	C	3850 ± 150					62°39.4′	69°34.4′	470570	6947300	8
P-708	C	3814 ± 69	-23e			3834 ± 77e	62°44.8′	69°39.2′	466000	6956800	18
GSC-596	C	3750 ± 140					62°54′	69°51.5′	456374	6974539	3
P-710	C	3577 ± 69	-23e			3597 ± 78e	62°39.4′	69°34.4′	470570	6947300	15
M-1531	C	3480 ± 200	-23e			3500 ± 205e	62°39.5′	69°34.2′	470570	6947300	11
GSC-1051	C	3420 ± 210	-26.8			3390 ± 210	62°39.2′	69°34.9′	470200	6947200	18
P-699	C	3043 ± 63	-23e			3063 ± 72e	62°44.5′	69°39.6′	466000	6957500	10
P-698	C	2608 ± 50	-23e			2628 ± 60e	62°39.2′	69°34.3′	470570	6947300	6
M-1535	C	2410 ± 120	-23e			2430 ± 125e	62°39.2′	69°34.4′	470570	6947300	12
M-1528	C	2390 ± 150	-23e			2410 ± 155e	62°39.2′	69°34.3′	470570	6947300	6
GaK-1284	C	2380 ± 80	-20e			2460 ± 80e	62°39.2′	69°34.4′	470570	6947300	12
GaK-1286	C	2370 ± 100	-25e			2370 ± 100e	62°39.2′	69°34.4′	470570	6947300	12
GaK-1280	C	2360 ± 100	-25e			2360 ± 100e	62°39.2′	69°34.3′	470570	6947300	6
GSC-820	C	2350 ± 140	-23e			2370 ± 145e	62°39.2′	69°34.3′	470570	6947300	6
M-1528A	C	2250 ± 130					62°39.2′	69°34.3′	470570	6947300	6
GaK-1279 *	C	2220 ± 100	-25e			2220 ± 100e	62°39.2′	69°34.4′	470570	6947300	12
M-1534	C	2200 ± 120	-23e			2220 ± 125e	62°39.3′	69°34.4′	470570	6947300	8.5
M-1530a*	C	2180 ± 120	-23e			2220 ± 125e	62°39.3′	69°34.4′	470570	6947300	10
GaK-1287	C	2110 ± 80	-15e			2270 ± 80e	62°39.2′	69°34.4′	470570	6947300	12
GSC-794	C	2040 ± 130	-25e			2040 ± 130e	62°39.3′	69°34.4′	470570	6947300	8.5
GaK-1493	C	2010 ± 80	-23e			2030 ± 85e	62°39.2′	69°34.4′	470570	6947300	12
P-704	C	1916 ± 61	-25e			1916 ± 61e	62°39.2′	69°34.4′	470570	6947300	12
GaK-1494	C	1870 ± 110	-25e			1870 ± 110e	62°39.2′	69°34.4′	470570	6947300	12
P-706	C	1827 ± 61	-25e			1827 ± 61e	62°39.2′	69°34.4′	470570	6947300	12
M-1530b*	C	1790 ± 120					62°39.3′	69°34.4′	470570	6947300	10

[1]Identification numbers with * indicate the dates for that sample are suspect.
[2]C = conventional radiocarbon methods. AMS = accelerator mass spectroscopy.
[3]Laboratory/machine age uncorrected for sample isotopic fractionation or derivation of published age not known.
[4] $^{13}C/^{12}C$ ratios where known. For a number of samples in the Canadian Archaeological Radiocarbon Database (CARD), values have been estimated by R. Morlan (*see* footnote 12). These are given the suffix e.
[5]Age of marine organism, corrected following GSC convention, for fractionation to a $\delta^{13}C$ = 0‰ PDB. This is equivalent to subtracting a marine reservoir effect of 400 years, which is what is done if a normalized age is available.
[6]Normalized age corrected for a reservoir effect of 450 years, which is the convention of the Institute of Arctic and Alpine Research, University of Colorado. A few dates used by INSTAAR were converted from GSC corrected dates using a reservoir correction of 440 years. GSC error terms are halved by INSTAAR to give roughly a 1 sigma value.

Min. water depth	Marine limit[9] (m)	Material[10]	Site[11] italics = archeological site	Collector	Reference
HUDSON STRAIT					
	72-77	Mollusc *H.a.*	Glaciomarine	W. Manley	Manley, 1995, 1996; Manley and Jennings, 1996
	86	Molluscs *Mya t.?*	Glaciomarine	W. Manley	Manley, 1995, 1996; Manley and Jennings, 1996
	98	Mollusc *H.a.?*	Till	W. Manley	Manley, 1995, 1996; Manley and Jennings, 1996
	60	Mollusc *Mya t.*	Till	W. Manley	Manley, 1995; Manley and Jennings, 1996
	65	Mollusc	Till	W. Manley	Manley, 1995; Manley and Jennings, 1996
	98	Mollusc *Mya t.*	Till	W. Manley	Manley, 1995, 1996; Manley and Jennings, 1996
	56	Mollusc *H.a.*	Till	W. Manley	Manley, 1995; Manley and Jennings, 1996
	101	Molluscs *H.a.?*	Glaciomarine	W. Manley	Manley, 1995, 1996; Manley and Jennings, 1996
	67	Mollusc	Glaciomarine	W. Manley	Manley, 1995; Manley and Jennings, 1996
	77	Molluscs *H.a., A., B.*	Till	W. Blake & F. Synge	Blake, 1966; Lowden et al., 1967
	n/a	Forams & mollusc	Marine/glaciomarine	B. Maclean & W. Manley	Maclean et al., 1994; Manley and Jenkins, 1996
	n/a	Mollusc *P.a.*	Marine/glaciomarine	B. Maclean & W. Manley	Maclean et al., 1994; Manley and Jenkins, 1996
	n/a	Forams & ostracods	Marine/glaciomarine	B. Maclean & W. Manley	Maclean et al., 1994; Manley and Jenkins, 1996
	67*	Mollusc *P.a.*	Glaciomarine	W. Manley	Manley, 1995; Manley and Jennings, 1996
	115	Mollusc *P.a.*	Glaciomarine	W. Manley	Manley, 1995, 1996; Manley and Jennings, 1996
	102	Mollusc *H.a.*	Glaciomarine	W. Manley	Manley, 1995, 1996; Manley and Jennings, 1996
	110	Molluscs *H.a., Mya, Mac.*	Glaciomarine	W. Blake & F. Synge	Blake, 1966; Lowden et al., 1967
	95	Mollusc *Mya t .*	Glaciomarine	W. Manley	Manley, 1995, 1996; Manley and Jennings, 1996
	91	Molluscs *H.a., Mya t.*	Glaciomarine	W. Blake & F. Synge	Blake, 1966; Lowden et al., 1967
	90	Mollusc	Rock outcrop	P. Clark	Andrews and Short, 1983; Clark, 1985
	92	Mollusc *H.a.*	Glaciomarine	W. Manley	Manley, 1995, 1996; Manley and Jennings, 1996
	95	Mollusc *P.a.?*	Glaciomarine	W. Manley	Manley, 1995, 1996; Manley and Jennings, 1996
	138	Mollusc *P.a.*	Glaciomarine	W. Manley	Manley, 1995, 1996; Manley and Jennings, 1996
	98	Molluscs *H.a., Mya t.*	Glaciomarine	W. Manley	Manley, 1995, 1996; Manley and Jennings, 1996; McNeely, 2001
	67*	Molluscs *Mya t., H.a., P.a., S.g., C.i.*	Glaciomarine	W. Manley	Manley, 1995; Manley and Jennings, 1996; McNeely, 2001
	56	Mollusc *Mya t., Pec., B, A., Mac., H.a.*	Glaciomarine	W. Manley	Manley, 1995; Manley and Jennings, 1996
	95	Mollusc *Mya t.*	Glaciomarine	W. Manley	Manley, 1995; Manley and Jennings, 1996
	91	Molluscs *H.a., Mya t.*	Glaciomarine	W. Blake & F. Synge	
	95	Mollusc *Mya t.*	Glaciomarine	W. Manley	Manley, 1995, 1996; Manley and Jennings, 1996
	101	Mollusc *Mya t.*	Glaciomarine	W. Manley	Manley, 1995, 1996; Manley and Jennings, 1996
	98	Molluscs *H.a.*	Glaciomarine	W. Manley	Manley, 1995, 1996; Manley and Jennings, 1996
	90	Molluscs *B., Mac.b., Mya t., H.a., Hem.*	Glaciomarine	P. Clark	Andrews and Short, 1983; Clark, 1985
	101	Mollusc *Mya t.*	Glaciomarine	W. Manley	Manley, 1995, 1996; Manley and Jennings, 1996
	89**	Charred fat	Midden *Closure (Cape Tanfield)*	A. Dekin	Lowdon et al., 1972
	89**	Charred fat	*Closure (Cape Tanfield)*	M. Maxwell	Kigoshi et al., 1969, p. 245–326
	89**	Charred fat	*Closure/Cape Tanfield*	M. Maxwell	Stuckenrath et al., 1966, p. 348–385
	88**	Charred fat	*Kakela (Tanfield Valley)*	M. Maxwell	Crane and Griffen 1966, p. 274–279; Maxwell, 1973
	88**	Charred fat	*Kakela (Tanfield Valley)*	M. Maxwell	Crane and Griffen 1966, p. 274–279; Maxwell, 1973
	87**	Charred fat	*Annawak*	M. Maxwell	Stuckenrath et al., 1966, p. 348–385
	91	Molluscs *Mya t.*	Glaciomarine	W. Blake & F. Synge	Lowden et al., 1967
	88**	Charred fat	*Loon (Tanfield Valley)*	M. Maxwell	Stuckenrath et al., 1966, p. 348–385
	88**	Charred fat	*Site13 (Tanfield Valley)*	M. Maxwell	Crane and Griffen 1966, p. 274–279
	89**	Charred fat(contaminated?)	Midden *Closure (Cape Tanfield)*	A. Dekin	Lowdon et al., 1970
	87**	Charred fat	*Killilugak*	M. Maxwell	Stuckenrath et al., 1966, p. 348–385
	88**	Charred fat	*Tanfield (Tanfield Valley)*	M. Maxwell	Stuckenrath et al., 1966, p. 348–385
	88**	Charred fat	*Nanook (Tanfield Valley)*	M. Maxwell	Crane and Griffen 1966, p. 274–279
	88**	Charred fat	*Tanfield (Tanfield Valley)*	M. Maxwell	Crane and Griffen 1966, p. 274–279
	88**	Seal skin, caribou	*Nanook (Tanfield Valley)*	M. Maxwell	Wilmeth, 1969
	88**	*Salix* sp.	*Nanook (Tanfield Valley)*	M. Maxwell	Wilmeth, 1969
	88**	Sod, twigs	*Tanfield (Tanfield Valley)*	M. Maxwell	Kigoshi et al., 1969, p. 245–326
	88**	Charred fat	Midden *Tanfield (Tanfield Valley)*	M. Maxwell	Lowdon et al., 1969
	88**	Charred fat	*Tanfield (Tanfield Valley)*	M. Maxwell	Crane and Griffen 1966, p. 274–279
	88**	Sod	*Nanook (Tanfield Valley)*	M. Maxwell	Wilmeth, 1969; Maxwell, 1973
	88**	Charred fat	*Kemp (Tanfield Valley)*	M. Maxwell	Crane and Griffen 1966, p. 274–279
	88**	Charred fat	*Avinga (Tanfield Valley)*	M. Maxwell	Crane and Griffen 1966, p. 274–279; Maxwell, 1973
	88**	Baleen	*Nanook (Tanfield Valley)*	M. Maxwell	Wilmeth, 1969
	88**	Driftwood	Midden *Kemp (Tanfield Valley)*	M. Maxwell	Lowden et al., 1969
	88**	Charred fat	*Nanook (Tanfield Valley)*	M. Maxwell	[12]Morlan 2000.09.05
	88**	Plant material	*Nanook (Tanfield Valley)*	M. Maxwell	Stuckenrath et al., 1966, p. 348–385
	88**	Sod	*Nanook (Tanfield Valley)*	M. Maxwell	[12]Morlan 2000.09.05
	88**	*Salix* sp., twigs	*Nanook (Tanfield Valley)*	M. Maxwell	Stuckenrath et al., 1966, p. 348–385
	88**	Charred fat	*Avinga (Tanfield Valley)*	M. Maxwell	Crane and Griffen 1966, p. 274–279; Maxwell, 1973

[7]For all material for which isotopic fractionation values are available, ages are conventionally corrected to a $\delta^{13}C$ = -25‰ PDB (i.e. no marine reservoir correction applied to marine samples). Values have been estimated by R. Morlan (*see* footnote 12) for a number of samples in CARD and given the suffix e. ? = Value estimated by author.
[8]For some sites, the published co-ordinates have been revised on the basis of later maps.
[9]Published values are shown, except: * from other than primary published source; ** estimate from regional values; n/a = marine limit not applicable.
[10]*A: Astarte* sp., *A.s.: Astarte striatus*, *B: Balunus* sp., *C.c.: Clinocardium ciliatum*, *C.i.: Chlamys islandicus*, *H.a.: Hiatella arctica*, *Hem.: Hemithyris*, *L.s.: Littorina saxatilis*, *Mac.: Macoma* sp., *Mac.b.: Macoma baltica*, *Mac.c.: Macoma calcarea*, *Mya: Mya* sp., *Mya t.: Mya truncata*, *P.: Portlandia* sp., *P.a.: Portlandia arctica*, *Pec.: Pectin* sp., *S.g.: Serripes groenlandicus*, *V.d.: Volsella demissa*, *Y.g.: Yoldia glacialis*, *Y.s.: Yoldia sapotilla*. Names underlined and italicized are dated molluscs, names italicized only are other species present.
[11]Borden numbers of archaeological sites. *Sandy:* KdDq-2, *Tanfield*: KdDq-7, *Avinga*: KdDq-8, *Kemp*: KdDq-8-2 (sic), *Kakela*: KdDq-8-3, *Nanook*: KdDq-9-1,2, *Loon*: KdDq-10, *Closure*: KdDq-11, *Site 13*: KdDq-13, *Kiluktee*: KdDq-19, *Annawak*: KeDr-1 (sic), Killilugak: KeDr-3 (sic), *Shaymarc*: KkDn-2.
[12]Morlan, R., 2000.09.05: Canadian Archaeological Radiocarbon Database; http://www.canadianarchaeology.com/radiocarbon/card/crd.htm

Table 1 (cont.)

Lab. Id.[1]	Method[2]	Uncorrected age[3]	$\delta^{13}C$[4]	Corrected age (GSC)[5]	Corrected age (INSTAAR)[6]	Normalized age[7]	Lat. ′W[8]	Long. ′E[8]	Easting	Northing	Elev. (m a.s.l.)
GSC-708	C	1790 ± 130					62°34′	68°52′	506854	6937117	38
M-1533	C	1670 ± 150	-23e			1690 ± 150e	62°40.5′	69°31.1′	474300	6956500	4
M-1529	C	1470 ± 110	-25e			1470 ± 110e	62°36.8′	69°31.3′	473100	6942300	4
GaK-1285	C	1400 ± 80	-25e			1400 ± 80e	62°39.2′	69°34.4′	470570	6947300	12
GSC-591	C	680 ± 180					62°51′	69°50′	457572	6968952	76
GaK-1288	C	580 ± 80	-25e			580 ± 80e	62°39.2′	69°34.4′	470570	6947300	12
GSC-639 inorg	C	0 ± 130					63°10′	70°53′	405155	7005352	-12
GSC-639 org	C	0 ± 150					63°10′	70°53′	405155	7005352	-12
GSC-659 inorg	C	10 ± 130					63°10′	70°53′	405155	7005352	-12
GSC-659 org	C	0 ± 200					63°10′	70°53′	405155	7005352	-12
FROBISHER BAY											
QC-903	C	9875 ± 130					63°15.5′	68°10.6′	541400	7014300	27
AA-15125	AMS			9065 ± 100	9015 ± 100	9465 ± 100	63°12.4′	68°03.7′	547500	7018500	52
AA-15124	AMS			9060 ± 75	9010 ± 75	9460 ± 75	63°13.4′	67°57.2′	552500	7011000	17
AA-17861	AMS			8955 ± 75	8905 ± 75	9355 ± 75	63°26.2′	68°25.4′	528800	7034100	28
AA-15131	AMS			8935 ± 75	8885 ± 75	9335 ± 75	63°26.2′	68°25.4′	528800	7034100	28
GSC-5895	C	8850 ± 110	0.69	8860 ± 110	8820 ± 55	9260 ± 110	63°13.2′	68°13.9′	539000	7010000	66
AA-15127	AMS			8820 ± 75	8770 ± 75	9220 ± 75	63°15.4′	68°10.6′	541300	7014300	11
GSC-3157	C	8690 ± 120	0.86	8710 ± 120		9110 ± 120	63°13′	68°13′	538600	7010300	82
AA-16403	AMS			8700 ± 80	8650 ± 80	9100 ± 80	63°24.9′	68°26.2′	528200	7031700	4
AA-15126	AMS			8630 ± 75	8580 ± 75	9030 ± 75	63°13.0′	68°13.3′	539000	7010000	64
GSC-3666	C	8560 ± 100	1.5	8590 ± 100		8990 ± 100	63°15.5′	68°11′	541001	7014435	25
GX-8159	C		0.8	8450 ± 190		8850 ± 190?	63°39′	68°06′	544400	7057600	39
GSC-462	C	8230 ± 240					63°23.5′	68°25′	529152	7029164	87
GX-8696	C	8225 ± 450					63°37′	68°11′	540570	7054510	1
QC-904	C	7985 ± 130					63°15.3′	68°16.9′	536100	7013900	32
AA-15123	AMS			7950 ± 70	7900 ± 70	8350 ± 70	63°38.5′	68°06.5′	544200	7057400	16
AA-15130	AMS			7925 ± 75	7875 ± 75	8325 ± 75	63°21.7′	68°22.3′	531500	7025800	18
QC-905	C	7800 ± 150					63°41.6′	68°15.5′	536700	7062800	5
AA-15128	AMS			7760 ± 70	7710 ± 70	8160 ± 70	63°15.4′	68°19.5′	533900	7014200	38
AA-15129	AMS			7655 ± 70	7605 ± 70	8055 ± 70	63°15.4′	68°19.6′	533800	7014100	30
Beta-1872	C	7595 ± 130					63°26 10′	68°30′	525000	7034400	15
QC-902	C	7510 ± 320					63°42′	68°14′	537800	7063300	34
GSC-2771	C	7380 ± 220					63°43′	68°15′	537056	7065463	11
QC-901	C	7340 ± 135					63°42.7′	68°17.8′	534800	7064800	13
Beta-1871	C	7140 ± 115					63°25′	68°27′	528000	7031900	14
GX-8160	C		1.1	7080 ± 175		7480 ± 175?	63°44. 5′	68°36′	521000	7069000	16
GSC-5903	C	7060 ± 120		7080 ± 120	7040 ± 60	7480 ± 120	63°36.6′	68°10.4′	541000	7053700	1
GSC-464	C	6750 ± 170					63°43.5′	68°27.5′	526755	7066287	15
GSC-533	C	6440 ± 160					63°45′	68°32′	523030	7069044	3
GX-8695	C	6430 ± 225					63°37′	68°11′	540570	7054510	2
GSC-503	C	6140 ± 170					63°43.5′	68°27.5′	526755	7066287	15
GSC-6204	C	5420 ± 90	-24.4			5420 ± 90	63°05.25′	69°10.83′	490881	6995153	250
AA-6526	AMS					4905 ± 100	63°39′	68°21′	532191	7057980	15.5
GSC-6208	C	4440 ± 70	-25.1			4440 ± 70	63°05.25′	69°10.83′	490881	6995153	250
GSC-849	C	4140 ± 130	-23e			4160 ± 135e	63°43.5′	68°32.5′	521385	7069032	15
GSC-6226	C	3660 ± 60	-25.4			3650 ± 60	63°05.25′	69°10.83′	490881	6995153	250
AA-6525	AMS					3605 ± 75	63°39′	68°21′	532191	7057980	15.5
GX-8385	C					2575 ± 140	63°42′	68°16′	534200	7064300	<30
Beta-1087	C	2035 ± 70					63°41′	68°16′	534200	7064300	<30
Beta-1622	C	1460 ± 70					63°41′	68°16′	534200	7064300	<30
GX-8384	C	1345 ± 135					63°42′	68°16′	534200	7064300	<30
GX-8380	C	955 ± 130					63°46′	68°42′	514797	7070852	17
Beta-1086	C	905 ± 100					63°41′	68°16′	534200	7064300	<30
GX-8383	C	905 ± 130					63°42′	68°16′	534200	7064300	<30
AECV-1708C	C					880 ± 50	63°45.7′	68°41′	515600	7070200	10
AECV-1349C	C					740 ± 70	63°45.7′	68°41′	515600	7070200	16
AECV-1350C	C					740 ± 80	63°45.7′	68°41′	515600	7070200	16
AA-6524	AMS					970 ± 150	63°39′	68°21′	532191	7057980	15.5
AECV-1348C	C					550 ± 60	63°45.7′	68°41′	515600	7070200	6
AECV-1351C	C					490 ± 70	63°45.7′	68°41′	515600	7070200	8
GX-8381	C	475 ± 125					63°46′	68°42′	514797	7070852	17
GSC-467	C	440 ± 150					63°33.5′	68°45′	512421	7047627	21
GX-8382	C	420 ± 125					63°42′	68°16′	534200	7064300	<30

[1]Identification numbers with * indicate the dates for that sample are suspect.
[2]C = conventional radiocarbon methods. AMS = accelerator mass spectroscopy.
[3]Laboratory/machine age uncorrected for sample isotopic fractionation or derivation of published age not known.
[4] $^{13}C/^{12}C$ ratios where known. For a number of samples in the Canadian Archaeological Radiocarbon Database (CARD), values have been estimated by R. Morlan (*see* footnote 12). These are given the suffix e.
[5]Age of marine organism, corrected following GSC convention, for fractionation to a $\delta^{13}C$ = 0‰ PDB. This is equivalent to subtracting a marine reservoir effect of 400 years, which is what is done if a normalized age is available.
[6]Normalized age corrected for a reservoir effect of 450 years, which is the convention of the Institute of Arctic and Alpine Research, University of Colorado. A few dates used by INSTAAR were converted from GSC corrected dates using a reservoir correction of 440 years. GSC error terms are halved by INSTAAR to give roughly a 1 sigma value.

Min. water depth	Marine limit[9] (m)	Material[10]	Site[11] italics = archeological site	Collector	Reference
	n/a	Organic debris	Under solifluction	W. Blake	Lowden and Blake, 1968
	86**	Charred fat	*Killuktee*	M. Maxwell	Crane and Griffen 1966, p. 274–279
	90**	Charcoal	*Sandy (Juet I.)*	M. Maxwell	Crane and Griffen 1966, p. 274–279
	88**	Sod	*Nanook (Tanfield Valley)*	M. Maxwell	Wilmeth, 1969
	n/a	Peat	Under solifluction	W. Blake	Lowden et al., 1967
	88**	*Salix* sp.	*Nanook (Tanfield Valley)*	M. Maxwell	Wilmeth, 1969
	n/a	Live molluscs *L.s.*	Modern marine	W. Blake	Blake, 1988
	n/a	Live molluscs *L.s.*	Modern marine	W. Blake	Blake, 1988
	n/a	Live molluscs *L.s.*	Modern marine	W. Blake	Blake, 1988
	n/a	Live molluscs *L.s.*	Modern marine	W. Blake	Blake, 1988
FROBISHER BAY					
>30	119	Molluscs	Glaciomarine not in situ	M. Algus	Osterman et al., 1985
	121	Mollusc *P.*	Glaciomarine	W. Manley	Manley, 1995; Manley and Jennings, 1996
	123	Mollusc *Mac.c.*	Glaciomarine	W. Manley	Manley, 1995; Manley and Jennings, 1996
>42	120*	Mollusc *Mac.c.*		W. Manley	Manley, 1995; Manley and Jennings, 1996
>42	120*	Mollusc *Mac.c.*	Glaciomarine	W. Manley	Manley, 1995; Manley and Jennings, 1996
	129	Molluscs *H.a.*	Glaciomarine	W. Manley	Manley, 1995; Manley and Jennings, 1996
	114	Mollusc *P.*	Glaciomarine	W. Manley	Manley, 1995; Manley and Jennings, 1996
	>104	Molluscs *H.a.*, *A.s.*		E. Lind	Lind, 1982; Blake, 1982; Andrews and Short, 1983
	120*	Mollusc *P.a.*	Glaciomarine	W. Manley	Manley, 1995; Manley and Jennings, 1996
	129**	Mollusc *H.a.*	Glaciofluvial	W. Manley	Manley, 1995; Manley and Jennings, 1996
	114**	Molluscs *H.a.*	Glaciomarine	J. Jacobs & W. Mode	Blake, 1988
>42	119	Molluscs	Nearshore?	W. Mode & J. Jacobs	Andrews and Short, 1983; Jacobs et al., 1985b
	103	Molluscs *Mac.b.*, *Y.g.*, *H.a.*	Glaciomarine?	W. Blake & F. Synge	Blake, 1966; Lowdon et al., 1967
	<90	Bulk organics	Lake core into marine sediments	J. Jacobs	Squires, 1984
>46	119**	Molluscs	Deltaic	M. Algus & A. Colvill	Andrews and Short, 1983
>34	119*	Mollusc *Mac.c.*	Glaciofluvial	W. Manley	Manley, 1995; Manley and Jennings, 1996
>21	122	Mollusc *P.a.*	Glaciomarine	W. Manley	Manley, 1995; Manley and Jennings, 1996
	43	Molluscs	Marine	M. Algus & A. Colvill	Jacobs et al., 1985b
	48-119	Mollusc *P.*	Glaciomarine	W. Manley	Manley, 1995; Manley and Jennings, 1996
>48	48-119	Mollusc *H.a.*	Glaciofluvial	W. Manley	Manley, 1995; Manley and Jennings, 1996
	88	Molluscs *H.a.*, *Mac.c.*	Marine	E. Lind	Lind, 1982; Andrews and Short, 1983
	43*	Molluscs		M. Algus	Andrews and Short, 1983
>14	43*	Molluscs *Mya t.*, *Mya*, *Mac., P.*	Deltaic	L. Ostermann	Andrews and Short, 1983; Jacobs et al., 1985b
	40*	Molluscs	Deltaic	M. Algus	Andrews and Short, 1983
	88	Molluscs *P.a.*, *Mya t.*	Marine	E. Lind	Lind, 1982; Andrews and Short, 1983
	29	Molluscs *Mya t.*	Marine	W. Mode & J. Jacobs	Andrews and Short, 1983; Jacobs et al., 1985b
>18	96	Molluscs *Mya t.*	Glaciomarine	W. Manley	Manley, 1995; Manley and Jennings, 1996; McNeely, 2001
<30	30	Molluscs Mya t.	Deltaic	W. Blake & R. McNeely	Blake, 1966; Lowdon et al., 1967
<8	30	Molluscs *Mya t.*, *Mac. c.*, *H.a.*, *P.a., C.c., S.g., Y.s., V.d.*	Deltaic	B. Matthews	Blake, 1966; Lowdon et al., 1967; Matthews, 1967
	>9	Bulk organics	Lake core into marine sediments	J. Jacobs	Squires, 1984
<30	30*	Molluscs *Mya t.*, *H.a.*, *A.*	Deltaic	B. Matthews	Blake, 1966; Lowdon et al., 1967; Matthews, 1967
	n/a	Plant material	Fluvial	D. Hodgson	This report
	n/a	Humic acids	Lake core	G. Miller & M. Abbott	Abbott, 1991; Miller 1992; Kaufman and Williams, 1992
	n/a	Plant material	Fluvial	D. Hodgson	This report
	30	Charred fat	Midden *(Shaymarc)*	M. Maxwell	Lowdon et al., 1970; Maxwell, 1973
	n/a	Plant material	Fluvial	D. Hodgson	This report
	n/a	Humic acids	Lake core	G. Miller & M. Abbott	Abbott, 1991; Miller 1992; Kaufman and Williams, 1992
	n/a	Peat	Peat	J. Jacobs	Andrews and Short, 1983; Jacobs et al., 1985b
	n/a	Peat	Peat	J. Jacobs	Short and Jacobs, 1982; Andrews and Short, 1983; Jacobs et al., 1985b
	n/a	Peat	Peat	J. Jacobs	Short and Jacobs, 1982; Andrews and Short, 1983; Jacobs et al., 1985b
	n/a	Peat	Peat	J. Jacobs	Andrews and Short, 1983; Jacobs et al., 1985b
	n/a	Peaty sand	Plants & eolian?	J. Jacobs	Andrews and Short, 1983; Jacobs et al., 1985b
	n/a	Peat	Peat	J. Jacobs	Short and Jacobs, 1982; Andrews and Short, 1983; Jacobs et al., 1985b
	n/a	Peat	Peat	J. Jacobs	Andrews and Short, 1983
	n/a	Bone *(Rangifer tarandus)*	*Tungatsivvik*	D. Stenton	Manley and Jennings, 1996
	n/a	Bone *(Rangifer tarandus)*	*Tungatsivvik*	D. Stenton	Manley and Jennings, 1996
	n/a	Wood	*Tungatsivvik*	D. Stenton	Manley and Jennings, 1996
	n/a	Humic acids	Lake core	G. Miller & M. Abbott	Abbott, 1991; Miller 1992; Kaufman and Williams, 1992
	n/a	Bone *(Rangifer tarandus)*	*Tungatsivvik*	D. Stenton	Manley and Jennings, 1996
	n/a	Bone (*Rangifer tarandus*)	*Tungatsivvik*	D. Stenton	Manley and Jennings, 1996
	n/a	Peaty sand	Plants & eolian?	J. Jacobs	Andrews and Short, 1983
	n/a	Molluscs *H.a.*, *Mya*	Beach	W. Blake	Lowdon et al., 1967
	n/a	Peat	Peat	J. Jacobs	Andrews and Short, 1983

[7]For all material for which isotopic fractionation values are available, ages are conventionally corrected to a $\delta^{13}C$ = -25‰ PDB (i.e. no marine reservoir correction applied to marine samples). Values have been estimated by R. Morlan (*see* footnote 12) for a number of samples in CARD and given the suffix e. ? = Value estimated by author.
[8]For some sites, the published co-ordinates have been revised on the basis of later maps.
[9]Published values are shown, except: * from other than primary published source; ** estimate from regional values; n/a = marine limit not applicable.
[10]*A:* *Astarte* sp., *A.s.*: *Astarte striatus*, *B:* *Balunus* sp., *C.c.:* *Clinocardium ciliatum*, *C.i.:* *Chlamys islandicus*, *H.a.:* *Hiatella arctica*, *Hem.:* *Hemithyris*, *L.s.:* *Littorina saxatilis*, *Mac.:* *Macoma* sp., *Mac.b.:* *Macoma baltica*, *Mac.c.:* *Macoma calcarea*, *Mya:* *Mya* sp., *Mya t.:* *Mya truncata*, *P.:* *Portlandia* sp., *P.a.:* *Portlandia arctica*, *Pec.:* *Pectin* sp., *S.g.:* *Serripes groenlandicus*, *V.d.:* *Volsella demissa*, *Y.g.*: *Yoldia glacialis*, *Y.s.:* *Yoldia sapotilla*. Names underlined and italicized are dated molluscs, names italicized only are other species present.
[11]Borden numbers of archaeological sites. *Sandy:* KdDq-2, *Tanfield*: KdDq-7, *Avinga*: KdDq-8, *Kemp*: KdDq-8-2 (sic), *Kakela*: KdDq-8-3, *Nanook*: KdDq-9-1,2, *Loon*: KdDq-10, *Closure*: KdDq-11, *Site 13*: KdDq-13, *Kiluktee*: KdDq-19, *Annawak*: KeDr-1 (sic), Killilugak: KeDr-3 (sic), *Shaymarc*: KkDn-2.
[12]Morlan, R., 2000.09.05: Canadian Archaeological Radiocarbon Database; http://www.canadianarchaeology.com/radiocarbon/card/crd.htm

SURFICIAL MATERIALS AND QUATERNARY LANDFORMS

Bedrock

Units mapped on land by St-Onge et al. (1999b, c, d, e, f, g, h) and offshore by MacLean et al. (1986) and Sanford and Grant (2000) are shown on Figure 3. For this report, bedrock is grouped into five broad categories by hardness, which is a major control on susceptibility to weathering. They are listed below from least to most resistant.

Limestone (unit Ol)

Northwest of the head of Frobisher Bay, several small outliers of the Ordovician Frobisher Bay and Amadjuak formations of the southeast Arctic Platform are composed of lime mud that outcrops as light grey, frost-rived rock to pebble-size, angular clasts and silt. Similar age limestone underlies Hudson Strait offshore from the map area. Erratics from terrestrial and marine outcrops of platform rocks commonly stand out on shield rocks and till by nature of their white to buff weathered surface; however, they frost rive and chemically weather much faster than most shield rocks.

Clastic and metasedimentary rocks (unit Ps)

Semipelite, pelite, and psammite; minor calc-silicate, quartzite, and monzogranite are the dominant rock types.

Extensive outcrop to narrow belts occur on the southwest flank of Meta Incognita Peninsula, in the Paleoproterozoic Sugluk Group, Lake Harbour Group, and Blandford Bay Assemblage. They are a minor presence farther north in the Cumberland batholith. Outcrops of metasedimentary rocks vary from buff or rust, frost-rived competent rock to recessive units of pebble- to granule-size clasts in ferruginous sand or silt matrix.

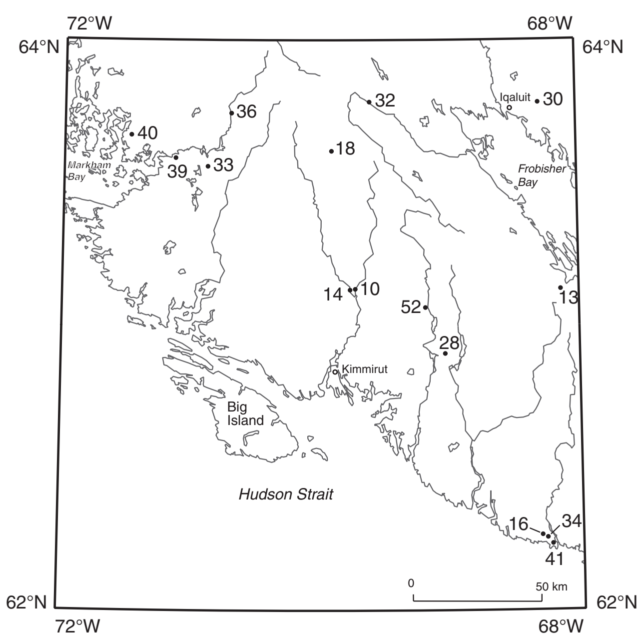

Figure 9. Locations of photographs in this report.

Marble (unit Pc)

Belts of marble and calc-silicate rocks are numerous between Markham Bay and Kimmirut and scattered elsewhere on the southwest flank of Meta Incognita Peninsula. The marble is mostly part of the Paleoproterozoic Lake Harbour Group. The distinctive white rock commonly weathers to 1 m or more depth of sandy granular sediment (pea gravel) with core stones (Fig. 9, 10). It is generally recessive and pitted by lakes.

Tonalite and monzogranite gneiss and quartzite (unit APt)

Orthogneiss bodies occur throughout the map area, though note that rocks of the Cumberland batholith are classified separately (*see* 'Monzogranite (unit PCg)' section below). They

***Figure 10.** Light-toned, weathered marble outcrop in foreground (person circled for scale) surrounded by psammite. Light-toned, gravelly sand outwash terraces of Soper River in centre, tonalite in background; (intersection of Soper and Livingstone rivers, Fig. 9). Photograph by D.A. Hodgson. GSC 2001-379A*

are mostly part of the Archean Superior craton and Paleoproterozoic Ramsay River orthogneiss and Narsajuaq arc. They outcrop as intact and fractured buff rock, or as frost-rived block fields (angular or subangular large clasts) and sand or silty sand. Despite their competency, in the map area microrelief on exposed surfaces is generally rough; uncovered glacial striations and grooves do not appear to survive more than a few years of subaerial processes.

Monzogranite (unit Pg)

The Paleoproterozoic Cumberland batholith outcrops over much of the north and east of the map area. The intact to fractured tan to pink rock and frost-rived block fields are more resistant to subaerial processes than monzogranite of other (older) units.

Units Ol, Pc, and Pg are relatively homogeneous and massive. Units Ps and APt can display numerous minor ridges and scarps resulting from differential weathering. Glacier flow over units Ps, APt, and Pg has scoured some zones exposing relatively smooth, unfractured rock. Wave washing during marine overlap has left outcrop more common below the postglacial marine limit than immediately above. Areas mapped as bedrock can include up to a 40% cover of till, block fields, or colluvium, with very minor fluvial deposits, muck, or raised marine nearshore and shoreline deposits.

Subglacial bedrock landforms

The classification used here follows Benn and Evans (1998, Table 9.1; *after* Sugden and John (1976)).

Landscape-scale forms

In a study relating bedrock roughness to degree of glacial scouring and hence basal glacier temperature, Sugden (1978) measured from topographic maps of Canada the number of lakes of area 0.5–2.0 km^2. The results showed a moderate number of lake basins (50–100 per 400 km^2) in southeast Baffin Island, though elsewhere in the paper, Sugden (1978) indicated heavy scouring on Meta Incognita Peninsula except in the centre. For southeast Baffin Island, Muller (1980) used per cent lake area in 400 km^2 units as an indication of lake density. Water areas were obtained by scanning a LANDSAT image. The results showed lowest (<5%) lake cover on central Meta Incognita Peninsula, and highest cover (>10%, locally >20%) on the Hudson Strait coast. Higher values also were present on Bird's (1958) Baffin Surface. Andrews et al. (1985) measured all lake areas (for the map area) in a 625 km^2 grid, again showing lowest values (<5%) on central Meta Incognita Peninsula and highest on the Hudson Strait coast (>30%).

Lake area is not a satisfactory measure of rock roughness in the map area because some large lakes are enclosed by till or outwash. To reduce the influence of these larger lakes, the number of lakes (any size) per 25 km^2 was counted on 1:250 000 topographic maps (Fig. 11). This shows no lakes to twenty-five lakes per 25 km^2 still with a similar pattern to Muller (1980) and Andrews et al. (1985) — i.e. high density along parts of the Hudson Strait shore, especially immediately west of Kimmirut on an extensive outcrop of metasedimentary rocks where ribbed terrain results from differential erosion of the sedimentary rocks. Other highs occur around obvious glacial outlets such as Markham Bay and Crooks Inlet, and less obvious locations such as parts of Big Island and flanking the middle reaches of Ramsay River. Moderate densities are present elsewhere along the Hudson Strait coast, except low in the centre of extensive thick till. The southeast, where cross-strait ice moved onshore, does not stand out in this criterion. Patches of moderate density in otherwise low-density areas occur around Frobisher Bay, despite this being a known glacial outlet (though on the relatively homogeneous Cumberland batholith with much large-scale topographic irregularity); and locally on the high elevation 'Baffin Surface', at the east edge of the map area, distal to the Frobisher Bay Moraine System. More than a third of the area has fewer than five lakes per 25 km^2, mainly in the centre of the peninsula on rock and till.

Megascale erosional forms

Cirques. On the basis of their erosional form, 64 cirques were identified in the map area (Fig. 12). Many contain overdeepened basins but none contain glaciers and no cirque glacier deposits were observed (Fig. 13). The few visited faced down the regional ice flow, hence striations in and around the cirques accord with that flow. Colvill (1982) reported that a cirque due west of Cape Rammelsberg contained glacial deposits unrelated to cirque erosion and thus postdated cirque glaciation. Backwall scarps range in plan from shallow arcs to almost-enclosed circles, with semicircles the norm. Widths vary from 300 m to 2400 m, mean 1000 m;

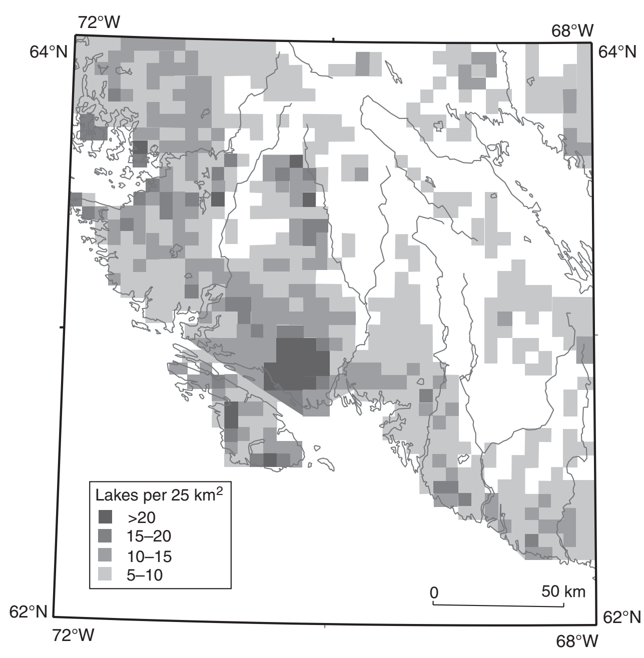

Figure 11. *Lake density: number of lakes of any size in 25 km^2 squares, as an indicator of landscape roughness. Measured from 1:250 000-scale topographic maps.*

backwall heights average slightly over 100 m. Most are eroded into orthogneiss or monzogranite (units APt and Pg), though some cut metasedimentary rocks (unit Ps).

Two distinct clusters are present on western and central Meta Incognita Peninsula (Fig. 12). Over half the cirques lie 5–20 km inland (southwest) of Frobisher Bay, on the eastern rim or summit of the upland surface; a smaller population lies close to sea level along the Hudson Strait coast or connected inlets. A majority of the upland cirques (36, or 56% of all cirques) are east of the peninsula height of land, and, not surprisingly, 75% of them face between 020° and 090°; the remaining nine are oriented 110°–320°. These cirques have a mean backwall top 600 m a.s.l. and a floor at 480 m. Of the twelve upland cirques west of the height of land, more than half face 200°–250°; mean backwall tops are 630 m and floors 540 m. Most of the sixteen in the Hudson Strait coast population also face 200°–250°, but their backwall tops are at a mean 190 m and floors 50 m (some are drowned: e.g. at Henderson Harbour).

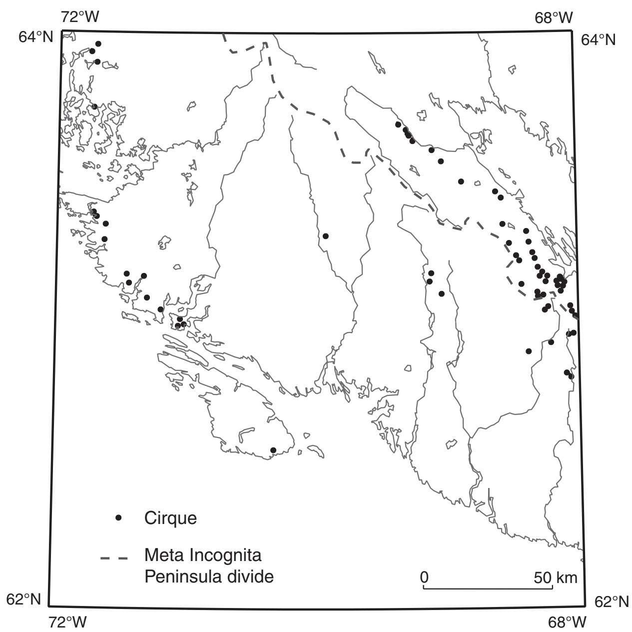

Figure 12. *Location of recognized cirques.*

Mercer's (1956) contention that no Meta Incognita Peninsula cirques lie within the limits of the last regional glaciation is disproved by the presence of several cirques proximal to the Frobisher Bay Moraine System, i.e. distribution crosscuts deglacial margins of the last glaciation. It is clear that topography (upland, northeast aspect) is the primary control for the larger population. The Hudson Strait population also appears to have developed where relief is high. The most spectacular cirques on the peninsula are developed in the highest terrain (Everett Mountains), 50 km down Frobisher Bay from the map area, where backwall heights reach 800 m. Some northeast-facing cirques are occupied by glaciers and others are free of ice, but with floors below sea level (Mercer, 1956).

Rock sags. Rock sags, probably initiated by glacier and meltwater deepening of valleys cut in rock with appropriate strength, bedding planes, and jointing, were observed on airphotos at several sites near the junction of Soper and Livingstone rivers (Fig. 14). An investigated sag covering 250 m by 250 m developed on a 15° slope in metasedimentary rocks. Transverse cracks to 5 m wide by 5 m deep appear to align with the local joint pattern.

Mesoscale erosional forms

Ice-streamlined rock ridges or troughs upwards of several hundred metres long were identified on airphotos in two main clusters: around the head of Frobisher Bay in a drawdown pattern (in association with drumlins), and southwest-trending around Markham Bay, extending to islands forming the margin of Hudson Strait (Fig. 15). As with cirques, development is mostly restricted to resistant rock units. Roches

Figure 13. *Northeast-facing cirque near the height of land (800 m), 3 km southwest of Hidden Bay (off Frobisher Bay). Width of the lake is 500 m; height of the backwall is over 100 m. Photograph by D.A. Hodgson. GSC 2001-379B*

Figure 14. *Rock-sag failure scarps (5 m high). Tonalite at junction of Soper and Livingstone rivers. Photograph by D.A. Hodgson. GSC 2001-379C*

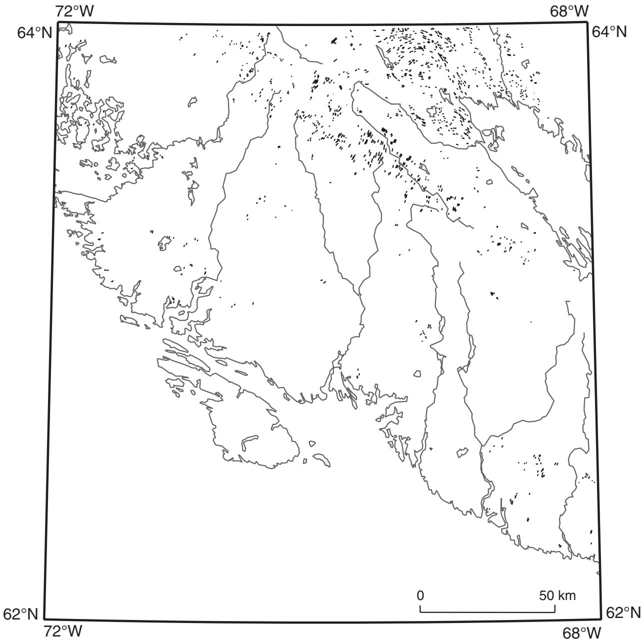

Figure 15. Glacier-moulded bedrock and streamlined till, including rock drumlins, drumlins, and till lineations (not to scale).

moutonnées, rock drumlins, and whalebacks are common in the same two clusters, but also were observed in the field elsewhere, including the flanks of Frobisher Bay, in the Frobisher Bay Moraine System, in Markham Bay, and adjacent to Hudson Strait in the southeast of the map area.

Microscale erosional forms

Striations, grooves, and other small-scale forms are uncommon on most exposed rock surfaces in the map area, though relatively more common on Cumberland batholith granite around Frobisher Bay (where occurrence also could be related to scouring by a Frobisher Bay glacier). They are rare on marble and weaker metasedimentary rocks, even on surfaces protected by till. On many competent rocks, such as tonalite, microrelief on exposed surfaces is generally rough; uncovered striations do not appear to survive more than tens of years of subaerial processes or were never inscribed. Possibly a higher content of unstable elements, including iron (*see* 'Till geochemistry', below), increases weathering in the map area relative to some other parts of the shield (though paucity of exposed striations was observed by Gray (2001) on the south shore of Hudson Strait). Pyritic units are reported to be common in some of the metasedimentary rocks (M.R. St-Onge, pers. comm., 2000) These iron sulphide minerals, which after oxidation are the main source of acid in shield rocks, may be leached by the relatively high precipitation received by this area percolating through the coarse structure of the local till.

The method used to detect microscale forms was to find outcrop smooth to the touch adjacent to overlapping till and excavate a feathered edge. Even then, it was often necessary to brush and wet the surface and view against the sun to see striations (cf. Miller and Kauffman, 1990; Manley, 1995). For the majority of striation measurements, the sense of direction was not determined (bidirectional) due to poor preservation and conflicting evidence presented by fracture marks or cracks. In some cases, exposed grooves provided definitive ice-flow direction (Fig. 16). In order to determine regional flow patterns, an effort was made to find striations on regional topographic high points (Fig. 17). Numerous measurements were taken on some ground traverses, therefore the symbols on Figure 17 have been thinned compared to Maps 2042A–2048A. Where observations of the writer are scarce, striations from other sources are shown, mostly Manley (1995,1996) along the Hudson Strait coast east of Crooks Inlet, and Davison (1958) around Kimmirut, but also from Bell (1885, 1901b), Blake (1966), Lind (1983), Clark (1985), and bedrock geologists of the Geological Survey of Canada 'South Baffin Project'. A total of 305 observations were made for this study (168 on regional high points) and a further 126 by other observers have been compiled (Tables 2, 3).

The general pattern of striations along the north-central coast of Hudson Strait was established by Bell (1901b) and others to be a southwest flow, except southeast on southernmost Big Island. This study extends the southwest flow pattern across Markham Bay and inland to the peninsula fluvial divide — even east of the height of land in the Hone River area (Fig. 17). It also confirms Manley's (1995, 1996) determination of onshore flow from the south-southwest in the southeastern part of the report area. Manley found evidence of the latter flow as far west as Carew Bay, but did not establish an inland limit. In the present study, definite onshore striations, grooves, and whalebacks were found up to 20 km north of the mouth of Wight Inlet. The apparent reciprocity between this onshore flow and regional Meta Incognita Peninsula flows in the southeast is confusing. Regional flows

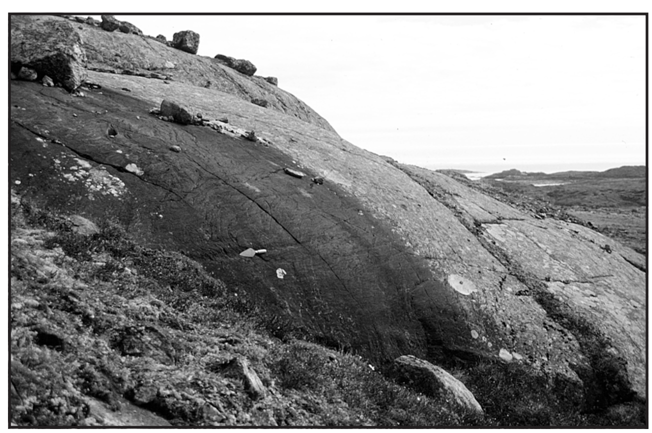

***Figure 16.** Ice-moulded grooves (trend indicated by trowel) in whaleback, west of Wight Inlet, 3 km inland from Hudson Strait (distant background). Direction of the photograph is 200°. The regional ice flow from Meta Incognita Peninsula, also 200°, would have flowed over rather than around the up-ice end of the outcrop. Therefore, the groove was eroded by the reciprocal (20°) onshore-flowing Labrador ice (possible Noble Inlet advance), wrapping around the 'tail' of the landform. Photograph by D.A. Hodgson. GSC 2001-379D*

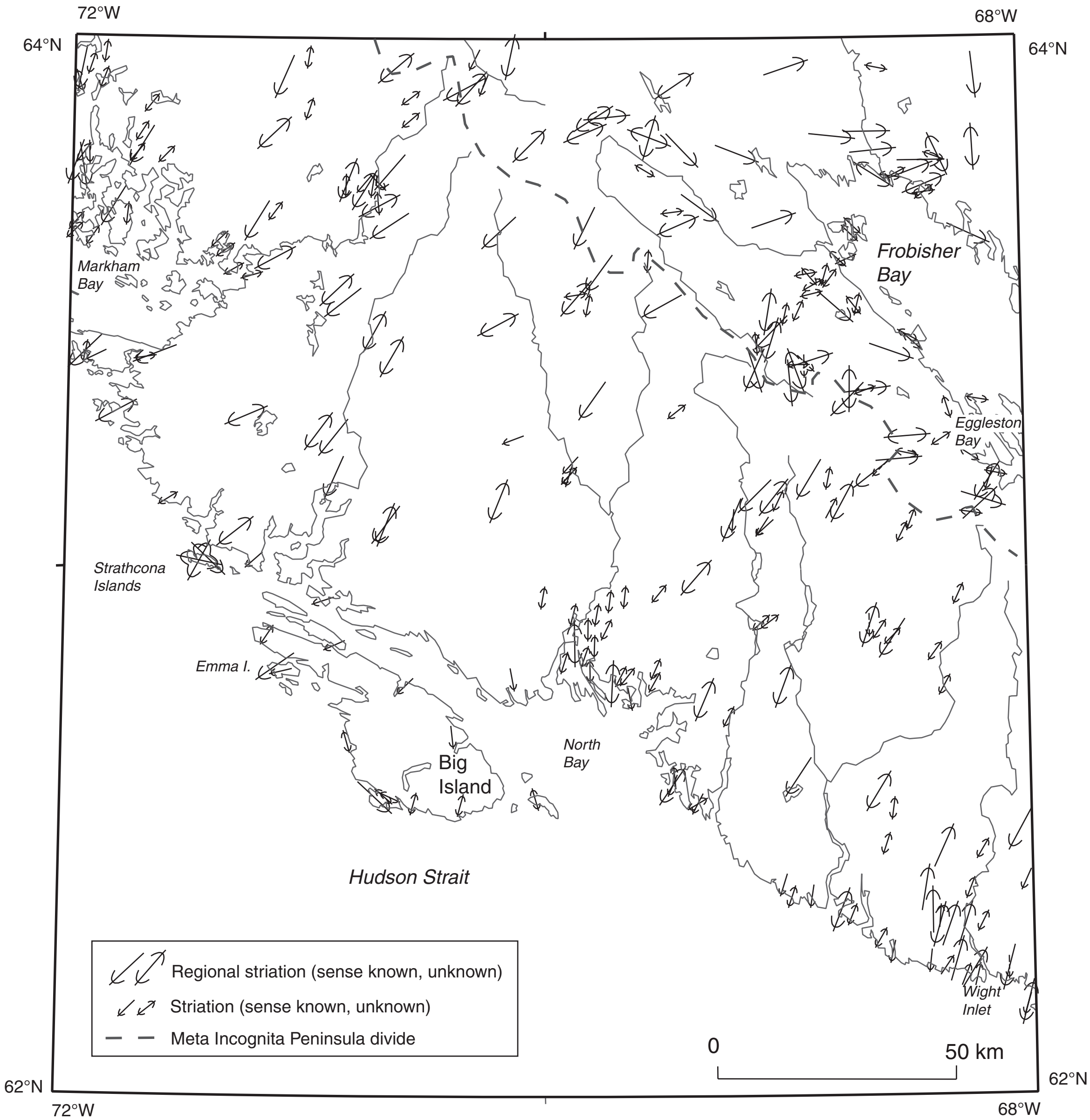

Figure 17. *Striation orientations and sense of direction, where known (concentrations of observations have been thinned). Regional striations measured on regional topographic high points. Some data* after *Davison (1958), Blake (1966), Lind (1983), Clark (1985), and Manley (1995).*

throughout the map area are uninterrupted by local topography such as the major south-trending valleys and the coastal upland southeast of Markham Bay, other than slightly convergent flows into Markham and North bays. Manley (1995) noted either downstrait flow or diverging ice from Crooks Inlet on Strathcona Islands, northwest of Big Island, where crosscutting striations provided no clear sense of direction. The present study found a similar pattern on adjacent Glencoe Island, though no evidence of anything but offshore flow on Emma Island, which is both farther from Crooks Inlet and closer to the centre of Hudson Strait.

For inner Frobisher Bay, a generally downbay (southeast) flow was reported by Blake (1966) and Colvill (1982). Additionally, Manley and Moore (1995) observed younger (than downbay) eastward-trending striations on mid-bay islands on the eastern margin of the map area, older eastward-trending striations on the south side of the bay at Eggleston Bay, and younger eastward-trending striations in, and proximal to, the Frobisher Bay Moraine System belt on Hall Peninsula. Observations for this report also found on Hall Peninsula southward striations distal to the Frobisher Bay Moraine System outer ridge and eastward flow proximal to Frobisher Bay Moraine System. On the west side of the bay, striations within a few kilometres of the shore are downbay (southeast), whereas towards the height of land ice flow is registered as flowing northeast or east, orthogonal to the shore. West and northwest of the head of the bay, striations (and till landforms) swing from northeast on uplands to southeast in lowlands.

Table 2. Striations measured for this study.

Identification	Zone	Easting	Northing	NTS	Regional flow[1]	Angle	Type[2]	Sense[3]	Till sample
HCA-95-2-8-7	19	394900	6972000	25 L					HCA-95-B1
HCA-95-3-8-14	19	427600	6943500	25 L					HCA-95-B2
HCA-95-4-8-1	19	472600	6989700	25 N					HCA-95-B3
HCA-95-5-8-1	19	456100	7008400	25 N		223	1	1	
HCA-95-5-8-2	19	456200	7008100	25 N		215	1	2	
HCA-95-5-8-3	19	456100	7007700	25 N		203	1	2	
HCA-95-5-8-5Aa	19	455800	7006200	25 N		198	1	1	
HCA-95-5-8-5Ab	19	455800	7006200	25 N		223	1	2	
HCA-95-5-8-5Ba	19	455800	7006200	25 N		223	1	2	
HCA-95-5-8-5Bb	19	455800	7006200	25 N		203	1	2	
HCA-95-5-8-6	19	455600	7006000	25 N					HCA-95-B4
HCA-95-8-8-1A	19	459900	7046500	25 N		232	1	2	
HCA-95-8-8-1B	19	459900	7046500	25 N		222	1	2	
HCA-95-8-8-1C	19	459900	7046500	25 N		237	1	2	
HCA-95-8-8-2	19	459800	7044500	25 N		192	1	2	
HCA-95-8-8-3	19	459400	7044600	25 N		202	1	2	
HCA-95-8-8-4	19	457800	7044500	25 N		262	1	2	
HCA-95-9-8-1	19	452700	7046800	25 N					HCA-95-B5
HCA-95-10-8-1	19	460500	7047600	25 N		212	1	2	
HCA-95-10-8-2a	19	462800	7049000	25 N	x	217	1	1	
HCA-95-10-8-2b	19	462800	7049000	25 N		227	1	2	
HCA-95-10-8-3	19	463200	7048700	25 N		222	1	1	
HCA-95-10-8-5	19	463200	7046800	25 N	x	217	1	2	
HCA-95-10-8-9A	19	460400	7042300	25 N		192	1	2	
HCA-95-10-8-10	19	459900	7042200	25 N		227	1	2	
HCA-95-10-8-11	19	457900	7043800	25 N	x	222	1	2	
HCA-95-10-8-12	19	458700	7046700	25 N					HCA-95-B6
HCA-95-12-8-1	19	506700	7004600	25 N	x	212	1	1	HCA-95-B7
HCA-95-12-8-3	19	510800	7004800	25 N		192	1	2	
HCA-95-16-8-1	19	529400	7070100	25 N	x	70	1	1	
HCA-95-16-8-2	19	531500	7072200	25 N	x	90	1	1	
HCA-95-16-8-3	19	534300	7073000	25 N		110	1	2	
HCA-95-16-8-4A	19	535000	7073000	25 N		150	1	1	
HCA-95-16-8-4B	19	535000	7073000	25 N		155	1	1	
HCA-95-16-8-5	19	535000	7073400	25 N	x	155	1	2	
HCA-95-16-8-6	19	534100	7073300	25 N		115	1	2	
HCA-95-17-8-1	19	522200	7072900	25 N	x	90	1	1	
HCA-95-17-8-2	19	521400	7074400	25 N	x	85	1	1	
HCA-95-17-8-3	19	520600	7076700	25 N	x	80	1	1	
HCA-95-17-8-4	19	520200	7078400	25 N	x	90	1	1	
HCA-96-27-6-6	19	394103	7053634	25 M/11	x	243	1	2	
HCA-96-28-6-5	19	378473	7065131	25 M/11					HCA-96-B8
HCA-96-29-6-7	19	365662	7077598	25 M/13	x	208	2	2	
HCA-96-29-6-8	19	366300	7078025	25 M/13	x	213	1	1	HCA-96-B9
HCA-96-30-6-1	19	360021	7065312	25 M/12	x	213	1	1	
HCA-96-30-6-4	19	362839	7063819	25 M/12					HCA-96-B10
HCA-96-30-6-5	19	362979	7063609	25 M/12		188	1	2	HCA-96-B11
HCA-96-1-7-2	19	353919	7094580	25 M/13	x	193	1	1	
HCA-96-1-7-3	19	354269	7094293	25 M/13					HCA-96-B12
HCA-96-1-7-4	19	355598	7094446	25 M/13	x	190	1	2	
HCA-96-1-7-4	19	355598	7094446	25 M/13	x	193	2	1	
HCA-96-1-7-6	19	358602	7092643	25 M/13		203	1	2	HCA-96-B13
HCA-96-3-7-2	19	382636	7039305	25 M/6					HCA-96-B14
HCA-96-4-7-1	18	630926	7057152	35 P/9		211	1	2	
HCA-96-4-7-2	18	631934	7056990	35 P/9		233	1	2	
HCA-96-4-7-3	18	632871	7056794	35 P/9					HCA-96-B15
HCA-96-4-7-4	18	633316	7056973	35 P/9	x	210	1	2	
HCA-96-4-7-5	18	633600	7056911	35 P/9	x	198	1	2	
HCA-96-4-7-7	18	636400	7056100	35 P/9		223	1	2	
HCA-96-5-7-3	19	390437	7061545	25 M/11	x	213	1	1	

[1]x = topographic high (regional ice flow)
[2]1 = striation; 2 = groove
[3]1 = flow direction known; 2 = not known

Table 2 (cont.)

Identification	Zone	Easting	Northing	NTS	Regional flow[1]	Angle	Type[2]	Sense[3]	Till sample
HCA-96-5-7-8	19	394394	7063537	25 M/11		218	1	2	HCA-96-B16
HCA-96-6-7-1	19	355164	7076807	25 M/13		180	1	1	HCA-96-B17
HCA-96-6-7-2	19	353940	7076745	25 M/13		218	1	2	
HCA-96-6-7-3	19	353580	7076427	25 M/13		173	1	2	
HCA-96-6-7-4	19	352381	7075758	25 M/13		208	1	1	
HCA-96-6-7-4	19	352381	7075758	25 M/13		188	1	1	
HCA-96-6-7-6	19	351717	7075119	35 P/16	x	185	1	2	
HCA-96-6-7-7	19	352221	7074750	25 M/13	x	201	1	1	HCA-96-B18
HCA-96-6-7-7	19	352221	7074750	25 M/13	x	175	1	1	
HCA-96-6-7-9	19	353808	7073906	25 M/13	x	173	1	1	
HCA-96-7-7-1	19	366150	7033112	25 M/5		263	1	2	HCA-96-B19
HCA-96-7-7-3	19	368200	7033764	25 M/5	x	250	1	1	
HCA-96-7-7-4	19	368620	7033567	25 M/5					HCA-96-B20
HCA-96-8-7-2	19	418548	7032104	25 M/7	x	211	1	2	
HCA-96-8-7-3	19	414971	7037517	25 M/7	x	210	1	2	HCA-96-B21
HCA-96-10-7-1	19	408094	7043245	25 M/10					HCA-96-B22
HCA-96-10-7-2	19	408333	7043826	25 M/10	x	233	1	1	
HCA-96-10-7-3	19	407126	7046536	25 M/10	x	228	1	2	
HCA-96-10-7-5	19	405881	7052303	25 M/10					HCA-96-B23
HCA-96-12-7-1	19	409964	7069800	25 M/10	x	203	1	2	HCA-96-B24
HCA-96-12-7-3	19	409445	7068692	25 M/10		183	1	2	
HCA-96-12-7-4	19	410221	7068763	25 M/10	x	203	1	2	
HCA-96-12-7-5	19	412128	7069248	25 M/10	x	223	1	2	
HCA-96-12-7-6	19	413322	7068955	25 M/10		221	1	1	
HCA-96-12-7-7	19	413395	7067641	25 M/10	x	213	1	2	HCA-96-B25
HCA-96-12-7-9	19	413815	7067418	25 M/10	x	210	1	2	
HCA-96-12-7-10	19	415127	7068423	25 M/10		190	1	1	
HCA-96-13-7-1	19	397191	7096116	25 M/14	x	207	1	2	HCA-96-B26
HCA-96-13-7-2	19	397440	7094334	25 M/14	x	208	1	2	
HCA-96-13-7-4	19	396842	7092049	25 M/14	x	205	1	1	
HCA-96-13-7-5	19	395864	7089841	25 M/14					HCA-96-B27
HCA-96-14-7-1	19	396229	6971825	25 L/14					HCA-96-B28
HCA-96-14-7-3	19	413338	6938483	25 L/10	x	134	1	1	HCA-96-B29
HCA-96-14-7-4	19	424082	6950312	25 L/9					HCA-96-B30
HCA-96-14-7-5	19	427475	6939537	25 L/9					HCA-96-B31
HCA-96-14-7-6	19	437735	6939978	25 L/9					HCA-96-B32
HCA-96-14-7-7	19	446848	6937963	25 L/9					HCA-96-B33
HCA-96-14-7-9	19	448317	6981547	25 L/16					HCA-96-B34
HCA-96-14-7-10	19	436174	6978883	25 L/16					HCA-96-B35
HCA-96-14-7-11	19	426004	6982014	25 L/16					HCA-96-B36
HCA-96-14-7-12	19	418068	6984879	25 L/15					HCA-96-B37
HCA-96-16-7-1	19	356759	7032627	25 M/5					HCA-96-B38
HCA-96-16-7-2	19	356334	7033067	25 M/5		243	1	2	
HCA-96-16-7-3	19	355690	7033697	25 M/5		245	1	1	HCA-96-B39
HCA-96-16-7-4b	19	353498	7034516	25 M/5		193	1	2	
HCA-96-16-7-4c	19	353350	7034541	25 M/5	x	227	1	1	
HCA-96-17-7-1	19	418482	7059906	25 M/10	x	238	1	1	HCA-96-B40
HCA-96-17-7-3	19	416492	7064232	25 M/10	x	243	1	2	HCA-96-B41
HCA-96-17-7-4	19	416436	7064988	25 M/10		166	1	1	
HCA-96-17-7-5	19	416231	7064714	25 M/10		176	1	2	
HCA-96-18-7-1	19	418792	7071269	25 M/15	x	222	1	1	HCA-96-B42
HCA-96-18-7-2	19	417786	7070322	25 M/15	x	203	1	2	
HCA-96-18-7-3a	19	416651	7070036	25 M/10		181	1	1	
HCA-96-18-7-3b	19	416398	7069782	25 M/10		178	1	2	
HCA-96-20-7-1	19	460965	7022007	25 N/5	x	216	1	1	HCA-96-B43
HCA-96-20-7-2	19	478881	7019425	25 N/6		233	1	2	HCA-96-B44
HCA-96-20-7-3	19	497505	7022866	25 N/6					HCA-96-B45
HCA-96-20-7-4	19	509297	7022842	25 N/7					HCA-96-B46
HCA-96-20-7-5	19	524726	7031615	25 N/8	x	110	1	1	HCA-96-B47
HCA-96-20-7-6	19	527745	7013588	25 N/8	x	266	1	2	HCA-96-B48

[1]x = topographic high (regional ice flow)
[2]1 = striation; 2 = groove
[3]1 = flow direction known; 2 = not known

Identification	Zone	Easting	Northing	NTS	Regional flow[1]	Angle	Type[2]	Sense[3]	Till sample
HCA-96-20-7-7	19	519859	7001570	25 N/2					HCA-96-B49
HCA-96-20-7-8	19	495136	7001216	25 N/3	x	226	1	1	HCA-96-B50
HCA-96-20-7-9	19	475386	6998278	25 N/3					HCA-96-B51
HCA-96-21-7-1	19	448562	7076456	25 M/16	x	226	1	2	HCA-96-B52
HCA-96-21-7-2	19	467321	7084786	25 N/13	x	248	1	2	HCA-96-B53
HCA-96-21-7-3	19	465097	7082184	25 N/13	x	231	1	2	
HCA-96-21-7-3	19	465097	7082184	25 N/13	x	265	1	2	
HCA-96-21-7-4	19	464215	7082379	25 N/13	x	248	1	2	
HCA-96-21-7-5	19	462203	7081939	25 N/13	x	238	1	2	
HCA-96-21-7-6a	19	460509	7080195	25 N/13	x	233	1	2	
HCA-96-21-7-6b	19	460508	7079998	25 N/13					HCA-96-B54
HCA-96-21-7-7	19	460403	7078896	25 N/13	x	248	1	2	
HCA-96-22-7-1	19	479533	7088676	25 N/14	x	57	1	2	HCA-96-B55
HCA-96-22-7-2	19	487607	7094540	25 N/14					HCA-96-B56
HCA-96-22-7-3	19	503249	7092214	25 N/15	x	72	1	1	HCA-96-B57
HCA-96-22-7-4	19	522365	7091958	25 N/15		102	1	2	HCA-96-B58
HCA-96-22-7-5	19	542879	7090110	25 N/16	x	174	1	1	HCA-96-B59
HCA-96-22-7-6	19	542431	7074836	25 N/16	x	177	1	2	HCA-96-B60
HCA-96-22-7-7	19	541390	7056508	25 N/9	x	115	1	1	HCA-96-B61
HCA-96-22-7-8	19	512813	7077473	25 N/15	x	97	1	1	HCA-96-B62
HCA-96-22-7-9	19	492593	7074038	25 N/14	x	112	1	1	HCA-96-B63
HCA-96-22-7-10	19	480921	7074886	25 N/14	x	137	1	1	HCA-96-B64
HCA-96-22-7-11	19	473997	7077696	25 N/13	x	282	1	2	
HCA-96-22-7-11	19	473997	7077696	25 N/13	x	112	1	2	
HCA-96-22-7-11	19	473997	7077696	25 N/13	x	197	1	2	
HCA-96-22-7-12	19	472961	7070721	25 N/13		122	1	2	
HCA-96-23-7-1	19	441682	7058075	25 M/9	x	228	1	1	HCA-96-B65
HCA-96-23-7-2	19	459927	7058757	25 N/12	x	207	1	1	HCA-96-B66
HCA-96-23-7-3	19	479726	7058940	25 N/11	x	247	1	2	HCA-96-B67
HCA-96-23-7-4	19	484538	7062609	25 N/11	x	127	1	1	HCA-96-B68
HCA-96-23-7-5	19	500165	7059748	25 N/11	x	72	1	1	HCA-96-B69
HCA-96-23-7-6	19	512961	7041221	25 N/7	x	132	1	1	HCA-96-B70
HCA-96-23-7-7	19	498581	7040341	25 N/6	x	10	1	2	HCA-96-B71
HCA-96-23-7-8	19	475992	7041880	25 N/11	x	242	1	1	HCA-96-B72
HCA-96-23-7-9	19	441255	7038523	25 M/8	x	243	1	2	HCA-96-B73
HCA-96-24-7-1	19	420482	7093410	25 M/15	x	231	1	2	HCA-96-B74
HCA-96-24-7-2	19	444768	7095357	25 M/16	x	193	1	2	HCA-96-B75
HCA-96-24-7-5	19	437185	7094831	25 M/16		208	1	1	HCA-96-B76
HCA-96-26-7-1	19	416170	7069249	25 M/10		171	1	1	
HCA-96-26-7-1	19	416170	7069249	25 M/10		136	1	1	
HCA-96-26-7-2	19	416531	7069221	25 M/10		178	1	1	
HCA-96-28-7-1	19	376143	6996296	25 M/3					HCA-96-B77
HCA-96-28-7-3	19	384625	6995704	25 M/3	x	233	1	2	HCA-96-B78
HCA-96-29-7-1	19	379445	6989048	25 M/3		278	1	1	
HCA-96-29-7-3	19	378844	6989925	25 M/3	x	315	1	2	HCA-96-B79
HCA-96-29-7-3	19	378844	6989925	25 M/3	x	275	1	2	
HCA-96-29-7-4	19	376911	6989631	25 M/3	x	283	1	2	HCA-96-B80
HCA-96-29-7-4	19	376911	6989631	25 M/3	x	210	1	2	
HCA-96-31-7-1	19	388531	7005120	25 M/3					HCA-96-B81
HCA-96-31-7-2	19	406670	7015601	25 M/7					HCA-96-B82
HCA-96-31-7-3	19	405844	7015210	25 M/7	x	220	1	1	
HCA-96-31-7-4	19	402712	7016585	25 M/7	x	218	1	2	
HCA-96-31-7-6	19	395082	7013059	25 M/3					HCA-96-B83
HCA-96-1-8-1	19	405823	7006670	25 M/2	x	205	1	1	HCA-96-B84
HCA-96-2-8-1	19	439079	7089454	25 M/16		203	1	1	
HCA-96-2-8-2	19	436390	7088709	25 M/16	x	223	1	2	
HCA-96-2-8-3	19	434820	7088638	25 M/16	x	243	1	1	HCA-96-B85
HCA-96-5-8-2	19	391935	6966687	25 L/14					HCA-96-B86
HCA-96-5-8-4	19	392581	6966754	25 L/14	x	236	1	1	
HCA-96-5-8-5a	19	393788	6965692	25 L/14		258	1	1	

Table 2 (cont.)

Identification	Zone	Easting	Northing	NTS	Regional flow[1]	Angle	Type[2]	Sense[3]	Till sample
HCA-96-5-8-5b	19	39395	696525	25 L/14	x	243	1	2	
HCA-96-6-8-1	19	394441	7080131	25 M/14	x	228	1	2	HCA-96-B87
HCA-96-7-8-1	19	389369	7030366	25 M/6					HCA-96-B88
HCA-96-7-8-2	19	387407	7020287	25 M/6	x	248	1	2	HCA-96-B89
HCA-96-7-8-3	19	378835	7008071	25 M/6					HCA-96-B90
HCA-96-7-8-4	19	359805	7021800	25 M/6	x	243	1	2	HCA-96-B91
HCA-96-7-8-5	19	366924	7020401	25 M/6					HCA-96-B92
HCA-96-8-8-1	19	416666	6996433	25 M/2	x	203	1	2	HCA-96-B93
HCA-96-8-8-1	19	416666	6996433	25 M/2	x	218	1	1	
HCA-96-8-8-2	19	440751	7001048	25 M/1	x	203	1	2	HCA-96-B94
HCA-96-8-8-3	19	443977	7013993	25 M/8		250	1	1	HCA-96-B95
HCA-97-3-7-4	19	490443	6996079	25 N		186	1	1	
HCA-97-3-7-5	19	490180	6996213	25 N	x	204	1	1	
HCA-97-3-7-5	19	490180	6996213	25 N		225	2	1	
HCA-97-4-7-1	19	497156	6994562	25 N		229	1	1	
HCA-97-4-7-2	19	496651	6994718	25 N		214	1	1	
HCA-97-4-7-2	19	496651	6994718	25 N		225	2	1	
HCA-97-4-7-7	19	494375	6998766	25 N		224	1	1	
HCA-97-4-7-7	19	494375	6998766	25 N		225	2	1	
HCA-97-4-7-8	19	494039	6999468	25 N	x	224	1	1	
HCA-97-5-7-2	19	495586	7028013	25 N	x	163	1	1	
HCA-97-5-7-2	19	495586	7028013	25 N	x	205	1	1	
HCA-97-5-7-13	19	495429	7025149	25 N					HCA-97-B96
HCA-97-7-7-1	19	496100	6974300	25 K		229	1	2	
HCA-97-7-7-3	19	497901	6974494	25 K		234	1	2	HCA-97-B97
HCA-97-8-7-1	19	515103	7021549	25 N	x	225	1	1	
HCA-97-8-7-1	19	515103	7021549	25 N		225	2	1	
HCA-97-8-7-2	19	515101	7022028	25 N	x	218	1	2	
HCA-97-8-7-2	19	515101	7022028	25 N		45	2	1	
HCA-97-8-7-3	19	514908	7023610	25 N		38	1	1	
HCA-97-8-7-4	19	515603	7023735	25 N	x	1	1	2	
HCA-97-8-7-4	19	515603	7023735	25 N		45	2	1	
HCA-97-8-7-6	19	516000	7023600	25 N		43	1	2	
HCA-97-8-7-6	19	516000	7023600	25 N		225	2	1	
HCA-97-8-7-8	19	518914	7023408	25 N	x	250	1	2	
HCA-97-8-7-9	19	519489	7023590	25 N	x	83	1	1	
HCA-97-8-7-10	19	519938	7023035	25 N		85	1	2	
HCA-97-9-7-1	19	499267	7034339	25 N	x	198	1	2	
HCA-97-9-7-2	19	499177	7035955	25 N	x	243	1	2	
HCA-97-9-7-2	19	499177	7035955	25 N	x	225	1	1	
HCA-97-9-7-3	19	500015	7037815	25 N		3	1	1	
HCA-97-9-7-4	19	502192	7039799	25 N		193	1	2	
HCA-97-10-7-1	19	500602	6960845	25 K	x	201	1	2	HCA-97-B98
HCA-97-10-7-2	19	503475	6941405	25 K	x	214	1	1	HCA-97-B99
HCA-97-10-7-12	19	512739	6926119	25 K					HCA-97-B100
HCA-97-11-7-6	19	512512	6998317	25 N					HCA-97-B101
HCA-97-11-7-8	19	511367	6998469	25 N		29	1	1	
HCA-97-12-7-3	19	520171	7005710	25 N	x	233	1	1	
HCA-97-12-7-6	19	521951	7006802	25 N	x	65	1	2	
HCA-97-12-7-6	19	521951	7006802	25 N		225	2	1	
HCA-97-12-7-8	19	524909	7008161	25 N	x	65	1	2	
HCA-97-12-7-10	19	525910	7008782	25 N	x	86	1	1	
HCA-97-12-7-11	19	526949	7009704	25 N	x	76	1	2	
HCA-97-12-7-12	19	527600	7009966	25 N		102	1	2	
HCA-97-13-7-1	19	546408	7005534	25 N		102	1	2	
HCA-97-13-7-3	19	545437	7004796	25 N		193	1	2	
HCA-97-13-7-4	19	544911	7004221	25 N		199	1	1	
HCA-97-13-7-5	19	544538	7003836	25 N	x	214	1	2	
HCA-97-13-7-6	19	543978	7003572	25 N		194	1	2	
HCA-97-13-7-6	19	543978	7003572	25 N		225	2	1	

[1]x = topographic high (regional ice flow)
[2]1 = striation; 2 = groove
[3]1 = flow direction known; 2 = not known

Identification	Zone	Easting	Northing	NTS	Regional flow[1]	Angle	Type[2]	Sense[3]	Till sample
HCA-97-13-7-8	19	543292	7002872	25 N		179	1	1	
HCA-97-13-7-9	19	542859	7002421	25 N		199	1	2	
HCA-97-15-7-1	19	464269	6961819	25 K	x	184	1	2	HCA-97-B102
HCA-97-15-7-2	19	476749	6939958	25 K	x	215	1	2	HCA-97-B103
HCA-97-15-7-3	19	483808	6958133	25 K	x	204	1	2	HCA-97-B104
HCA-97-15-7-4	19	482431	6984078	25 K	x	222	1	2	HCA-97-B105
HCA-97-16-7-3	19	517746	7003634	25 N	x	239	1	1	
HCA-97-16-7-4	19	517592	7003288	25 N		239	1	2	
HCA-97-16-7-6	19	513677	6999793	25 N	x	209	1	2	
HCA-97-18-7-1	19	505065	7023980	25 N		230	1	1	
HCA-97-18-7-2	19	504620	7024147	25 N	x	230	1	2	
HCA-97-18-7-3	19	503903	7025004	25 N	x	223	1	2	
HCA-97-18-7-4	19	503052	7025170	25 N	x	175	1	1	
HCA-97-18-7-4	19	503052	7025170	25 N		180	2	1	
HCA-97-18-7-6	19	503790	7027143	25 N	x	177	1	2	
HCA-97-18-7-7	19	504324	7027845	25 N	x	160	1	2	
HCA-97-18-7-7	19	504838	7029050	25 N		90	1	2	
HCA-97-19-7-2	19	498200	6920300	25 K					HCA-97-B106
HCA-97-19-7-3	19	512178	6913104	25 K	x	202	1	2	HCA-97-B107
HCA-97-19-7-4	19	534630	6904994	25 K		215	1	2	HCA-97-B108
HCA-97-19-7-5	19	551633	6892978	25 K	x	195	1	2	HCA-97-B109
HCA-97-19-7-6	19	547626	6900362	25 K	x	195	1	1	HCA-97-B110
HCA-97-19-7-6	19	547626	6900362	25 K		180	2	1	
HCA-97-19-7-7	19	541519	6919947	25 K					HCA-97-B111
HCA-97-19-7-8	19	550380	6929640	25 K	x	209	1	1	HCA-97-B112
HCA-97-19-7-9	19	540026	6941712	25 K					HCA-97-B113
HCA-97-19-7-10	19	520519	6938158	25 K	x	212	1	2	HCA-97-B114
HCA-97-20-7-1	19	523824	6970636	25 K	x	214	1	1	HCA-97-B115
HCA-97-20-7-3	19	523912	6971055	25 K		226	1	2	
HCA-97-20-7-4	19	523692	6972028	25 K	x	209	1	1	
HCA-97-20-7-6	19	523318	6972359	25 K					HCA-97-B116
HCA-97-20-7-7	19	523309	6972326	25 K					HCA-97-B117
HCA-97-20-7-9	19	521191	6972568	25 K		214	1	2	
HCA-97-20-7-10	19	519055	6973502	25 K	x	199	1	2	
HCA-97-20-7-10	19	519055	6973502	25 K		180	2	1	
HCA-97-21-7-2	19	505510	7027368	25 N	x	253	1	2	
HCA-97-21-7-3	19	505385	7027591	25 N	x	231	1	2	
HCA-97-21-7-5	19	506073	7028684	25 N		143	1	2	
HCA-97-21-7-5	19	506073	7028684	25 N		180	2	1	
HCA-97-21-7-6	19	506007	7028818	25 N		78	1	1	
HCA-97-21-7-7	19	506486	7029264	25 N		263	1	2	
HCA-97-21-7-7	19	506486	7029264	25 N		163	1	2	
HCA-97-21-7-7	19	506486	7029264	25 N		135	2	1	
HCA-97-21-7-8	19	507504	7029913	25 N	x	73	1	1	
HCA-97-21-7-9	19	508443	7030227	25 N		233	1	2	
HCA-97-21-7-10	19	509425	7030943	25 N	x	241	1	2	
HCA-97-22-7-1	19	542964	6999101	25 N	x	48	1	1	HCA-97-B118
HCA-97-22-7-2	19	543000	6999500	25 N		37	1	2	
HCA-97-22-7-3	19	543415	6999687	25 N		30	1	2	
HCA-97-22-7-4	19	543233	7000108	25 N		63	1	2	
HCA-97-22-7-5	19	543409	7000868	25 N	x	48	1	2	
HCA-97-22-7-6	19	543333	7001669	25 N	x	53	1	2	
HCA-97-22-7-7	19	543669	7002922	25 N		113	1	1	
HCA-97-22-7-8	19	543708	7000025	25 N	x	108	1	1	
HCA-97-23-7-1	19	538608	6898932	25 K		205	1	2	
HCA-97-23-7-2	19	538283	6900065	25 K		202	1	2	
HCA-97-23-7-4	19	536963	6901888	25 K	x	195	1	2	HCA-97-B119
HCA-97-23-7-5	19	536700	6902400	25 K	x	17	1	1	
HCA-97-23-7-5	19	536700	6902400	25 K		10	2	1	
HCA-97-23-7-6	19	536375	6903475	25 K	x	198	1	2	

Table 2 (cont.)

Identification	Zone	Easting	Northing	NTS	Regional flow[1]	Angle	Type[2]	Sense[3]	Till sample
HCA-97-25-7-4	19	494916	6963367	25 K					HCA-97-B120
HCA-97-26-7-1b	19	532949	6909623	25 K		5	1	2	
HCA-97-26-7-1c	19	533016	6909680	25 K		11	1	2	
HCA-97-26-7-1d	19	533016	6909680	25 K	x	16	1	2	
HCA-97-26-7-2	19	533275	6911242	25 K	x	15	1	2	
HCA-97-26-7-3	19	533169	6911520	25 K		5	1	1	
HCA-97-26-7-4	19	532060	6912099	25 K		10	1	2	
HCA-97-26-7-5	19	531664	6912864	25 K	x	360	1	1	
HCA-97-26-7-6	19	531307	6913986	25 K	x	10	1	1	
HCA-97-26-7-7	19	530446	6915817	25 K	x	10	1	2	
HCA-97-26-7-8	19	530182	6917619	25 K	x	10	1	1	
HCA-97-26-7-9	19	530250	6918100	25 K	x	15	2	1	
HCA-97-26-7-10	19	530003	6919033	25 K		5	1	2	
HCA-97-26-7-11	19	530208	6919324	25 K		25	1	2	
HCA-97-26-7-12	19	530547	6920096	25 K	x	20	1	2	
HCA-97-27-7-1	19	544438	6974528	25 K					HCA-97-B121
HCA-97-27-7-2	19	538414	6958930	25 K					HCA-97-B122
HCA-97-27-7-3	19	534202	6926438	25 K	x	25	1	1	HCA-97-B123
HCA-97-30-7-1	19	500136	7000154	25 N		206	1	2	HCA-97-B124
HCA-97-30-7-2	19	499153	7000912	25 N	x	219	1	2	
HCA-97-30-7-6	19	495050	7001183	25 N	x	222	1	2	
HCA-99-10-7-1	19	524100	7069050	25 N		123	1	2	
HCA-99-11-7-1	19	526080	7069450	25 N		63	1	1	
HCA-99-11-7-2	19	526240	7069630	25 N		80	1	2	
HCA-99-11-7-2	19	526240	7069630	25 N		92	1	2	
HCA-99-11-7-5a	19	525580	7069060	25 N		98	1	2	
HCA-99-11-7-5b	19	524930	7068880	25 N		123	1	2	
HCA-99-11-7-5c	19	524930	7068880	25 N		98	1	2	
HCA-99-11-7-6a	19	521720	7069230	25 N		103	1	2	
HCA-99-11-7-6b	19	521460	7069210	25 N	x	123	1	2	
HCA-99-11-7-7	19	521480	7069410	25 N	x	128	1	2	
HCA-99-11-7-9	19	520720	7071080	25 N		123	1	2	
HCA-99-12-7-3	19	532040	7065410	25 N		83	1	2	
HCA-99-12-7-3	19	532040	7065410	25 N		53	1	2	
HCA-99-12-7-5	19	532100	7067080	25 N	x	68	1	2	
HCA-99-14-7-1	19	454150	6966410	25 K		198	1	2	
HCA-99-15-7-2a	19	456410	6970460	25 K	x	180	1	2	
HCA-99-18-7-5	19	537730	6904280	25 K	x	20	1	2	
HCA-99-18-7-7	19	536180	6903880	25 K	x	25	1	2	
HCA-99-18-7-8	19	536450	6902920	25 K		23	1	2	
HCA-99-18-7-9	19	536620	6902970	25 K		25	1	1	
HCA-99-19-7-3	19	540380	6900410	25 K	x	32	1	1	
HCA-99-19-7-5b	19	538980	6901320	25 K	x	20	1	2	
HCA-99-22-7-1a	19	537920	6909450	25 K	x	21	1	1	
HCA-99-22-7-1b	19	537920	6909450	25 K	x	15	1	1	
HCA-99-22-7-2	19	538440	6909850	25 K		3	1	2	
HCA-99-22-7-3	19	538530	6909860	25 K	x	18	1	1	
HCA-99-23-7-3	19	536040	6908710	25 K		18	1	2	
HCA-99-23-7-5	19	535250	6909810	25 K	x	20	1	1	
HCA-99-23-7-6a	19	538130	6906890	25 K		4	1	1	
HCA-99-23-7-6b	19	538130	6906890	25 K		20	1	1	
HCA-99-24-7-1	19	537780	6906690	25 K		3	1	1	
HCA-99-24-7-2	19	537700	6906690	25 K		15	1	1	
HCA-99-24-7-3	19	537350	6906690	25 K		15	1	2	
HCA-99-24-7-5	19	537700	6907060	25 K		16	1	2	
HCA-99-25-7-1	19	537700	6907150	25 K	x	17	1	2	
HCA-99-25-7-2	19	535550	6906300	25 K		25	1	2	
HCA-99-25-7-3	19	534860	6906110	25 K		15	1	2	

[1]x = topographic high (regional ice flow)
[2]1 = striation; 2 = groove
[3]1 = flow direction known; 2 = not known

Table 3. Striations (data from other studies)

Recorder[1]	NTS	Zone	Easting	Northing	Angle	Type[2]	Sense[3]
Unknown	25 N	19	473300	7051500	5	1	2
Unknown	25 N	19	496000	7033600	355	1	2
Unknown	25 N	19	505000	7040500	25	1	2
Unknown	25 N	19	478600	7061800	83	1	2
Unknown	25 N	19	516800	7058400	315	1	2
D.M. Carmichael	25 M	19	355500	7059100	216	1	2
D.M. Carmichael	25 M	19	351700	7060300	228	1	2
D.M. Carmichael	25 M	19	352200	7061000	214	1	2
D.M. Carmichael	25 M	19	352100	7062300	222	1	2
D.M. Carmichael	25 M	19	365300	7076600	222	1	2
D.M. Carmichael	25 M	19	366450	7081100	214	1	2
D.M. Carmichael	25 M	19	366900	7081900	218	1	2
D.M. Carmichael	25 M	19	371500	7076050	226	1	2
D.M. Carmichael	25 M	19	389100	7050000	255	1	2
D.M. Carmichael	25 M	19	385300	7051450	242	1	2
D.M. Carmichael	25 M	19	383600	7055500	236	1	2
D.M. Carmichael	25 M	19	382600	7055900	228	1	2
D.M. Carmichael	25 M	19	382400	7057800	228	1	2
D.J. Scott	25 M	19	356000	7095700	200	1	2
D.J. Scott	25 M	19	359100	7098200	190	1	2
D.J. Scott	25 M	19	402000	7085100	200	1	2
D.J. Scott	25 M	19	402100	7096100	190	1	2
M.R. St-Onge	25 M	19	423400	7082300	231	1	2
M.R. St-Onge	25 M	19	423500	7087000	234	1	2
D.J. Scott	25 K	19	537700	6909500	13	1	2
D.J. Scott	25 K	19	538500	6909600	15	1	2
D.J. Scott	25 K	19	542300	6910300	27	1	2
M.R. St-Onge	25 K	19	539600	6912400	11	1	2
M.R. St-Onge	25 K	19	539600	6912400	200	2	1
N. Wodicka	25 K	19	551600	6919000	205	1	1
D.J. Scott	25 K	19	532300	6914800	201	1	2
D.J. Scott	25 K	19	534000	6914500	197	1	2
D.J. Scott	25 K	19	534600	6914300	189	1	2
D.J. Scott	25 K	19	536300	6914600	186	1	2
D.J. Scott	25 K	19	542400	6925700	211	1	2
M.R. St-Onge	25 K	19	539700	6917400	202	1	2
M.R. St-Onge	25 K	19	522000	6927000	199	1	2
D.J. Scott	25 K	19	523600	6934500	188	1	2
D.J. Scott	25 K	19	534850	6960600	209	1	2
D.J. Scott	25 K	19	532900	6967750	217	1	2
D.J. Scott	25 K	19	518900	6971800	221	1	2
N. Wodicka	25 K	19	538000	6979900	205	1	2
M.R. St-Onge	25 N	19	526300	6993250	27	1	2
M.R. St-Onge	25 N	19	528200	6995800	21	1	2
L. Piper	25 N	19	541000	6997200	99	1	2
Blake (1966)	25 K	19	501700	6916000	199	1	2
Blake (1966)	25 K	19	488900	6954400	208	1	2
Blake (1966)	25 K	19	457300	6966600	178	1	2
Blake (1966)	25 K	19	457500	6967900	186	1	2
Blake (1966)	25 K	19	456500	6974200	207	1	2
Blake (1966)	25 N	19	513700	7051400	119	1	2
Blake (1966)	25 N	19	506750	7048250	81	1	2
Blake (1966)	25 N	19	536300	7019600	163	1	2
Blake (1966)	25 N	19	540900	7009500	123	1	2
Blake (1966)	25 M	19	368600	7087000	220	1	2
Blake (1966)	25 M	19	353400	7092000	175	2	2
Blake (1966)	25 M	19	353400	7092000	165	1	2
Blake (1966)	25 L	19	415200	6938700	132	1	2
Bell (1885)	25 L	19	416500	6938500	115	1	2
Bell (1901b)	25 L	19	407500	6950500	165	1	2
Davison (1958)	25 K	19	461200	6976500	191	1	2

[1]Italicized names are geologists from concurrent bedrock mapping
[2]1= striation; 2= groove
[3]1= flow direction known; 2= flow direction not known

Table 3. (cont.)

Recorder[1]	NTS	Zone	Easting	Northing	Angle	Type[2]	Sense[3]
Davison (1958)	25 K	19	449800	6980300	191	1	2
Davison (1958)	25 K	19	464000	6979300	188	1	2
Davison (1958)	25 K	19	467200	6980200	187	1	2
Davison (1958)	25 K	19	474500	6980800	220	1	2
Davison (1958)	25 K	19	459300	6973400	182	1	2
Davison (1958)	25 K	19	460300	6974100	190	1	2
Davison (1958)	25 K	19	463200	6973300	207	1	2
Davison (1958)	25 K	19	455900	6968900	185	1	2
Davison (1958)	25 K	19	460600	6969800	183	1	2
Davison (1958)	25 K	19	456000	6971200	195	1	2
Davison (1958)	25 K	19	455900	6966500	190	1	2
Davison (1958)	25 K	19	456200	6965400	179	1	2
Davison (1958)	25 K	19	458500	6967600	200	1	2
Davison (1958)	25 K	19	459600	6964500	180	1	2
Davison (1958)	25 K	19	466100	6963300	209	1	2
Davison (1958)	25 K	19	467500	6963250	220	1	2
Davison (1958)	25 K	19	467500	6963250	180	1	2
Davison (1958)	25 K	19	473250	6962000	210	1	2
Davison (1958)	25 K	19	473500	6964750	205	1	2
Davison (1958)	25 K	19	456200	6976600	195	1	2
Davison (1958)	25 K	19	458000	6976000	187	1	2
Davison (1958)	25 K	19	457200	6967000	185	1	2
Manley (1995)	25 K	19	551500	6892500	197	1	1
Manley (1995)	25 K	19	541000	6899000	14	1	1
Manley (1995)	25 K	19	538500	6899000	22	1	1
Manley (1995)	25 K	19	534500	6901000	35	1	1
Manley (1995)	25 K	19	531000	6902000	187	1	1
Manley (1995)	25 K	19	523000	6904000	193	1	1
Manley (1995)	25 K	19	520500	6907000	211	1	2
Manley (1995)	25 K	19	514500	6912000	203	1	2
Manley (1995)	25 K	19	512178	6913104	203	1	1
Manley (1995)	25 K	19	506000	6916000	189	1	1
Manley (1995)	25 K	19	500000	6918500	198	1	1
Manley (1995)	25 K	19	482000	6936000	240	1	2
Manley (1995)	25 K	19	482000	6936000	208	1	1
Manley (1995)	25 K	19	476749	6939958	204	1	1
Manley (1995)	25 K	19	477200	6941700	355	1	1
Manley (1995)	25 K	19	477200	6941700	197	1	1
Manley (1995)	25 K	19	468000	6958500	170	1	1
Manley (1995)	25 L	19	447500	6937500	165	1	2
Manley (1995)	25 L	19	443000	6963000	170	1	1
Manley (1995)	25 L	19	430000	6951000	175	1	1
Manley (1995)	25 L	19	421500	6937000	196	1	2
Manley (1995)	25 L	19	420100	6962000	227	1	1
Manley (1995)	25 L	19	405250	6971000	247	1	1
Manley (1995)	25 L	19	391000	6973500	215	1	2
Manley (1995)	25 L	19	403000	6980500	253	1	1
Manley (1995)	25 L	19	431500	6936500	196	1	2
Manley (1995)	25 M	19	388500	6989500	230	1	1
Manley (1995)	25 M	19	370500	7003000	240	1	2
Lind (1983)	25 N	19	516200	7056800	135	1	2
Lind (1983)	25 N	19	513600	7051400	133	1	2
Lind (1983)	25 N	19	515300	7051300	66	1	2
Lind (1983)	25 N	19	510700	7048100	16	1	2
Lind (1983)	25 N	19	511800	7047300	37	1	2
Lind (1983)	25 N	19	507500	7047700	140	1	2
Lind (1983)	25 N	19	508200	7045900	61	1	2
Lind (1983)	25 N	19	507500	7044600	80	1	2
Lind (1983)	25 N	19	507900	7044000	77	1	2
Lind (1983)	25 N	19	516800	7041500	142	1	2
Lind (1983)	25 N	19	517500	7041700	14	1	2
Lind (1983)	25 N	19	529100	7033700	132	1	2
Lind (1983)	25 N	19	528200	7035000	119	1	2
Lind (1983)	25 N	19	542700	7021300	100	1	2
Lind (1983)	25 N	19	534900	7012900	57	1	2

[1]Italicized names are geologists from concurrent bedrock mapping
[2]1= striation; 2= groove
[3]1= flow direction known; 2= flow direction not known

Periglacial bedrock landforms

The extensive areas of rock outcrop have been widely subject to frost heave, a process reviewed for the eastern Arctic by Dredge (1992). Block fields resulting from disintegration by this process or by subglacial processes are particularly common on Big Island. Minor scarps and tors were observed on metasedimentary rocks at all elevations including an area above 700 m south of the cirques at Hidden Bay. At the latter site, part of the Baffin Surface, striations conform to the regional pattern.

Figure 18. *Clast-supported, typically bouldery till at distal margin of hummocky till; Frobisher Bay Moraine System, west of the Meta Incognita Peninsula height of land. Person for scale. Photograph by D.A. Hodgson. GSC 2001-379E*

Till

Till map units

Hummocky till (unit Th)

The thickest till is proximal to segments of the Frobisher Bay Moraine System. These extremely bouldery deposits (Fig. 18) have a rolling to hummocky surface obscuring all but the most irregular bedrock topography. Glacial ice may be preserved in this unit, contributing to the 1 m to more than 20 m thickness.

Till blanket (unit Tb)

Extensive areas of till blanket, 1–10 m thick, obscure bedrock structures normally visible on airphotos. The broadest cover lies in and proximal to the Frobisher Bay Moraine System (Fig. 19); on rising ground northwest of Frobisher Bay; northeast of the coastal upland (proximal slope) between Markham Bay and Crooks Inlet; and on interfluves in the

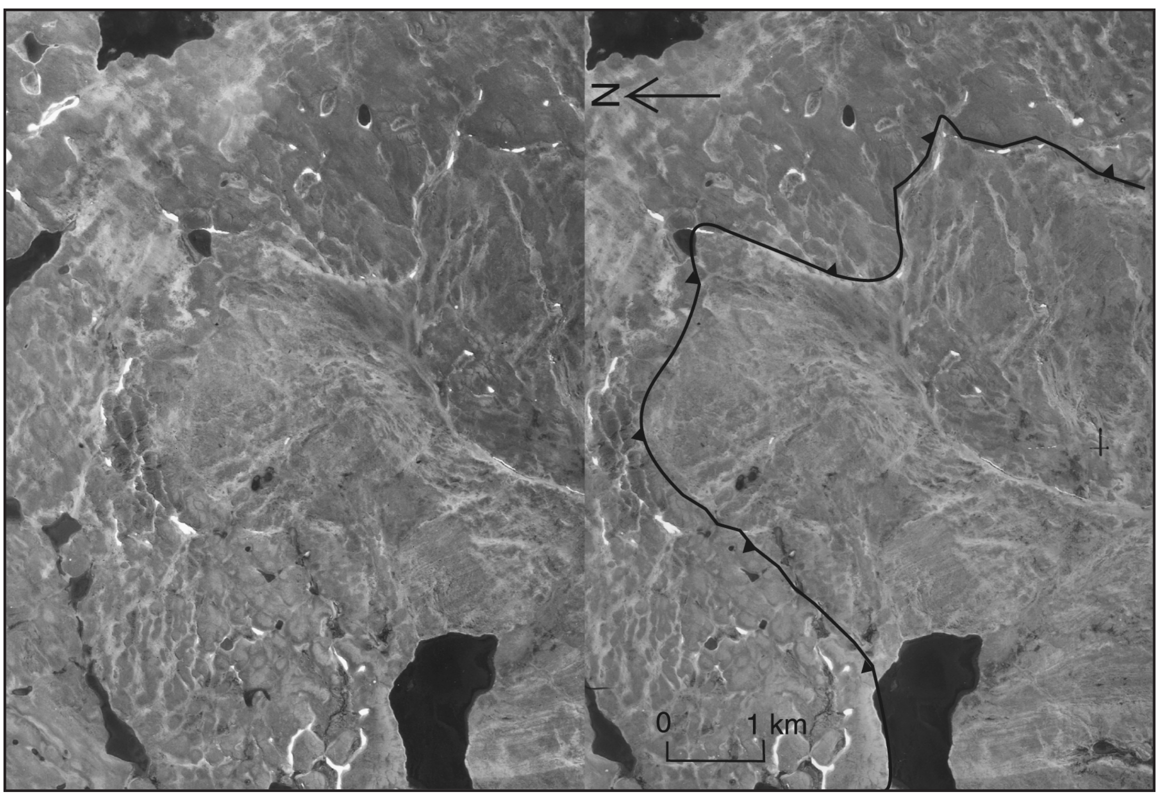

Figure 19. *Stereo-pair of western sector of Frobisher Bay Moraine System (domains 3a/4a). Hummocky till to the north of the moraine limit (shown by the line) bears southwest-trending lineations. Distal till veneer and bedrock is dissected by valley-side lateral drainage channels cut by an earlier retreating lobe of cold-based ice. NAPL A16322-35, A16322-36; scale 1:60 000 x 83%.*

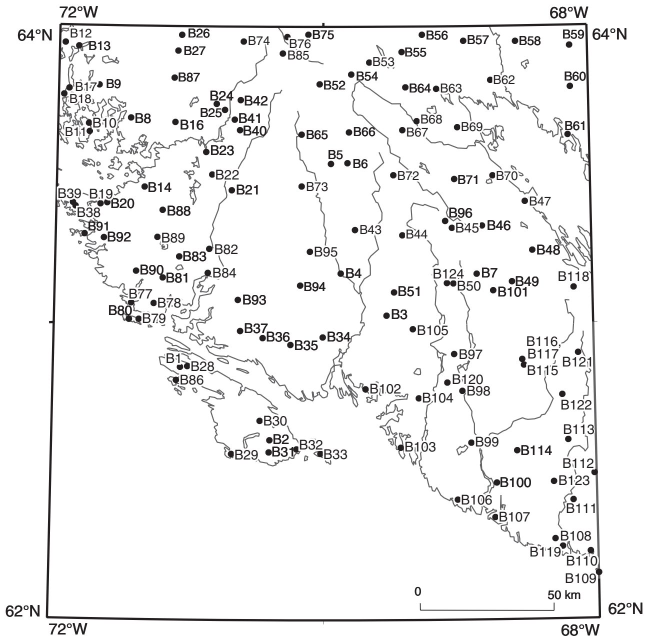

Figure 20. Till sample locations, this study. Sample numbers shown here are shortened to last digits to fit the figure; cf. Tables 2, 4.

southeast of the map area. This unit incorporates interlobate and ice-marginal moraines. There is no obvious relationship between till distribution or thickness and underlying or up-ice bedrock competency. Thicker till may be patterned by intersecting ice-filled frost-fissures. Offshore, MacLean et al. (1986) and MacLean et al. (1991a) reported that west of Big Island ice-contact sediments thicken to over 10 m towards the Western basin depocentre from 2 m or less thickness inshore. Southeast of the island, between basins, the sediment cover is very thin. Apparent multiple tills totalling over 100 m thick appear on some seismic records in the strait (MacLean et al., 2001).

Till veneer (unit Tv)

Thin, discontinuous veneers of till, less than 2 m thick, through which bedrock structure is evident, are widespread adjacent to thicker till described above. Included in this unit are block fields (angular or subangular large clasts), which are common in all topographic situations.

Till is notably rare on much of Big Island, on the coast from Markham Bay to Soper River, lower Soper valley, at the head of Crooks Inlet, on shores and islands of Markham Bay, on much of the Meta Incognita Peninsula height of land, the head of Frobisher Bay, and on Hall Peninsula east of the Frobisher Bay Moraine System.

Till composition

In a low-density till sampling program (1 sample/218 km^2) the majority of samples were collected from regional topographic highs, as with striation measurements; all were above marine limit (Fig. 20). Till from downslope sites is commonly finer grained. The bouldery till composition made excavating to a clear C-horizon difficult, therefore many samples were taken in frost boils at only 20–30 cm depth, but where the finer matrix was well mixed. Grain-size analyses showed a relatively uniform composition for most of the map area (Fig. 21, 22). Much of the till is clast supported (i.e. pebbles and larger fragments are in contact, constituting more than half of the till) with an acidic silty sand matrix (Fig. 23, 24). Clasts are dominantly subangular cobble- and boulder-size igneous and metamorphic rocks similar to local bedrock. A few carbonate clasts are present in till at the head of Frobisher Bay; a silty matrix-supported till is discontinuously present along the Hudson Strait coast, east of Big Island. East of Barrier Inlet, preglacial shells occur above the postglacial marine limit in till or glacial marine deposits.

Only one till has been has been observed at any site, though the bouldery composition of the till throughout most of the map area and the consequent instability of natural incisions precludes preservation of clean exposures; hence, no stratigraphy has been observed. The short transport distance of most local lithologies indicates a deformation or lodgement origin. Block fields in this area may be deformation till deposits derived from adjacent bedrock or they may be the residue after removal of fines from conventional coarse till by glacial meltwater, or, locally, scouring by higher postglacial seas, glacial lakes, and Holocene nival processes. Many block fields are surrounded by indicators of active glaciation and there is no particular evidence for them being relict features predating the last glaciation, as Muller (1980) suggested for Jackman Sound, 75 km east of the map area, and Dredge (2000a) found to be the case for granite and gneiss of Melville Peninsula.

Stravers (1986) classified till on the peninsula east of the map area as Meta Incognita Drift — a sandy, locally derived till. Adjacent to outer Frobisher Bay, Stravers (1986) identified Hall Drift, composed of loam with carbonate clasts deposited by a Frobisher Bay outlet glacier. This till is now understood to have been deposited by cross-Hudson Strait ice (Manley et al., 1996).

pH

Weakly to moderately acidic values (pH 6.2–4.2) were measured for all till that was analyzed (mostly from a cross-section of the central Meta Incognita Peninsula), for a mean of 5.2, except for a weakly alkaline site (7.2, site HCA-96-B57) overlying Paleozoic limestone at the head of Frobisher Bay (Fig. 25; Table 4, on CD-ROM). Till samples above marine limit from other studies (Table 5) provides a mean pH of 5.6. From central-eastern Meta Incognita Peninsula, east of the map area, Stravers (1986) determined pH values of 4.3–6.5, with a mean of 5.0, for Meta Incognita Drift. Values of 6.0 and more were obtained from shelly till in the southeast (HCA-97-B108, HCA-97-B119), from a silty till anomaly (HCA-97-B120) and from two otherwise unremarkable sites (HCA-95-B07, HCA-96-B94).

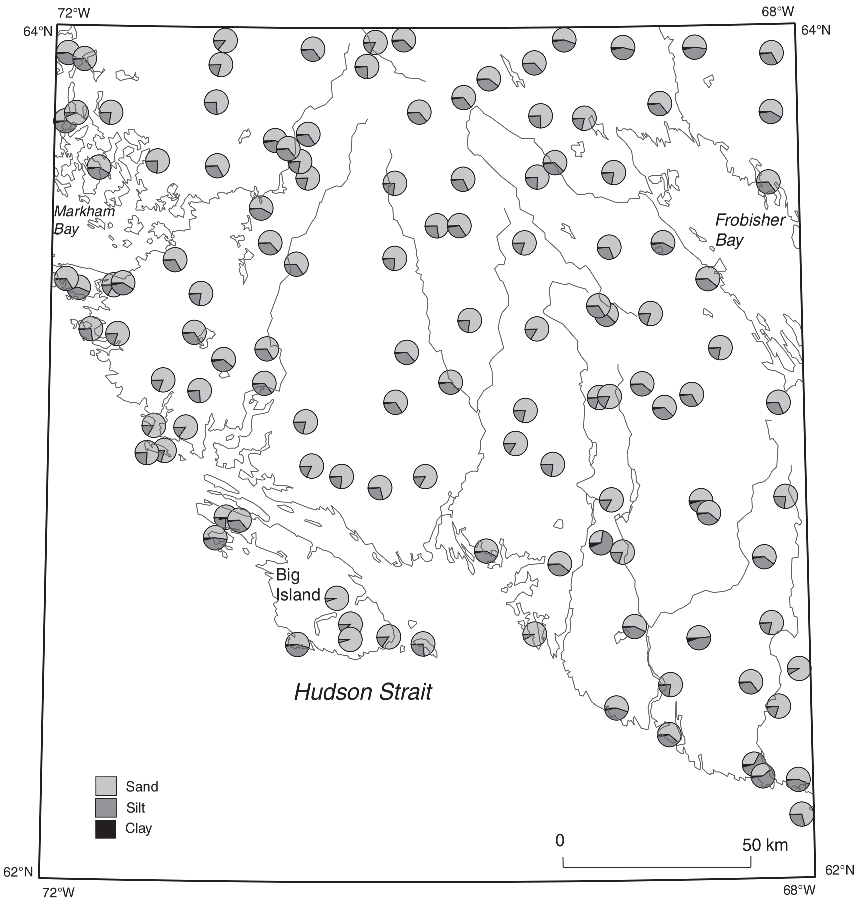

Figure 21. Till texture distribution (this study). Composition of regional till samples collected for this study for sand (2 mm to 63 µm), silt (<63 µm to 2 µm), and clay (<2 µm) fractions.

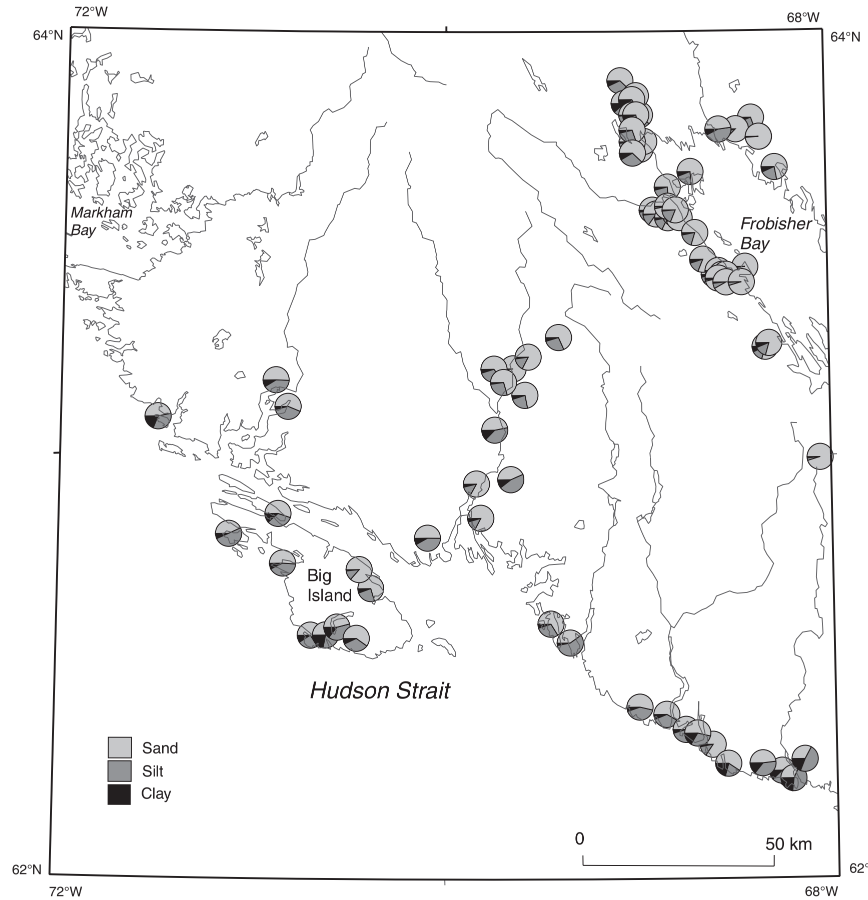

***Figure 22.** Till texture distribution (from other studies). Composition of till samples from other studies* (see *Fig. 24) for sand (2 mm to 63 µm), silt (<63 µm to 4 µm), and clay (<4 µm) fractions.*

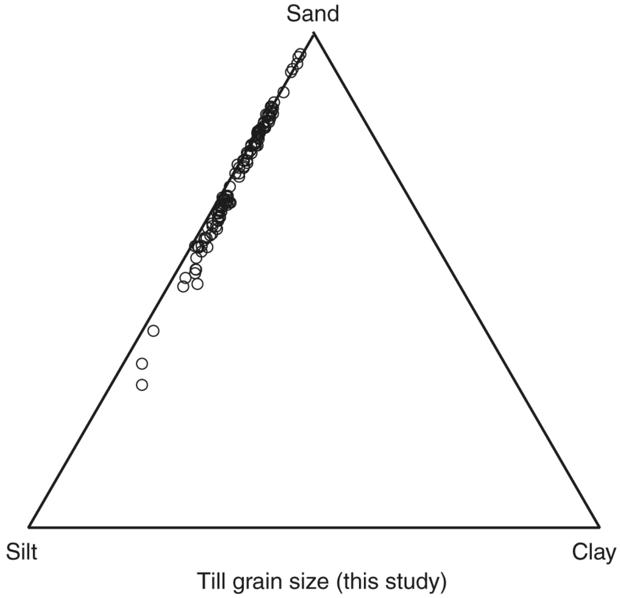

Figure 23. Till ternary diagram (this study) illustrating the silty sand regional till. Grain-size plot for matrix of 123 till samples collected for this study across the mapped area, mainly from regional topographic highs (Table 4, on CD-ROM). Grain-size analysis by sieving and sedimentation into sand (2 mm to 63 μm), silt (<63 μm to 2 μm), and clay (<2 μm) fractions.

Carbonate content

Samples were analyzed for carbonate content using a LECO carbon analyzer (the standard GSC method; R.A. Klassen, I. Girard, R.R. Lafromboise, and P.J. Lindsay, unpub. GSC report, 2000). Two separate analyses of each sample indicated low inorganic carbon content, but much more organic carbon, probably a result of the shallow excavations in the bouldery till barely reaching below the root zone (Table 4). The samples were re-analyzed using the Chittick method, which was also the procedure used by Manley (1995). This provided results more in agreement with field observations, which included some tests on surface samples with 10% HCl (Fig. 25). All of 123 total carbonate values were 4% or less (Table 4) except for till over Paleozoic outcrop (33.4%, HCA-96-B56; 25.1%, HCA-96-B57), till down-ice from the outcrop (8.9%, HCA-96-B62), shelly till on the southeast Hudson Strait coast (24.2%, HCA-97-B108; 24.6%, HCA-97-B108, HCA-97-B119), an adjacent coastal till site (19.6%; HCA-97-B103), the silty till anomaly (17.6%; HCA-97-B120), and a sample from the southeast, but well inland (10.7%, HCA-97-B112). On the other hand, the southwesternmost sample from Big Island (HCA-96-B29) had a carbonate content of only 0.9%. Thus, the mass of Paleozoic carbonate rocks towards and beyond Amadjuak Lake and in Hudson Strait (Fig. 4) are only peripherally recorded in the till of the map area. In the case of Frobisher Bay, Lind (1983) suggested that carbonate rocks from Foxe Basin were so comminuted that most did not reach the bay, though she obtained 15% carbonate content in till at Cape Rammelsberg. On the west side of Foxe Basin Dredge (1995)

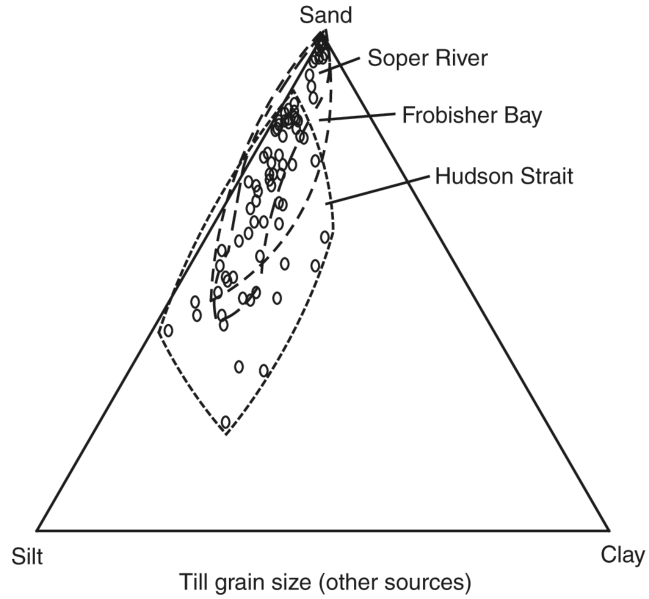

Figure 24. Till ternary diagram (from other studies). Grain-size plot for matrix of 77 till samples collected by other workers (Table 5) from vicinity of inner Frobisher Bay (Colvill, 1982; Lind, 1983; Squires, 1984; Stravers, 1986; Duvall, 1993), Soper River valley in central Meta Incognita Peninsula (Manley, 1995), and Hudson Strait coast in the map area (Manley, 1995). Grain-size analysis by sieving and sedimentation into sand (2 mm to 63 μm), silt (<63 μm to 4 μm), and clay (<4 μm) fractions. The greater clay content relative to Figure 23 is explained by the less elevated sample sites (closer to marine sediments) and the higher upper limit for clay particles.

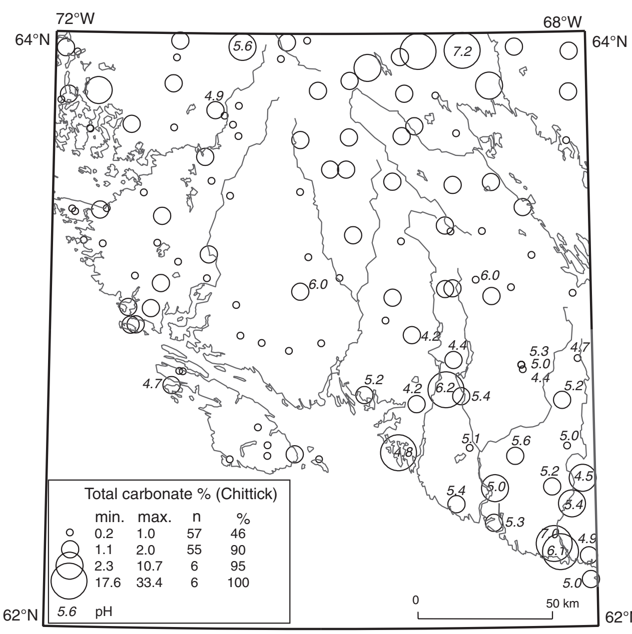

Figure 25. Total carbonate content (proportional circles) and pH (numerals) of till samples (by Chittick method).

documented carbonate values exceeding 50% in till over 100 km from source. As Manley (1995) and others found, the carbonate is dominantly calcite (75% for this study; Table 4). Dolomite is dominant for 13% of samples and the ratio is even for 11%. No particular correlation with Paleozoic or marble outcrop or with till origin was noted.

Till geochemistry

The less than 2 µm (clay) fraction of all 123 till samples was analyzed (aqua regia digestion, inductively coupled plasma emission spectroscopy) for a suite of 34 elements in a search for patterns in concentrations that could be related to direction of ice flows. Results are illustrated in Figure 26 and all data are shown in Table 4. They confirm the general homogeneity of till noted above; the cross-strait ice flow in the southeast is barely recorded (e.g. Ca). Only very minor exceptions to the normal abundance of elements occur (Rose et al., 1979). Lead is slightly elevated (>40 ppm) in the northwest though it has weak correlation with all other elements. Calcium and strontium, with the strongest correlation among the elements (r^2=0.9), have highest values in silty till containing carbonate erratics (head of Frobisher Bay, parts of southeast). Iron is relatively high everywhere, with 20% of samples containing more than 9%. The highest concentrations of metallic elements are along Hudson Strait in the vicinity of Big Island; this is also the area of sparsest till cover, hence samples might contain more weathered rock than till.

Till provenance

Till parameters at most sampled sites show a general homogeneity over the map area. Distinctive local lithologies such as red granite, quartz veins, and diabase dykes, commonly tail out a few tens to thousands of metres down-ice; however, conspicuous exotic erratics in the form of light-weathering, easily shattered Paleozoic carbonate rocks from the southeast Arctic Platform or Hudson Strait (Fig. 4) occur along coasts. Only those above the marine limit, which could not have been ice rafted, are useful in provenance studies. At greatest abundance, they are estimated to be less than 0.1% of till clasts at any site. Along Hudson Strait, they are found in till on southwest Big Island and the coast farther southeast (Blake, 1966; Clark, 1985; Stravers, 1986; Manley, 1995, 1996). Some are found in the vicinity of the southeasterly downstrait striations, but others were believed by Manley (1995, 1996) to have been reworked from glacial marine sediments by later southward ice flow. Carbonate erratics occur in the southeast of the map area, within the zone of onshore-heading striations, to at least 200 m altitude and 7 km inland. In the same area, pre-Late Wisconsinan marine shells have been transported onshore in a silty stony till (Blake, 1966; Manley, 1995, 1996), to elevations of 200 m (where marine limit is at 70 m) and 10 km inland. At the head of Frobisher Bay, Colvill (1982) and others recorded few carbonate erratics above marine limit, despite some till and rock landforms indicating last ice flow from the direction of the southeast extension of the Arctic Platform 50 km to the northwest, and even most of the erratics found were in the vicinity of platform outliers northwest of Foul Inlet.

Till landforms

Landforms at the megascale (e.g. end moraine complexes), mesoscale (interlobate and subaqueous push (deGeer) moraines, streamlined till), and microscale (periglacial processes modifying till) are discussed in order of assumed age.

Drumlins

Drumlins were identified proximal to the Frobisher Bay Moraine System only, mostly in several fields formed during final drawdown of ice from the northwest (east of peninsula height of land) into the head of Frobisher Bay (Fig. 15). They are commonly low and spindle-shaped, 500–1500 m long, and are associated with till lineations and streamlined rock. Clark (1985) noted a number of lee-side tills in the Kimmirut area. These small deposits (<1 km^2), together with till ramps, are found more rarely in other parts of the map area.

Till lineations

Ribbon-shaped till 'smears' up to 10 km long are recognizable by tonal differences on airphotos, but can rarely be seen on the ground. These bed forms are common on bouldery till blanket and veneer proximal to the Frobisher Bay Moraine System and are scattered over till blanket elsewhere (Fig. 15). They are probably narrow dispersion plumes (cf. Dredge, 2000b) in which boulders from a minor bedrock unit have different reflectance from adjacent, more uniform till. As with drumlins, they align with the regional striation pattern.

Moraines

Interlobate moraines. Isolated, but prominent ridges and cones on a number of interfluves between valleys draining to Hudson Strait in the southeast of the map area are presumed interlobate (medial) moraines and valley-rim moraines (Fig. 27, 28). The moraines take the form of single or multiple till ridges up to 50 m high and 5 km long. Slopes are steep and extremely bouldery (blocks up to 4 m diameter recorded). Gradients indicate formation within south- to southwest-flowing ice. On the basis of their form it is suggested that these moraines are no older than Late Wisconsinan, and were deposited in initial interlobate openings rather than being remnants of degraded ancient moraine systems. One interlobate-type moraine was identified within the zone of definite onshore-pointing striations: a 1 km long southwest-oriented ridge southeast of Balcom Inlet. Two smaller ridges on Big Island are much less bouldery and may have a different origin.

Large ice-marginal push moraines. Seismic reflection profiles in North Bay west of Cape Tanfield show several thick (>50 m) sediment ridges (Fig. 29, on CD-ROM) comprising two or more ice-contact sequences that were interpreted as moraines by MacLean et al. (1986, 2001), who suggested the moraines mark the limit of Baffin Island ice, and possibly record contact between that and Hudson Strait ice. The only end moraines on the Hudson Strait coast (Fig. 27) are a complex of ridges up to 10 m high wrapped around a 450 m

Table 5. Till analyses (data from other studies)

Sample number[1] Manley	Other collectors[2]	NTS	Zone	Easting	Northing	Gravel[3]	Sand[4]	Silt[5]	Clay[6]	Carbonate[7]	Calcite Dolomite[8]	pH
1	Stravers (1986)	25 N	19	548000	6984000	57.6	95.3	3.0	1.7	–	–	5.5
74	–	25 K	19	500000	6919000	8.4	53.6	41.2	5.2	1.9	7.4	7.0
75	–	25 K	19	507000	6917000	12.0	58.6	35.3	6.1	0	–	6.9
76	–	25 K	19	512000	6913000	3.7	46.1	49.3	4.6	0	–	6.6
77	–	25 K	19	515000	6912000	7.6	53.9	29.9	16.3	0	–	6.3
78	–	25 K	19	523000	6904000	7.6	59.4	20.0	20.6	0	–	6.4
79	–	25 K	19	532000	6904000	1.7	48.3	37.5	14.2	0	–	5.6
80	–	25 K	19	537000	6902000	5.2	41.4	46.7	11.9	0	–	6.2
81	–	25 K	19	539000	6901000	0.6	21.8	56.2	22.0	0	–	5.7
82	–	25 K	19	540000	6900000	9.4	32.2	44.4	23.4	22.1	0.7	8.1
83	–	25 K	19	543000	6905000	6.4	33.0	48.2	18.8	0	–	6.6
169	–	25 N	19	549000	7040000	–	–	–	–	0	–	–
170	–	25 N	19	549000	7044000	–	–	–	–	0	–	–
171	–	25 N	19	548000	7051000	–	–	–	–	0	–	–
172	–	25 N	19	544000	7059000	–	–	–	–	0	–	–
173	–	25 N	19	542000	7055000	–	–	–	–	0	–	–
174	–	25 N	19	540000	7054000	–	–	–	–	0	–	–
175	–	25 N	19	535000	7059000	–	–	–	–	0	–	–
176	–	25 N	19	536000	7063000	–	–	–	–	0	–	–
177	Squires (1984) 5	25 N	19	537000	7060000	25.6	72.1	21.3	6.6	–	–	–
178	–	25 N	19	534000	7067000	–	–	–	–	0	–	–
179	Squires (1984) 3	25 N	19	533000	7068000	15.6	84.2	14.7	1.1	–	–	–
180	Squires (1984) 1	25 N	19	531000	7073000	30.2	69.6	24.2	6.2	–	–	–
181	Squires (1984) 2	25 N	19	527000	7070000	30.2	87.2	8.0	4.8	–	–	–
182	–	25 N	19	526000	7071000	–	–	–	–	0	–	–
183	Duvall (1983)	25 N	19	524000	7070000	–	47.9	44.4	7.6	4	1.8	–
184	–	25 N	19	519000	7072000	–	–	–	–	0	–	–
185	Colvill (1982) G4	25 N	19	515000	7059000	34.2	73.8	20.3	5.9	0	–	–
186	Colvill (1982) G1	25 N	19	497000	7083000	13.7	62.3	31.0	6.7	0	–	–
187	Colvill (1982) E7	25 N	19	501000	7079000	33.8	74.0	18.2	7.8	0	–	–
188	Colvill (1982) E8	25 N	19	500000	7078000	24.9	65.7	24.1	10.2	15.2	–	–
189	Colvill (1982) G2	25 N	19	498000	7077000	22.7	74.8	13.8	11.4	0	–	–
190	Colvill (1982) B1	25 N	19	500000	7074000	24.0	81.9	16.9	1.2	1	–	–
191	Colvill (1982) B2	25 N	19	501000	7074000	28.1	71.8	22.8	5.4	0	–	–
192	Colvill (1982) E10	25 N	19	502000	7074000	20.4	62.0	26.6	11.4	17.2	–	–
193	Colvill (1982) C6	25 N	19	500000	7070000	24.5	69.7	26.8	3.5	0	–	–
194	Colvill (1982) E6	25 N	19	502000	7067000	32.1	82.8	16.1	1.1	0	–	–
195	Colvill (1982) E1	25 N	19	503000	7067000	27.7	75.9	19.8	4.3	0	–	–
196	Colvill (1982) E5	25 N	19	500000	7067000	16.5	75.3	22.8	1.9	0	–	–
197	Colvill (1982) E4	25 N	19	500000	7064000	19.3	62.3	29.3	8.4	0	–	–
198	Colvill (1982) E2	25 N	19	502000	7065000	36.7	76.2	21.6	2.2	0	–	–
199	Colvill (1982) G3	25 N	19	509000	7055000	15.4	74.1	22.2	3.7	0	–	–
200	Lind (1983) 58	25 N	19	509000	7050000	30.0	97.0	2.2	0.7	–	–	5.4
201	Lind (1983) 15	25 N	19	506000	7048000	40.4	85.0	13.7	1.4	0.2	–	5.2
202	Lind (1983) 24	25 N	19	509000	7047000	34.3	82.4	14.6	2.9	–	–	5.0
203	Lind (1983) 11	25 N	19	511000	7049000	39.6	81.2	17.4	1.4	0.3	–	5.6

[1]Samples are from Manley (1995, Appendix D, Tables D-1, D-2.
[2]Samples taken by other collectors by reference and sample number used in these references; – is no other reference for the sample
[3]Per cent 2–64 mm in total sediment fraction; – is no data
[4]Per cent 63 μm in total sediment fraction; – is no data
[5]Per cent 3.9– 63 μm in <2 mm fraction; – is no data
[6]Per cent <3.9 μm in <2 mm fraction; – is no data
[7]Per cent total carbonate in <2 mm fraction by Chittick method
[8]Sand, silt, and clay analyses by sieve and pipette except #177, 179–181 by sieve and hydrometer, #240–242 by sieve and SediGraph
Notes:– is no data

Sample number[1] Manley	Other collectors[2]	NTS	Zone	Easting	Northing	Gravel[3]	Sand[4]	Silt[5]	Clay[6]	Carbonate[7]	Calcite Dolomite[8]	pH
204	Lind (1983) 7	25 N	19	511000	7048000	21.7	83.4	13.2	3.4	–	–	4.7
205	Lind (1983) 169a	25 N	19	512000	7047000	15.1	95.2	2.5	2.2	0.4	–	5.8
206	–	25 N	19	514000	7045000	–	–	–	–	0	–	–
207	Lind (1983) 165	25 N	19	516000	7043000	39.1	79.7	17.3	3.0	0.2	–	5.7
208	Lind (1983) 156	25 N	19	518000	7036000	43.4	81.1	14.2	4.7	0.3	–	6.1
209	–	25 N	19	520000	7036000	–	–	–	–	0	–	–
210	Lind (1983) 142	25 N	19	522000	7033000	47.3	94.6	4.3	1.0	0.1	–	5.1
211	Colvill (1982) A6	25 N	19	521000	7032000	63.4	89.7	7.1	3.2	0	–	–
212	Colvill (1982) A7	25 N	19	522000	7031000	47.1	96.1	1.8	2.1	0	–	–
213	Colvill (1982) A8	25 N	19	524000	7030000	32.4	91.8	6.4	1.8	0	–	–
214	Colvill (1982) A5	25 N	19	523000	7032000	37.5	98.3	1.0	0.7	0	–	–
215	Colvill (1982) A4	25 N	19	524000	7032000	29.9	80.8	17.9	1.3	0	–	–
216	Lind (1983) 135	25 N	19	529000	7034000	6.4	97.8	1.5	0.7	–	–	4.5
217	–	25 N	19	526000	7031000	–	–	–	–	0	–	–
218	Lind (1983) 124	25 N	19	528000	7030000	18.3	95.4	3.7	0.9	0.2	–	5.5
219	–	25 N	19	532000	7025000	–	–	–	–	0	–	–
220	Colvill (1982) A2	25 N	19	534000	7013000	43.4	79.4	13.6	7.0	0	–	–
221	Colvill (1982) A3	25 N	19	535000	7014000	44.1	79.5	14.4	6.1	0	–	–
222	–	25 N	19	537000	7014000	–	–	–	–	0	–	–
223	–	25 N	19	538000	7014000	–	–	–	–	0	–	–
224	–	25 N	19	540000	7012000	–	–	–	–	0	–	–
225	–	25 N	19	542000	7015000	–	–	–	–	0	–	–
226	–	25 N	19	547000	7009000	–	–	–	–	0	–	–
227	–	25 N	19	549000	7011000	–	–	–	–	0	–	–
228	–	25 N	19	545000	7016000	–	–	–	–	0	–	–
229	–	25 N	19	549000	7017000	–	–	–	–	0	–	–
236	–	25 K	19	482000	6936000	0.1	40.3	56.9	2.7	0	–	5.9
237	–	25 K	19	477000	6941000	14.1	66.4	28.7	4.9	0	–	6.5
238	–	25 N	19	480000	7016000	1.8	68.5	27.1	4.4	0	–	5.5
239	–	25 N	19	464000	7008000	2.9	65.2	30.1	4.7	0	–	5.5
240	–	25 N	19	466000	7005000	10.4	70.4	27.6	1.9	0	–	5.3
241	–	25 N	19	471000	7001000	4.3	72.0	23.4	4.7	0	–	5.2
242	–	25 N	19	463000	6992000	0.9	47.0	40.4	12.5	0	–	5.2
243	–	25 K	19	467000	6979000	0.4	43.6	45.8	10.5	0	–	5.3
244	–	25 K	19	458000	6978000	8.7	83.1	13.0	3.9	0	–	5.3
245	–	25 K	19	459000	6969000	2.4	82.7	12.8	4.4	0	–	5.0
246	–	25 L	19	445000	6964000	0.7	50.5	41.5	8.0	0	–	–
247	–	25 L	19	430000	6951000	2.9	70.6	24.0	5.3	0	–	–
248	–	25 L	19	427000	6956000	13.4	86.4	11.8	1.8	0	–	–
249	–	25 L	19	420000	6961000	–	–	–	–	0	–	–
250	–	25 L	19	406000	6971000	3.8	55.3	33.3	11.4	0	–	–
251	–	25 L	19	393000	6980000	–	–	–	–	0	–	–
252	–	25 M	19	409000	6999000	12.5	56.5	39.6	3.9	0	–	–
253	–	25 M	19	406000	7006000	0.8	51.0	40.2	8.8	0	–	–
254	–	25 M	19	380000	6994000	–	–	–	–	0	–	–
255	–	25 M	19	375000	6997000	8.2	47.0	34.5	18.5	0	–	–
256	–	25 L	19	393000	6966000	0.7	43.4	50.1	6.4	0	–	–
257	–	25 L	19	407000	6958000	9.6	51.1	41.5	7.4	0	–	–
258	–	25 L	19	414000	6939000	5.2	66.3	24.7	9.1	0	–	5.7
259	–	25 L	19	418000	6939000	1.9	53.4	24.8	21.8	0	–	–
260	–	25 L	19	421000	6941000	5.0	46.5	39.3	14.2	23.6	1.1	–
261	–	25 L	19	426000	6938000	10.7	60.1	33.0	6.9	0	–	–
263	–	25 K	19	519000	6909000	34.5	84.6	12.6	2.8	0	–	6.5
265	–	25 N	19	472000	7011000	40.3	82.8	15.1	2.1	0	–	5.9
266	–	25 N	19	468000	7008000	39.2	98.3	0.9	0.8	0	–	6.3
267	Squires (1984) 4	25 N	19	533000	7068000	4.9	98.5	1.3	0.2	–	–	–
268	Lind (1983) 19	25 N	19	505000	7049000	25.2	83.0	14.5	2.4	–	–	4.5

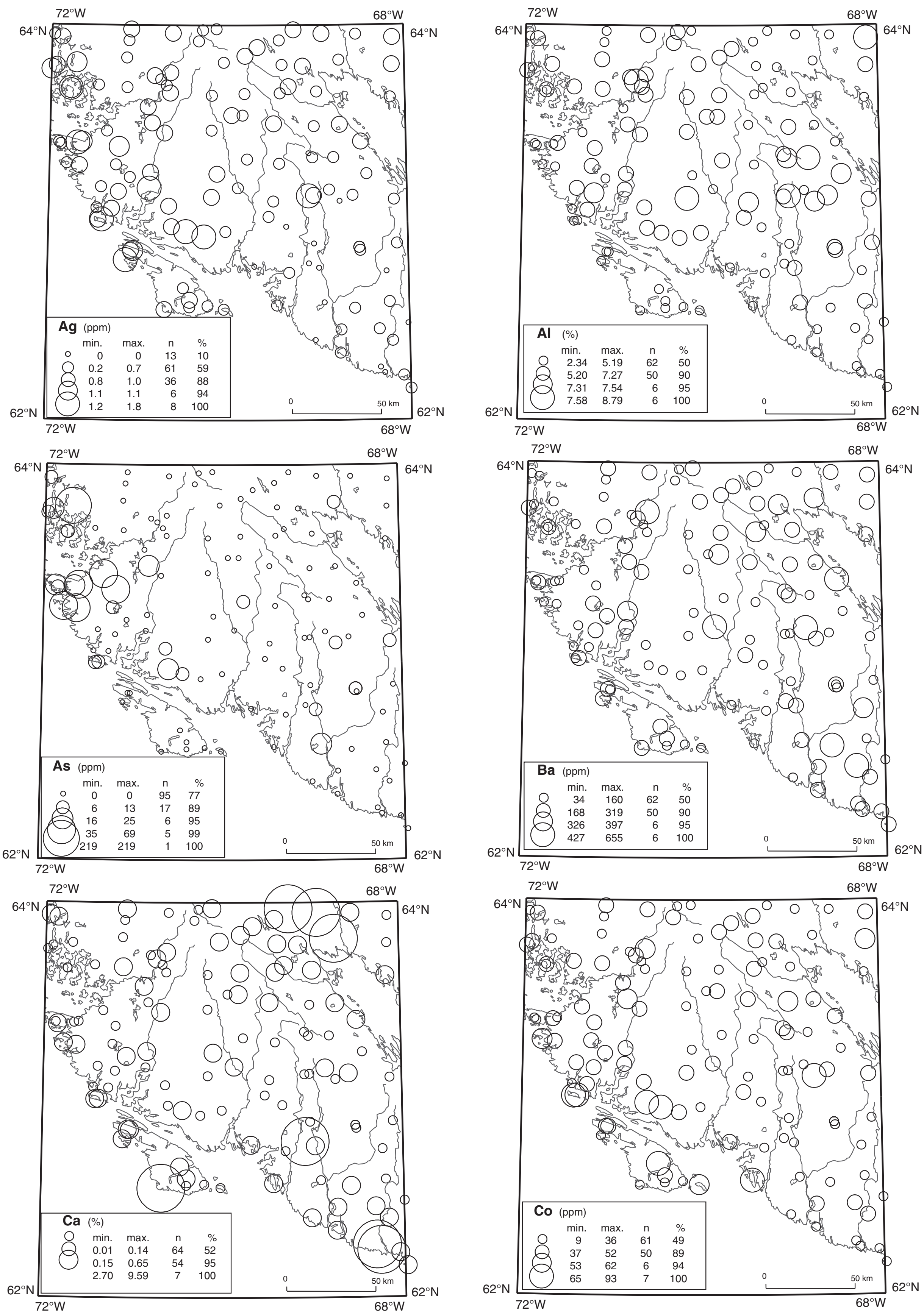

Figure 26. *Till geochemistry: geographic distribution of base-metal and trace elements from 2 μm (clay) fraction of till samples. Analytical method used was Instrument Neutron Activation Analysis (INAA).*

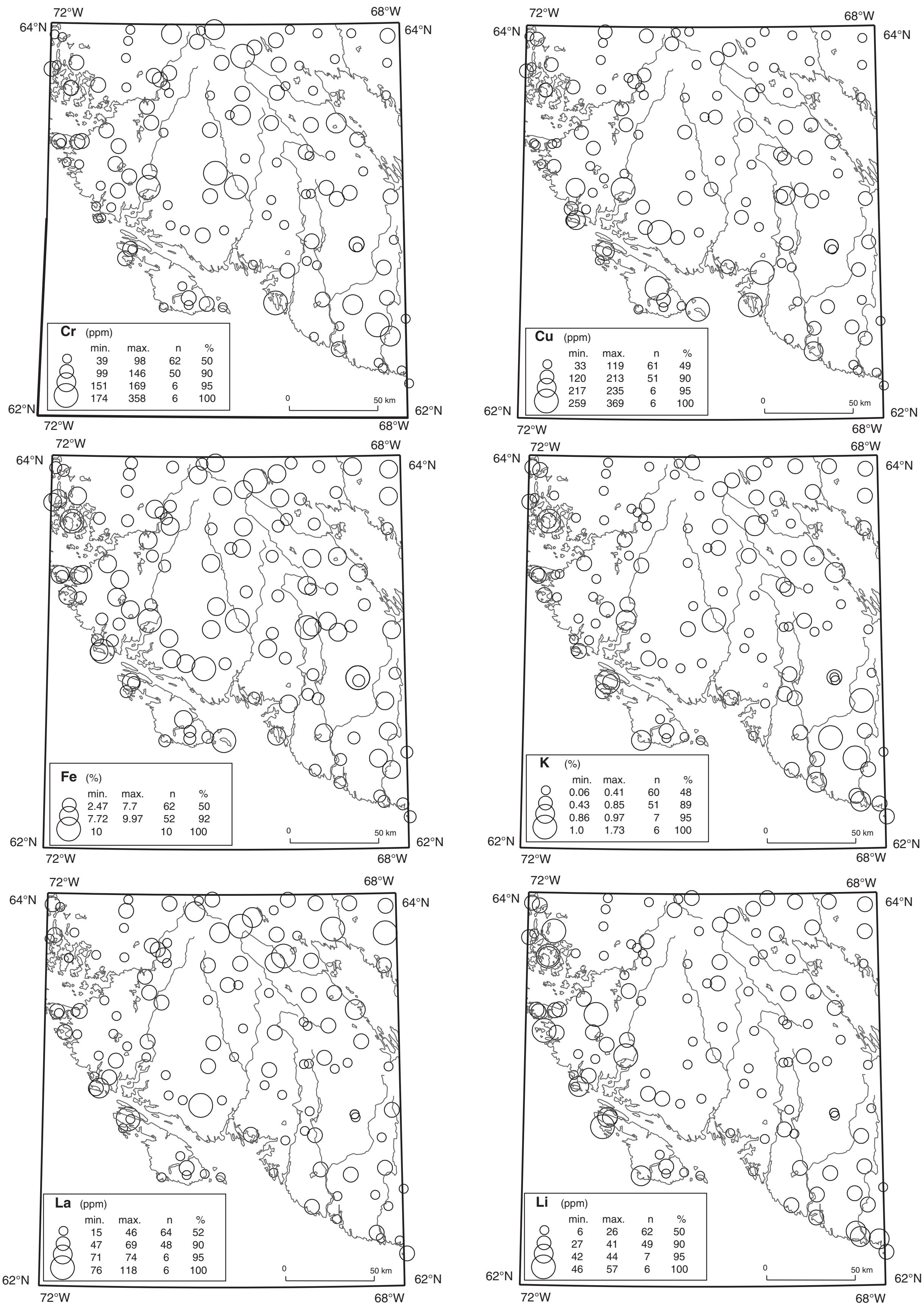

Figure 26 *(cont.)*

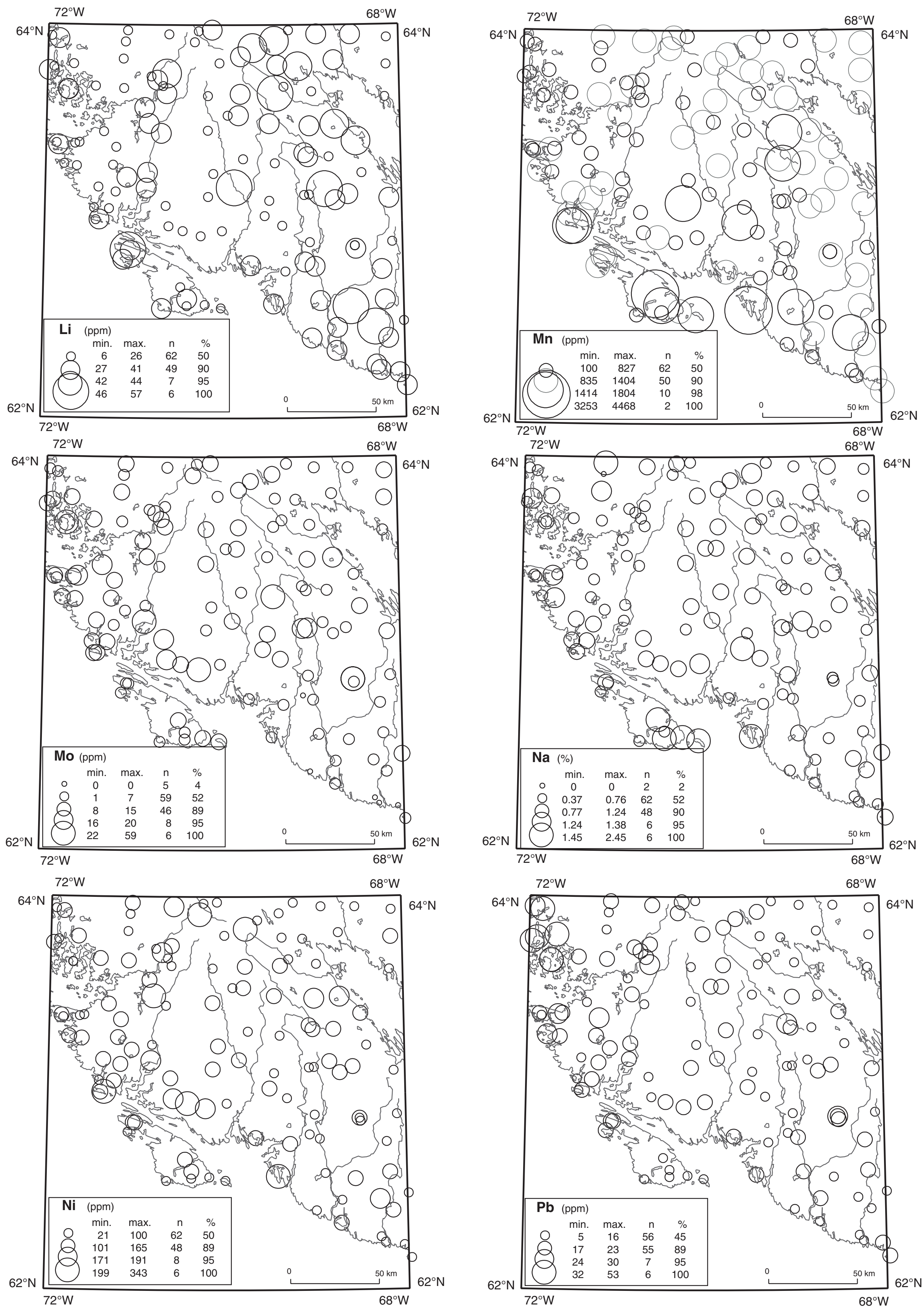

Figure 26 *(cont.)*

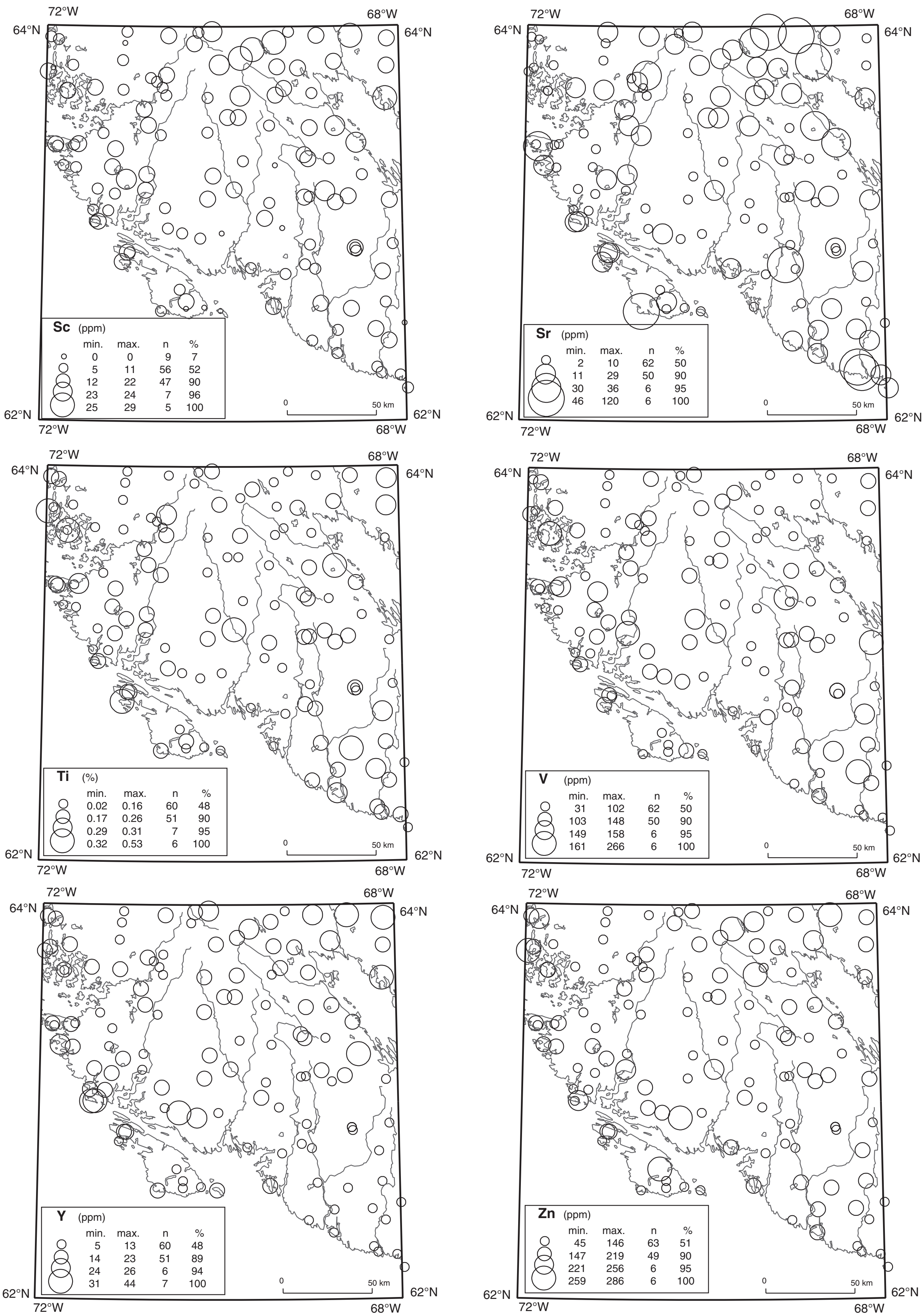

***Figure 26** (cont.)*

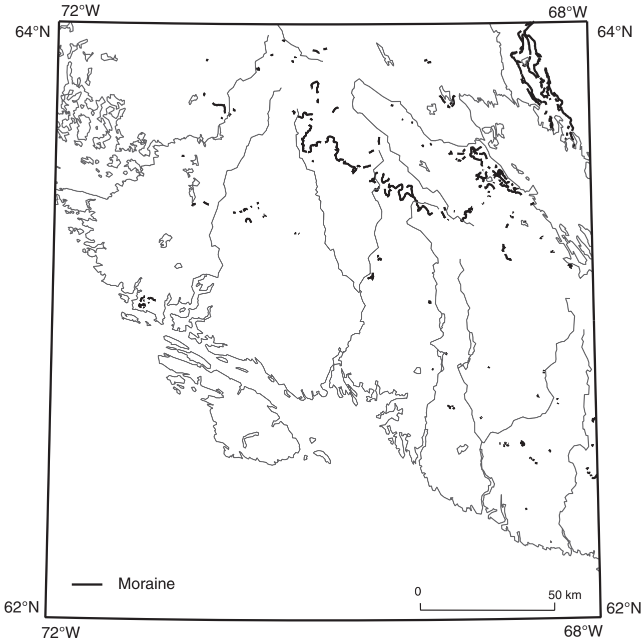

Figure 27. *End moraine and interlobate moraine ridge distribution.*

Figure 28. *Bouldery interlobate moraine knobs, foreground and background, on a drainage divide east of the river flowing to the head of Shaftesbury Inlet. Boulders to 4 m diameter, knolls to 50 m high. Photograph by D.A. Hodgson. GSC 2001-379F*

summit on the outer coast west of Crooks Inlet. These moraines mark the recession, or even the maximum position, of presumed southwest-flowing ice (southwest-oriented striations were found). Short lengths of recessional and/or minor readvance moraines are scattered across the mid-section of the western flank of Meta Incognita Peninsula. From west of Ramsay River to the river flowing into the head of Shaftesbury Inlet a few southward loops into valleys indicate associated ice flow to the south or southwest. Only shield rocks were observed in the moraines visited. From Shaftesbury Inlet drainage to the eastern margin of Map 2044A (on CD-ROM), several minor complexes of moraines and glaciofluvial deposits, observed only on airphotos, imply that an ice margin extended east-southeast. The distal and/or proximal sides of these features are not obvious from the airphotos; it is possible, but by no means certain, that they record the northern margin of onshore-flowing ice, where it met Meta Incognita Peninsula ice. Certainly, onshore-flowing ice did not extend farther north.

Frobisher Bay Moraine System. This most prominent glacial feature in the map area was treated as a single landform by Blake (1966) and Miller (1980), and was named the "Frobisher Bay Moraine" by Miller (1980). In fact, it is a system of landforms varying from sheets of thick till with few moraine ridges in a zone up to 15 km wide in the southwest, to a 10 km wide complex of ridges adjacent to Frobisher Bay. It is divided for this report into three sectors, covering the west and east flanks of Meta Incognita Peninsula and, across Frobisher Bay, the west flank of Hall Peninsula. Each sector has differences in landforms, though all sectors have thin or no till distal to the moraines and thick proximal till that suggests a readvance under changed glacial conditions rather than a simple stillstand. The composition of till in the moraine system is the typical bouldery silty sand described above.

In the western sector, the readvance combined with the concurrence in dip of the former ice surface, regional topography, and main valleys to form a sinuous ice front (Fig. 19). Commonly this readvance is marked by an abrupt thickening of till. Subdued moraine ridges occur locally at the distal limit of thick till and up to several kilometres proximal. To the west, the Frobisher Bay Moraine System was traced up to the river draining into the head of Blandford Bay, on interfluves 375 m a.s.l. In the east, the thickened till margin swings east and northeast across the height of land (at 750 m a.s.l.), an observation supported by the orientation of striations (Fig. 17). The till blanket has dammed a number of lakes along the upper course of the Armshow River.

The ice in the eastern sector of the Frobisher Bay Moraine System pushed upslope against Hall Peninsula with an ice front apparently parallel to pre-existing drainage, hence the linear ice front. Moraines rise from below marine limit in the south to 350 m in the north. Northeast of the map area, Blake (1966) showed traces of an end moraine crossing Hall Peninsula. There is a sharp contrast between thick till and glaciofluvial deposits of the moraine system and distal bedrock (Fig. 30). Squires (1984) identified five stillstands in a belt up to 9 km wide, recorded by till ridges up to 40 m high, but more commonly less than 10 m. The ridges break, bifurcate, or crosscut in several places, making an exact tally of stillstands difficult. Squires (1984) suggested that a subaerial ridge is superimposed on a subaqueous moraine in the lower 'Tasiujarjualaaq River' (Squires (1984) used the name 'Tatsiujarjualag River'; 'Tasiujarjualaaq' is the current local name for Burton Bay).

The moraine pattern on the east flank of Meta Incognita Peninsula is more complex than in the other sectors, mainly due to topography. Within the steep overall rise from tidewater to height of land, there are a number of valleys both parallel and transverse to the bay, isolating numerous bedrock ridges

Figure 30. Oldest (distal) Frobisher Bay Moraine System ridge (right centre, 10 m high) overlapping bedrock of Hall Peninsula, 12 km east of Iqaluit. Photograph by D.A. Hodgson. GSC 2001-379G

and knobs. Chains of moraine ridges loop around the knobs and re-enter valleys between Cape Rammelsberg and Bay of Two Rivers, as described by Colvill (1982) and Lind (1983). Farther inland, towards the height of land, terminal moraines trace several valley glaciers that descended to small piedmont lobes in cross-valleys (Fig. 31).

Small subaqueous push moraines. About 30 short, linear, cross-valley ridges were mapped in middle reaches and adjacent tributaries of the Armshow River where it is deeply incised into the upland surface. Raised shorelines in the same valley indicate a water depth of 200 m dammed by ice retreating downvalley to the southeast. The single field observation showed typical stony till, possibly more sandy towards the valley centre, in ridges measuring 500 m long and a few metres high, extending part-way up valley sides (Fig. 32). These are assumed to be annual subaqueous push moraines commonly known as De Geer moraines. Extrapolating the number of moraines, the lake existed for several hundred years. A few sets of similar moraines were mapped in other confined valleys between Frobisher Bay and the peninsula height of land.

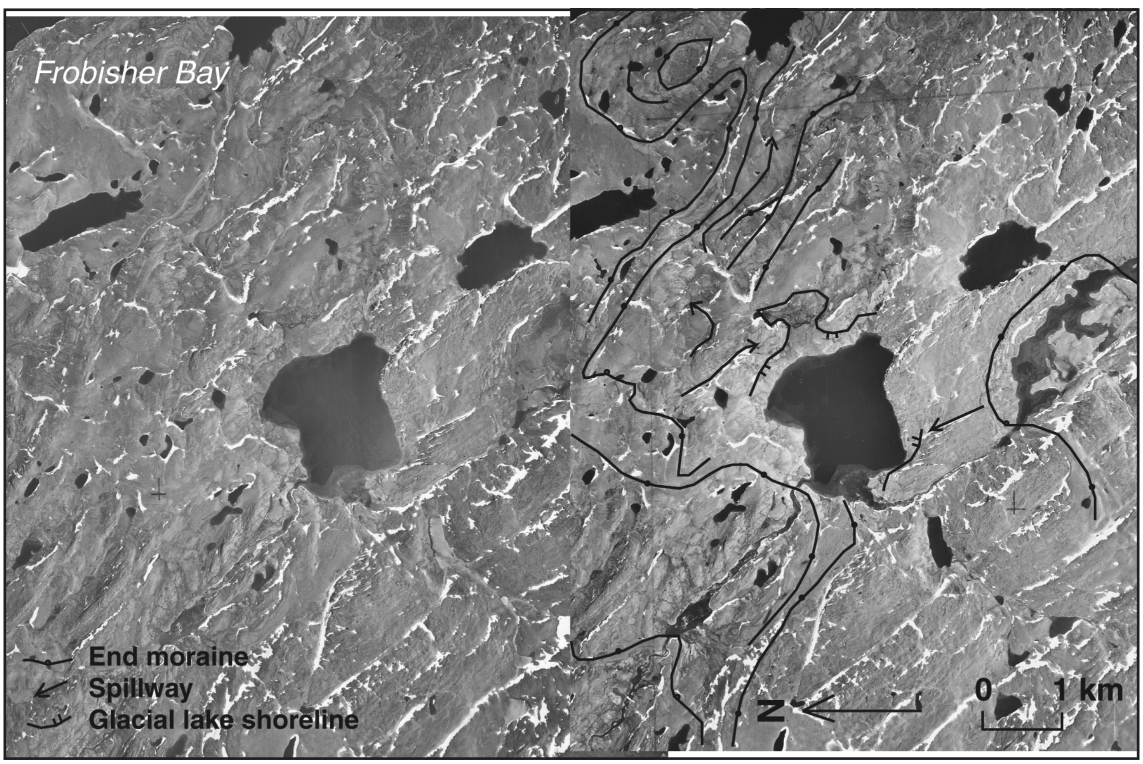

Figure 31. Stereo-pair of Frobisher Bay Moraine System on the southwest flank of Frobisher Bay (top left corner), west of Cape Rammelsberg (domain 4b). Successive lobes of readvancing ice from the Frobisher Bay glacier pushed southeast (left side), while a contemporary glacier (part of the Frobisher Bay Moraine System) descended from the Meta Incognita Peninsula height of land (right). Reduced 75% from NAPL A16165-53, A16165-54.

Figure 32. Subaqueous push moraines, 5 m high, running into a ponded section of the Armshow River (flow southeast, away from observer). Photograph by D.A. Hodgson. GSC 2001-379H

Periglacial landforms in till

Patterned ground is discontinuously present on thick and thin till. The critical factor in distribution of sorted patterns in the map area appears to be presence of sand or finer material — sorting is uncommon in coarse-grained, clast-supported till. Patches of finer material (whether part of the till or washed in by later glacial or nonglacial processes) are sufficiently widespread for frost boils to be common. Sorted nets and stripes are less common. Ice-wedge troughs resulting from frost fissures and ice wedges were observed mainly on thick till, especially hummocky till, which is commonly clast supported. Solifluction lobes are common on moderate to steep till-veneered slopes, and also occur on some slopes covered by a till blanket. A few detachment slides were observed in till veneer, with the failure plane at underlying, relatively smooth bedrock.

Glaciofluvial deposits

Deposition

Subglacial deposits

Eskers. Eskers are rare in the map area. Nonetheless, they were found both proximal and distal to the Frobisher Bay Moraine System and in the southeast zone of possible onshore flow, generally aligned with the regional ice-flow direction even where this crosses topographic grain. They are all single ridges not exceeding 10 km in length. The largest esker segment is an exceptional 27 m high where it crosses a valley (Fig. 33), but typically they are less than 10 m high (Fig. 34). Composition is cobbles, finer gravel, sand, boulders; minor sand and gravel segments occur. Eskers do not occur in the same valley reaches as flights of lateral drainage channels.

Proglacial deposits

Most proglacial deposits are associated with the Frobisher Bay Moraine System, hence their rarity in the southeast part of the map area (Fig. 35). Composition is mostly sand and gravel, though boulders and cobbles are locally dominant in narrow channels confined by bedrock. Where unvegetated, deflation has concentrated a thin lag of gravel or larger material. Most deposits are less than 10 m thick, but they can be as much as 30 m.

Kame terraces. Small terraces occur sporadically on valley sides throughout the map area, more particularly at ends of rock-cut lateral drainage channels. Extensive kames formed in the Frobisher Bay Moraine System belt on the west side of Frobisher Bay, where ice lobes filled or drained through valleys paralleling the shore (Blake, 1966).

Figure 33. Very large (for the map area) gravelly sand esker, up to 27 m high, between Markham Bay and Ramsay River. Photograph by D.A. Hodgson. GSC 2001-379I

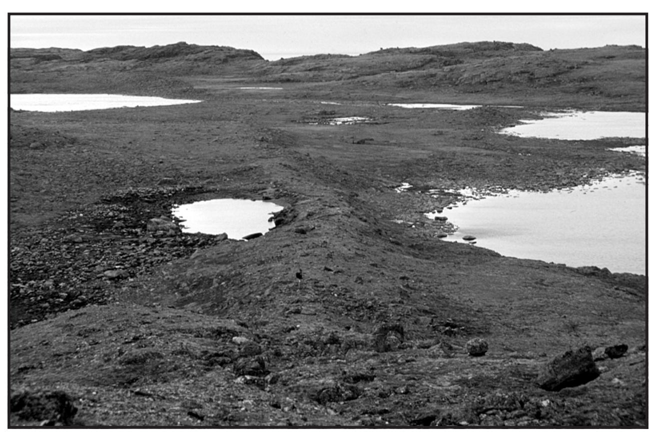

Figure 34. Small bouldery esker, typical of the few eskers in the map area; east of Wight Inlet. Photograph by D.A. Hodgson. GSC 2001-379J

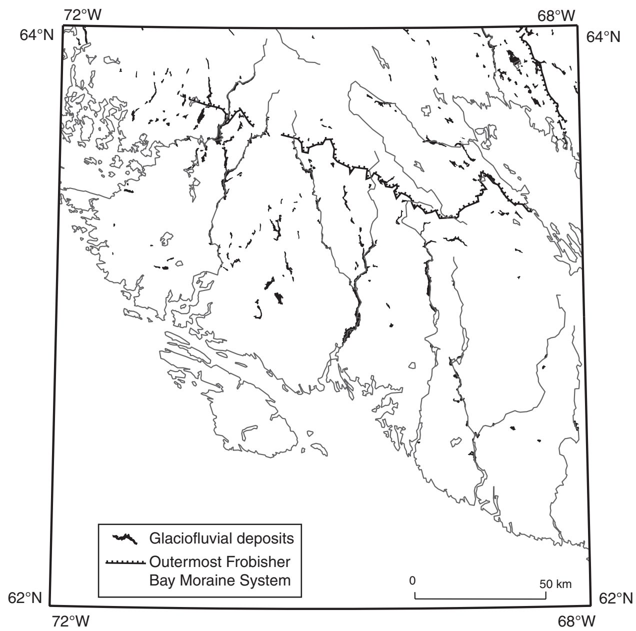

Figure 35. Relationship of main glaciofluvial deposits to Frobisher Bay Moraine System.

Figure 36. Kettled, valley-train gravelly sand, within the river valley draining to Blandford Bay. Tents in center of photograph for scale. Photograph by D.A. Hodgson. GSC 2001-379K

Sandar. Several large kettled outwash fans (>10 km^2) or small sandar were deposited into intermorainal basins on the east side of the Frobisher Bay glacier.

Valley trains. No sandar were deposited in front of the western sector of the Frobisher Bay Moraine System. The ice lobes drained into steep valleys that generally carried outwash to middle reaches of the major south-draining rivers before deposition. Trains of outwash run continuously for up to 50 km (e.g. Soper River); others are broken by kettle lakes and rock constrictions (Fig. 35, 36). Some outwash between Markham Bay and Soper River and around Jaynes Inlet was deposited from ice fronts distal to the Frobisher Bay Moraine System; other trains clearly postdate the retreat of ice from the head of Frobisher Bay (e.g. Sylvia Grinnell River). Outwash that originally filled valley bottoms up to 2 km wide has been dissected to varying degrees by postglacial drainage, commonly leaving terraces and a narrow modern floodplain.

Meltwater erosion

Subglacial erosion

There are isolated examples of subglacial (Nye) channels; most are small, with discontinuous courses or even reverse gradients. Water-scoured zones up to several kilometres wide occur in the local concentration of eskers in the vicinity of Sylvia Grinnell River. Several short (1 km) channels on the east margin of the map area, south of the peninsula height of land at 450 m, have plunge pools in their courses before terminating at fans. They are the westernmost links in a series of channels and deltas that extend 50 km east down the Meta Incognita Peninsula to where the 'York gorges' run northeast, transecting the peninsula. East of the map area, some of the channels terminate at major north-south valleys into which deltas with conventional subaerial forms have been deposited. Submarginal sheet flow may have washed fines out of till to leave extensive block fields. Some very large areas of bare to bouldery bedrock with sharp contacts with till blanket (e.g. area around the head of Crooks Inlet) could be meltwater-scoured zones, though in other areas topography on and around scoured rock makes a fluvial origin highly unlikely.

Subaerial erosion

Many existing watercourses have been enlarged by meltwater flow; however, the most informative channels are the largely abandoned lateral channels that outline former ice margins.

Lateral channels. Flights of meltwater drainage channels are locally abundant on valley sides or escarpments immediately distal to the Frobisher Bay Moraine System south of the Meta Incognita Peninsula height of land, and in and between the Soper and Ramsay drainage basins (Fig. 37). Flights occur also on proximal (northeast) slopes of coastal upland southeast of Markham Bay. The flights are commonly cut into outwash (i.e. they are coterminous with kame terraces) or till, and less commonly into bedrock. East of the Soper River, most channels are on the west side of valleys; in the Soper River valley they are on the east side; no explanation is obvious. The channels may record annual glacier margin retreat (Dyke, 1999). In the Ramsay River valley there are probably dozens or even hundreds of mostly poorly defined channels in a 50 km distance. Distribution of flights of channels in the Canadian Arctic is normally restricted to areas of formerly cold-based ice margins in the northern Arctic Islands, though they also occur in the Cordillera (Dyke, 1993).

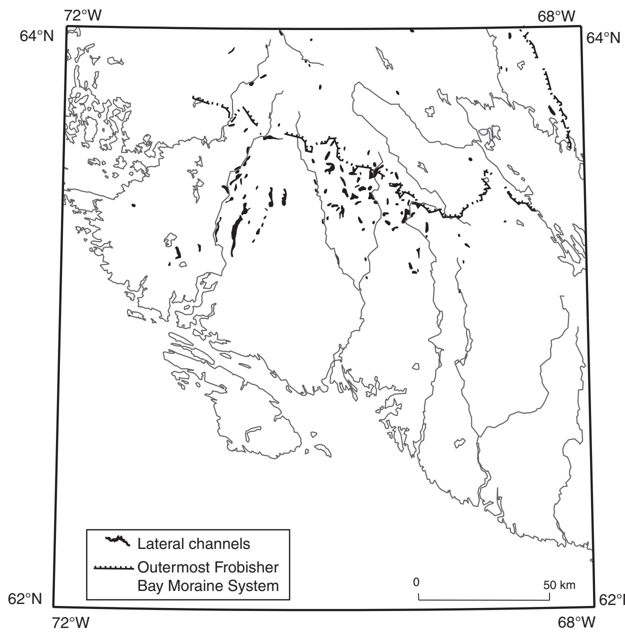

Figure 37. Concentrations of flights of lateral meltwater drainage channels.

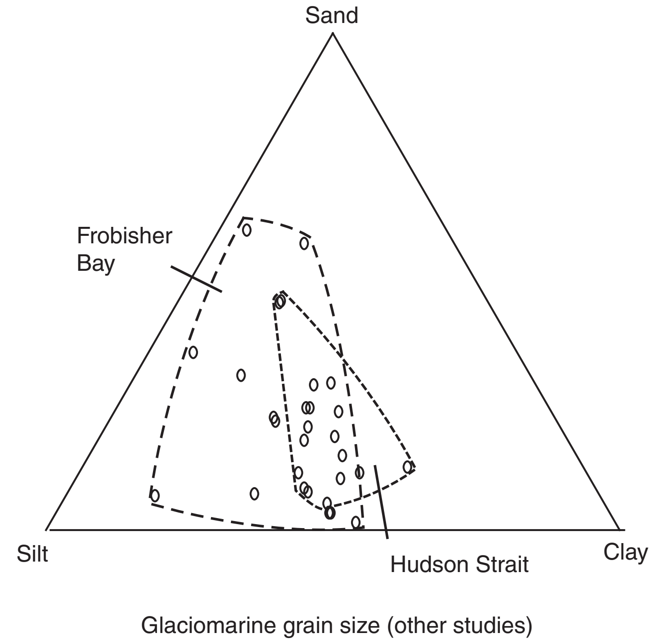

Figure 38. Texture of glacial marine sediments (nearshore and offshore) collected by other studies from vicinity of inner Frobisher Bay (Colvill, 1982; Lind, 1983) and Hudson Strait coast in the map area (Manley, 1995). Grain-size analysis by sieving and sedimentation into sand (2 mm to 63 µm), silt (<63 µm to 4 µm), and clay (<4 µm) fractions.

Glaciolacustrine deposits

The rugged topography and mostly upslope retreat of ice fronts west of the height of land gave rise to only minor glacial lakes and no measurable thickness of glaciolacustrine sediments. By far, the largest lake was east of the divide, outlined by a discontinuous trim line and scattered perched deltas at 490 m elevation in the middle Armshow River valley. The lake was dammed by a downriver-retreating ice mass in the valley with successive fronts at subaqueous moraines. The 30 km long lake spilled southwest across the peninsula divide, but was 200 m deep at the east end. There are traces of lower shorelines from later ice-retreat stages.

Squires (1984) described several proglacial deltas built into ice-dammed lakes along the 'Tasiujarjualaaq River' within the Frobisher Bay Moraine System belt east of Frobisher Bay. These sand and gravel features are not differentiated from glaciofluvial deposits on Map 2042A (on CD-ROM). Perched glaciolacustrine deltas immediately east of Iqaluit that are too small to map are built of up to 10 m of silty sand. Some of these deposits have been exploited in borrow pits.

The Frobisher Bay glacier dammed lakes among the moraines and kame terraces inland of the west shore of the bay (Blake, 1966; Colvill, 1982; Lind, 1983). The evidence is shorelines, perched deltas, kame terraces, and spillways (Fig. 31). A few glacial lakes elsewhere in the map area are partially outlined by trim lines or beaches of sand and rounded cobbles.

Glacial marine deposits

Sedimentation of outwash and ice-rafted detritus into proglacial seas in the map area occurred in a range of environments from ice-contact deltaic to offshore. Glacial marine sediments, which are predictably finer than the till (Fig. 38), are now exposed on a narrow strip of the mostly steep coastline that was previously immersed in the raised sea. The postglacial fall in sea level varies from a minimum of 28 m at the head of Frobisher Bay to at least 140 m at on a segment of Hudson Strait coast.

Raised deltas

Where valley trains reached the sea, they terminated as deltas. Composition is typically similar to outwash: medium- to coarse-grained sand with minor gravel; in a few instances boulders predominate at delta apices. The deltas are Gilbert-type in shape; however, the rarity of exposures in them means there is only scattered evidence that the coarse sediments prograded over fine-grained bottomsets (e.g. Porter Inlet: Manley and Jennings (1996, p. 101); Lewis Bay: Andrews and Short (1983, p. 25); Koojesse Inlet: McCann et al. (1981)). On the east side of Frobisher Bay, valley trains terminating in deltas include the 5 km^2 'Iqaluit' delta where a proto-Sylvia Grinnell River formerly flowed to Koojesse Inlet. Other deltas were deposited at the heads of Burton and

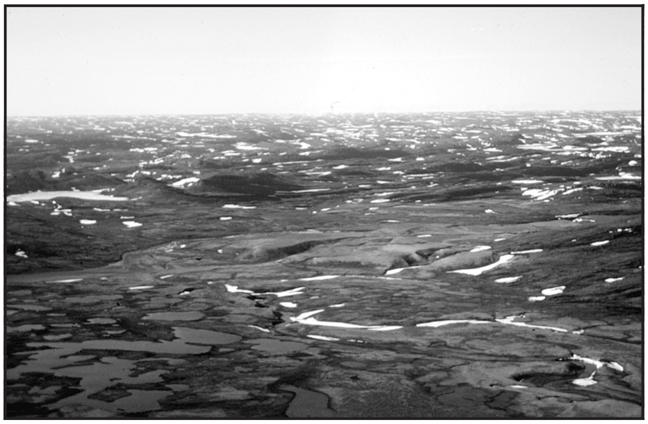

Figure 39. Raised glacial marine delta; meltwater flow right to left, bluffs 50 m high. Head of Blandford Bay, eastern Markham Bay. Photograph by D.A. Hodgson. GSC 2001-379L

Lewis bays; perched ice-contact deltas are present at the head of Tarr Inlet and at Apex Hill. On the west side of Frobisher Bay, between Bay of Two Rivers (Armshow River) and Eggleston Bay, there are numerous perched marine deltas associated with kame deposits as well as valley-train deltas. On Hudson Strait, large valley-train deltas formed in Blandford Bay (Fig. 39) and where the Ramsay River enters Crooks Inlet. The raised delta, at 69 m a.s.l., may have been built by outwash from the Frobisher Bay Moraine System, 20 km to the northeast. A small delta to the south, at 73 m, is related to a closer ice front, though it lies 22 m below a beach. At the head of Crooks Inlet, the main delta lies at 70 m a.s.l., 30 m below the marine limit, indicating most deposition occurred subsequent to Crooks Inlet deglaciation, probably at the same time that ice stood at the Frobisher Bay Moraine System, 60 km to the north (though note comments on tidal range in 'Marine limit' section). A 90 m a.s.l. elevation delta, 2 km down the inlet, was deposited by meltwater from an ice front less than 20 km inland. The Soper River valley does not contain a glacial marine (raised) delta: fluvial processes subsequent to the highest postglacial sea level eroded any deltas and continued prograding sediment down the rock-confined valley as it emerged. Valley-train and perched ice-contact deltas are common around the deep inlets of northern Markham Bay. Most are probably contemporaneous with deposition of the Frobisher Bay Moraine System. Raised deltas are rare on the Hudson Strait coast from Big Island eastwards, except for inner Barrier Inlet.

Nearshore and offshore deposits

Thick glacial marine sediments were identified only in Frobisher Bay, mainly associated with the Frobisher Bay Moraine System ice front in the vicinity of Cape Rammelsberg, in lesser deposits around Burton Bay, and at the head of Frobisher Bay. On airphotos extensive deposits have a characteristic dark tone (indicating they are well vegetated) and a distinctive lighter-toned rill pattern. The Cape Rammelsberg lowland is draped with a thick blanket of glacial marine sediments composed of bedded sand, some massive silty clay units, and a discontinuous veneer of large clasts. Several composite sections compiled by Lind (1983) were interpreted by her, on the basis of sediment analysis and foraminifera assemblages, as indicating a progression from outer proximal glacial marine to distal glacial marine to nearshore marine environments. Lind (1983, Fig. 4.8) also found glacial marine sand content increased from 10% offshore to 60–100% nearshore. Some of the deposits shown as marine veneer in the vicinity of Jaynes Inlet and on adjacent islands are likely glacial marine blankets. Surface samples collected by Lind (1983) from the Cape Rammelsberg and Jaynes Inlet areas have a fine-grained composition (Fig. 38) quite different from till composition. Carbonate content is clearly higher with a mean pH of 8.0 compared to 5.3 for Lind's (1983) till samples from above marine limit.

For the Hudson Strait coast below marine limit eastwards from (and including) Big Island, Manley (1995, 1996) identified calcareous silty diamicton as a glacial marine sediment, recognizing it as distinctly different from till above the marine limit (Fig. 38). It is not mapped (Maps 2044A, 2045A, 2048A, on CD-ROM) because it commonly forms only a discontinuous veneer, though here and around Frobisher Bay, small areas of thicker deposits probably underlie some of the marine veneer unit. Characteristics of glacial marine sediments along Hudson Strait include presence of Paleozoic limestone clasts and mollusc valves, a total weight per cent carbonate content commonly more than 30% , pH of 8.0, and predominantly silty composition compared to the silty sand till. Manley (1995) suggested sediments came from a limestone-bearing, calving ice margin, not necessarily in Hudson Strait.

Marine limit

Since Watson's (1897) observation of a washing limit on Big Island, numerous measurements of the limit of the postglacial marine inundation have been made, mostly using as a datum for altimeter readings the higher high-tide or storm-water mark (Blake, 1966; Matthews, 1967; Miller et al., 1988; this study), the mean high tide (Squires, 1984; Manley, 1995, 1996), or the top of the shore-fast ice foot where this obscured the shoreline (this study). Topographic maps of the area use mean sea level as datum. In the absence of good field evidence (see below) or of modelling of any tidal changes through the Holocene for the region, it must be assumed that present macrotidal conditions, with up to a 12 m range for large tides in Hudson Strait at Big Island and for inner Frobisher Bay, have continued since the opening of Hudson Bay between 9 ka and 8 ka, created an approximation of the present coastline. Prior to this, but following westward retreat of a Hudson Strait glacier, the ice-blocked strait may have contained equally high tides. The most widespread indicator of marine limit in the map area is a washing limit, usually recorded by the contact between bare wave or sea-ice-scoured rock and rock bearing either numerous glacier-transported boulders or unmodified till. Where discernible, usually on a moderate slope that was exposed to open sea, the contact may be sharp (bare rock to thick till or block field in a distance of 1–2 m, Fig. 40), gradational over many metres, or deformed by solifluction. Sea-ice thrusting and wave wash can extend the washed zone several metres above the highest tide level. Marine-limit beaches are rare; rounded cobble deposits are present preferentially in small cols which mostly lie several metres or more below any adjacent washing limits (Fig. 41). Nearshore glacial marine sediments might extend close to high-tide level. Ice-contact glaciofluvial sediments meeting the glacial marine environment (e.g. at deltas) grade to low-tide level. Hence, any difference in elevation between a washing limit and an adjacent ice-contact (i.e. contemporaneous) raised delta surface might give an indication of tide range at the time of formation. Clear examples of such pairs were not measured in the map area, though possible examples in Markham Bay and Crooks Inlet are noted below.

Marine limit southeast of the Frobisher Bay Moraine System at Cape Rammelsberg, on shores and islands of Frobisher Bay, was measured widely up to 122 m a.s.l. (Fig. 42) by Colvill (1982), Lind (1983), and Manley (*in* Manley and Jennings, 1996). Exceptionally, Manley (1995) recorded 129 m a.s.l. in Eggleston Bay, but only 114 m, 5 km to the north on Pugh Island. These are all washing limits. Blake (1966), Colvill (1982), Lind (1983), Manley (1995), and the present study measured several ice-contact and

Figure 40. *Limit of postglacial marine incursion where washed bedrock meets till blanket (sitting person for scale). Photograph by D.A. Hodgson. GSC 2001-379M*

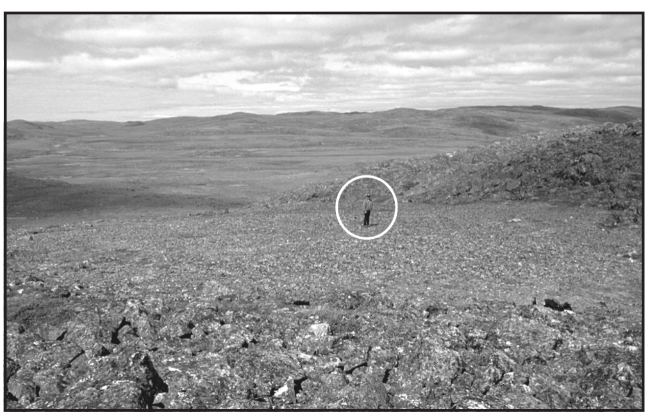

Figure 41. *Cobble pocket beach occupying a col close to marine limit, west of Wight Inlet (person for scale). Photograph by D.A. Hodgson. GSC 2001-379N*

valley-train deltas 10–20 m lower than marine limit, which is consistent with present tidal range. Southeast of the map area, Jacobs et al. (1985b) plotted a downbay decline in marine limit. Northwestwards from Cape Rammelsberg, washing limits and raised deltas also decline in elevation (Lind, 1983, Fig. 3.2) to a 28 m washing limit and 24 m highest raised beach at the head of the bay (Foul Inlet). Isolines for Frobisher Bay marine limits are drawn coast to coast across the bay, except for the valley west of Jaynes Inlet where an ice-contact delta formerly flanking east-flowing (Meta Incognita Peninsula) ice lies only 48 m a.s.l. (Manley *in* Manley and Jennings (1996)). This latter site indicates an isoline trend parallel to the Meta Incognita Peninsula axis.

On the northeast shore of Frobisher Bay, the highest recorded marine limit in the map area is a 119 m a.s.l. washing limit near Lewis Bay (Squires, 1984). This is immediately distal to the outermost Frobisher Bay Moraine System, and at a similar altitude to marine limit at Cape Rammelsberg on the opposite side of Frobisher Bay. As at the latter location, marine limit declines northwestwards (Squires, 1984, Fig. 15); the steepest drop is across the moraine system (Fig. 42). The washing limit is 103 m at the outermost moraine ridge at Lewis Bay (Squires, 1984) and 96 m proximal to this ridge in Porter Inlet (Manley *in* Manley and Jennings (1996)). On the distal side of this moraine ridge, within the 'Tasiujarjualaaq River' valley, it is 40 m (Squires, 1984) and at Apex Hill, proximal to the moraine system, about 30 m (Blake, 1966). Both Bird (1967) and Matthews (1967) suggested a 45 m washing limit for the Iqaluit area though replicate observations have not been made. From here, marine limit is subhorizontal to Peterhead Inlet (29 m; Squires (1984)) and the head of Frobisher Bay. The highest known delta built by meltwater from the Frobisher Bay Moraine System is north of the head of Lewis Bay, at 96 m a.s.l.; a glacial marine delta distal to the outermost Frobisher Bay Moraine System at the head of Lewis Bay is only 42 m a.s.l. (Squires, 1984). At the head of Burton Bay, proximal to outermost moraines, a large delta at 35 m a.s.l. has a smaller 43 m segment (Squires, 1984), apparently at the same height as washing limits. The small 27 m a.s.l. delta at the head of Tarr Inlet was deposited at an ice front in the inlet lying proximal to the innermost Frobisher Bay Moraine System. Blake (1966) and Matthews (1967) measured the ice-contact Apex Hill delta 21–24 m a.s.l.; the seaward limit of the much man-modified Iqaluit airport delta, terminating the Sylvia Grinnell River outwash train, is less than 20 m a.s.l.

For the segment of Hudson Strait coast that lies in the map area, subsequent to Watson's (1897) 90 m a.s.l. record of a washing limit on Big Island, Blake (1966) measured 110 m on southern Big Island and 87 m in the lower Soper valley, similar to Clark's (1985) determination of 90 m at Kimmirut (Lake Harbour); however, it was Manley's (1995, Fig. A-1, 2) numerous measurements of washing limits as far west as Canon Inlet that clearly indicated a consistent westward rise in marine limit, from 55 m at Wight Inlet to 141 m in the west (Fig. 42). Manley's (1995) isolines of emergence generally show less emergence inland. Manley's (1995) Figure A-2 isolines were drawn to link the southeasterly declining marine-limit elevations on both the Hudson Strait and

Frobisher Bay shores of Meta Incognita Peninsula; however, it is appropriate to realign the isolines to accord with the trend in Manley's (1995) Figure A-1: i.e. declining towards the axis of Meta Incognita Peninsula. This is supported by washing limit observations from Markham Bay, showing a decline eastwards from 135 m to 97 m along the south shore of the bay, and from 145 m on Hector Island (west of the map area in Hudson Strait) to 72 m inland from Ava Inlet northeast of the bay. The spot measurements show an irregular decline in the plane of the marine limit. Through much of the bay it is 100–90 m a.s.l., but in the southeast corner, it appears to decline from 120 m to 95 m in less than 20 km. As noted above, the valley train in the Ramsay River valley terminates in Crooks Inlet at a delta 70 m a.s.l., well below the local marine limit of 98 m. Similar differentials were observed in eastern Markham Bay (e.g. a 69 m delta and a 95 m washing limit at Blandford Bay), whereas northeast of Ava Inlet, the difference in elevation between deltas (60 m) and washing limit (72 m) is within the present tidal range.

Marine veneer

Raised nonglacial marine deposits of mappable extent are restricted to veneers over till blanket that survived immersion and washing, or to fine-grained glacial marine sediments that were modified by regressing shoreline processes. Complexes

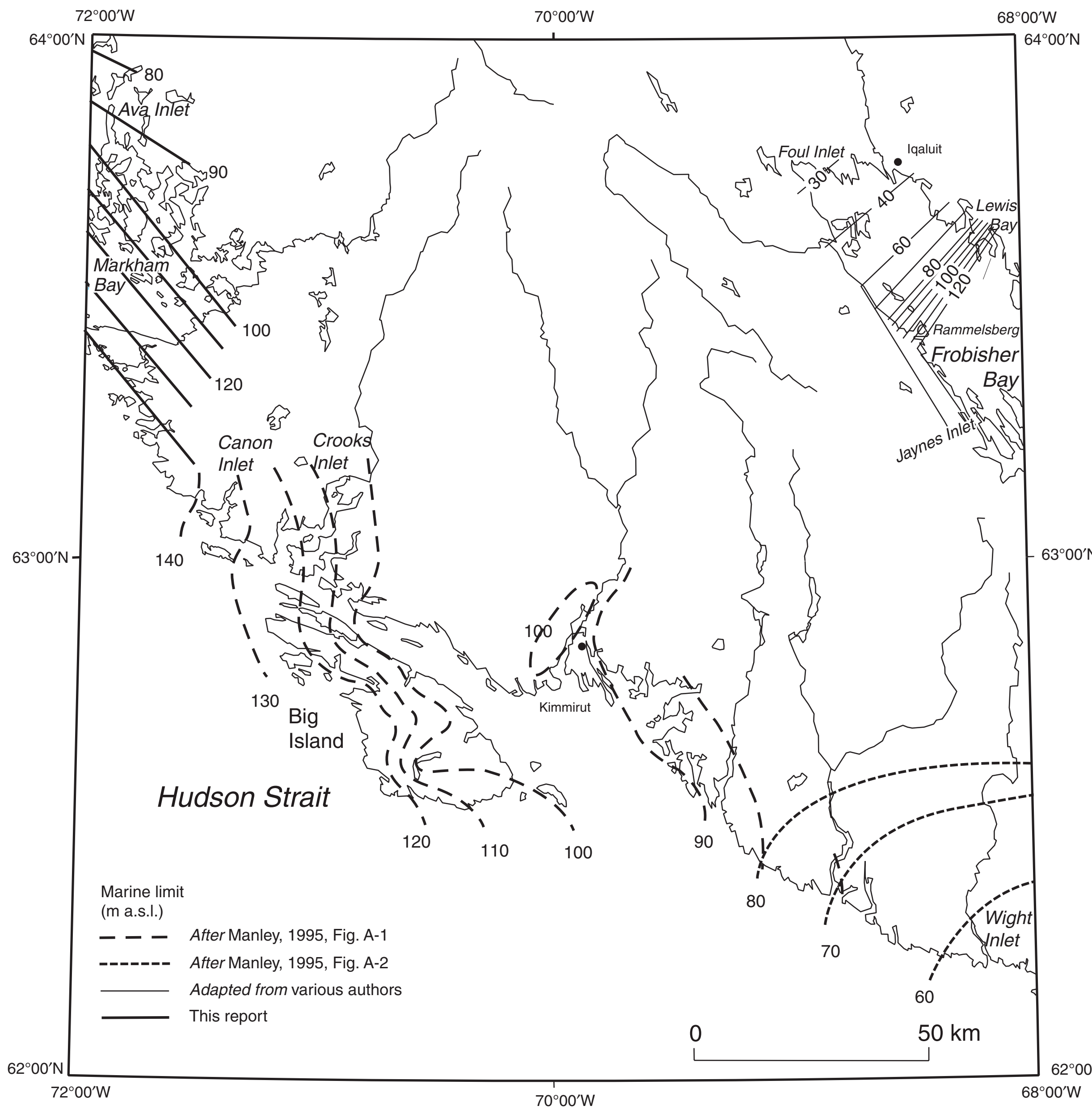

***Figure 42.** Marine limit isolines: new data used for Markham Bay; elevations for Frobisher Bay are from numerous sources (*see *text); Hudson Strait coast isolines* after *Manley (1995, Fig. A-1, A-2).*

of beach ridges are indicated by symbol on the maps. By far the most extensive area is southeast of Markham Bay, adjacent to and probably overlying thick till, where poorly organized flights of beaches to 102 m a.s.l. are composed of sand- to boulder-size material. Watson (1897) observed raised beaches scattered around Big Island. The smaller deposits elsewhere range through bouldery gravel to stony mud to clayey silt. Colvill (1982), Lind (1983), and others described postglacial marine terraces down to 14 m a.s.l. cut into glacial marine deposits of Cape Rammelsberg and Jaynes Inlet areas. Matthews (1967) described similar terraces at Iqaluit–Apex Hill.

Modern shoreline

Coastal waters in Frobisher Bay and along Hudson Strait are macrotidal and covered by ice for 8–9 months per year, which reduces the intensity of wave action. The semidiurnal tides have a mean large range of 12.6 m on southern Big Island and 11.6 m in Frobisher Bay, and a mean range of 7.8 m in Frobisher Bay (Canadian Hydrographic Service, 2000). Reversing falls are common where sea inlets markedly pinch or shoal. The modern shoreline should theoretically be classified as tide dominated, however, much of it is rock stripped of any previous till cover by wave action and so lacks landforms characteristic of any particular tidal environment. Pocket beaches of sand and cobbles have formed at the head of some rocky embayments. Beaches are common on the few per cent of the shoreline underlain by unconsolidated materials, though weaker glacial marine deposits may be eroded and cliffy. Intertidal flats of unconsolidated material, up to 1 km wide, are present along 10% of the coast at the head of Frobisher Bay, mainly in deeper embayments and estuaries (Dale, 1982). Tidal flats are rare along the rocky Hudson Strait coast.

The morphology and processes of the tidal flats of Koojesse Inlet (Iqaluit) were studied by Dale (McCann et al., 1981; Dale, 1982). Here, the substrate is indurated silt and clay (>80% silt or finer) with a thin cover of sandy sediment littered by cobbles and boulders. The silt and clay was suggested by McCann et al. (1981) to be an offshore glacial marine deposit; in view of the absence of foraminifers Dale (1982) suggested a glaciolacustrine origin; most likely it is a proglacial deposit laid in brackish water beyond the 'Iqaluit' delta. McCann et al. (1981) noted there is a sediment deficit under and at the edge of the ice foot — flats are being eroded and coarser surface material redistributed within the intertidal zone by entrainment in sea ice and by tidal current action.

Fluvial deposits

Deposits of mappable size lie within or downstream from valley trains. The floodplains, terraces, fans, or deltas are mainly sand and gravel reworked from the glaciofluvial deposits. The relatively steep valley gradients and the steady water flow from numerous lakes generally maintain a single channel, but some braided reaches occur. River beds other than on outwash are mainly on bedrock or till and are composed of boulders, cobbles, or rock. Streams and rivers drain into the numerous lakes via fans and deltas. On the Hudson Strait coast, such deposits are rare, and around Frobisher Bay some are underfits, possibly because of the upstream sediment traps and rapid deepening offshore. MacLean et al. (2001) remarked that the thin postglacial cover on the floor of Hudson Strait reflects a relatively starved sediment environment.

Icings which are seasonal or perennial sheets of ice accumulated by seepage of water from lakes down pre-existing watercourses during subfreezing conditions, were rarely observed on airphotos, though some are several square kilometres in area (Map 2042A, on CD-ROM).

Organic deposits

Peaty muck is common in low-lying areas on all materials. Accumulations of more than 25 cm are rare, except in the 'Tasiujarjualaaq River' valley (Jacobs et al., 1985b). Why thick peat fails to accumulate more widely in a low-arctic zone with abundant precipitation is possibly a function of the rugged topography at macro- to micro-scale offering few areas of quiescent seepage. Some of the more extensive lowlands are composed of sandy outwash which is subject to deflation, producing niveo-eolian peat deposits (Mode and Jacobs, 1987). Thin, organic-rich laminae alternate with thicker layers of sand eroded from nearby fluvial deposits and trapped in snowbanks.

Permafrost landforms

As noted above, some permafrost-controlled landforms are common in the map area, particularly rock pavement heave and convective sorting of finer grained deposits (frost boils). No pingos were observed, even though valley-bottom outwash seems a suitable environment for open-system pingos. Given the rarity of thick peat, the absence of palsen is not surprising.

AGE ESTIMATES OF SEDIMENTS AND LANDFORMS

Radiocarbon dating — ages and materials

The only absolute dating method to have been applied to Quaternary materials in the map area is conventional radiocarbon age determination and accelerator mass spectroscopy (AMS). A variety of organic materials have been sampled and dated for geological, archeological, and paleoenvironmental studies (Table 1; Fig. 43). Although radiocarbon dating is generally classified as an absolute method, corrections are necessary to produce a uniform radiocarbon time scale (the radiocarbon scale is used in this report) or to approximate calendar (astronomical) time.

Marine (oceanic) organisms have radiocarbon ages offset from those of terrestrial (atmospheric) organic materials due to the lengthy exchange time between atmosphere and ocean for radioactive carbon dioxide. Hence, for marine shells, a marine reservoir correction is applied, although there is much uncertainty as to what its value should be (Dyke et al., 1996b). The reservoir effect itself varies between different water masses by hundreds of years (Barber et al., 1999). Here, a correction of -400 years is used (according to GSC convention), compared to the -450 years correction in Table 1 of Manley (1996). Barber et al. (1999) indicated -400 years is 80 years younger than the present mean surface ocean age ('pre-hydrogen bomb') and 160 years younger than the mean for modern-day eastern Hudson Strait.

The radiocarbon time scale differs from the calendar-year time scale (calibrated age). For the range of dates critical to this report (6–9 ka) the calibrated age before present (BP) is about 1000 years older than the radiocarbon ^{14}C age (Stuiver et al., 1998).

The majority of dates cited in this report were determined by 'conventional' radiocarbon analysis, which requires tens to hundreds of grams of material for an accurate result. This frequently requires a mixture of individual components (e.g. more than one mollusc) with ensuing uncertainty as to whether the sample may be composed of individuals of different ages. Bulk organic samples from cores are particularly suspect because of the difficulty in examining the depositional environment (which may include bioturbation) and because of potential contamination by detrital carbonate. Near-surface samples of buried soils can be contaminated by roots. The accelerator mass spectroscopy (AMS) process used for 37 of the samples commonly permits fractions of grams of a sample (e.g. individual shells, twigs, seeds, etc.) to be dated, and mixed ages are avoided.

Marine molluscs

Half of the dates in Table 1 are for mollusc shells, mainly from three environments: 1) preglacial marine deposits which are undisturbed, reworked in marine sediments, or

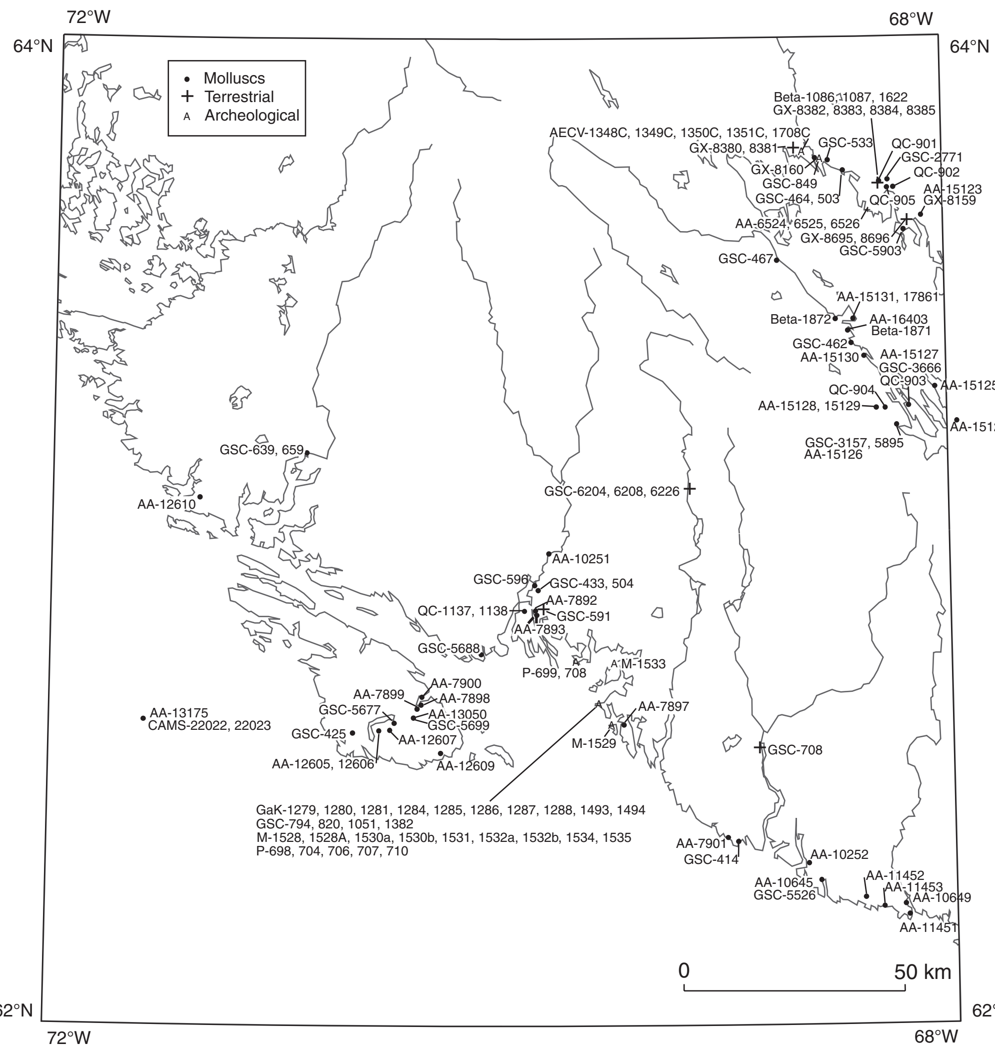

Figure 43. Radiocarbon date locations; see *Table 1.*

incorporated in (silty) till; molluscs are commonly concentrated at the surface in frost boils; 2) proglacial or postglacial nearshore sediments or raised beaches; molluscs may be in situ or displaced; and 3) submarine cores from offshore postglacial sediment, where stratigraphic 'succession' is assumed, though bioturbation can disturb this order.

Shells clearly not in situ in raised marine deposits may be dated to provide a minimum age for sea level when it lay at the altitude of the collection site, as well as a minimum date for deglaciation and influx of the sea. Mollusc shells are more likely to be preserved in carbonate-rich matrices because they are leached when in acidic shield-derived deposits (though permafrost tends to mitigate the process). This may partially explain the presence of early to middle Holocene shells in calcareous raised marine deposits and some coastal till along Hudson Strait from Big Island east (Manley, 1995, 1996) and in inner Frobisher Bay (Lind, 1983), and their apparent absence from raised deposits in Markham Bay, where unconsolidated material is all of shield origin (though abundant fresh water from outwash in the semienclosed bay is another possible factor).

Species and range

Mollusc species submitted for dating were generally the most robust or common in a collection, hence, sample descriptions may not include all species present at a site (Table 1), thus introducing a bias into the taxonomic data (Dyke et al., 1996a). Note that Lind (1983) identified the pelecypods in a number of undated collections from raised sediments on the west shore of Frobisher Bay. The great majority of raised pelecypods from both Hudson Strait and Frobisher Bay are the arctic–subarctic species *Hiatella arctica, Mya truncata*, and *Macoma calcarea*. Most of the other species recorded have a similar or greater range, hence Dyke et al. (1996a) showed the same "faunistic" zone (subarctic) for this area throughout the Holocene. Two of the westernmost samples from the Hudson Strait coast, dated ca. 7.7 ka (AA-12607, AA-12610, Table 1), are *Portlandia* sp., which favour ice-proximal conditions (Manley and Jennings, 1996). *Portlandia arctica* from an offshore Hudson Strait core dated 8.7 ka (AA-13175)(MacLean et al., 1994).

Ages

All pre-Late Wisconsinan dates are for marine shells from the shores of, or within Hudson Strait. These age determinations are at, or beyond the limit of the radiocarbon method and range from 43 360 BP to 30 200 BP, with two dates greater than ca. 43 ka. Half of the ten shore samples were identified by Manley (1996) as either undisturbed or reworked into silty glacial marine deposits, though GSC-414 is described by the collector (Blake, 1966) as being collected in till. The other five are reworked in silty diamicton described as till by Manley (Manley and Jenkins, 1996). An eleventh 'old' date (27 ka; CAMS-22022) is for molluscs and foraminifers below 8 m of stratified, ice-distal glacial marine sediments southwest of Big Island (core 93034-018, MacLean et al., 1994; MacLean et al., 2001). There is an absence of dates from the segment of the Hudson Strait coast under consideration here for the time interval 30 ka to 8.3 ka, unless any of the 'old' dates include material from that interval. (The offshore core (018) contained foraminifers and a mollusc collectively dated 27 ka at the base (-8 m) and a 8.7 ka mollusc at the top, which MacLean et al. (2001) suggested was reworked because it overlay 8.6 ka foraminifers and ostracods, in themselves suspect.) No mollusc younger than 6.2 ka has been dated, simply because collections were made in raised nearshore glacial marine sediments with the objective of dating the last deglaciation. The finite-age, onshore shells were collected between -4 m a.s.l. and 75 m a.s.l.

Molluscs from inner Frobisher Bay yielded finite Holocene ages from 9.1 ka to 6.1 ka, with the exception of anomalously old (9.9 ka) and young (0.4 ka/21 m a.s.l.) collections. Elevations of samples ranged from 4 m a.s.l. to 81 m a.s.l. Two-thirds of these shells were taken from deposits interpreted as nearshore or offshore glacial marine and most of the remainder from glacial marine deltas.

Other geological samples

More than half the age estimates that are not from molluscs are for niveo-eolian peat exposures, mostly composed of sedge, grass, willow, or *Sphagnum* moss from the Iqaluit area, plus a section in the upper reach of the river flowing to the head of Shaftesbury Inlet, all falling in the 5.4–0.4 ka interval. In addition to aiding vegetation and climatic reconstruction (Short and Jacobs, 1982; Jacobs et al., 1985b; Mode and Jacobs, 1987), some samples from 'Tasiujarjualaaq River' valley indicate the maximum sea level possible for the time when the dated material was deposited. Peaty material under solifluction lobes provided age estimates of 1.8 ka and 0.7 ka (Lowden et al., 1967; Lowden and Blake, 1968). Two lakes were cored, both on east side of Frobisher Bay, and organic fractions dated. 'Easy Lake' dammed by an outer Frobisher Bay Moraine System ridge provided bulk organic dates of 8.2 ka and 6.4 ka (Squires, 1984), and 'Upper Meech' lake in the inner moraines provided dates from humic acid of 4.9 ka to 0.6 ka (Abbott, 1991; Miller, 1992).

Archeological samples

Numerous samples from archeological investigations in the vicinity of Cape Tanfield on the Hudson Strait coast (Maxwell, 1973) and Iqaluit (Jacobs and Stenton, 1985) provide a record of human occupancy between 4.7 ka and 0.5 ka. Most of the samples are charred fat, but some wood, charcoal, and animal bones have been dated (Crane and Griffen, 1966; Stuckenrath et al., 1966; Kigoshi et al., 1969; Lowden et al., 1969, 1970, 1972; Wilmeth, 1969; Maxwell, 1973; Manley and Jennings, 1996). The oldest sample for any given elevation provides maximum sea level possible for the age of the dated material, and helps make up for the sparsity of late Holocene mollusc dates when constructing shoreline emergence curves (cf. Clark, 1985; Manley, 1996). It is generally assumed that coastal sites were occupied for sea-related activities and hence dwellings were placed close to contemporary sea level.

Relative dating methods

Several relative dating methods have been applied in or adjacent to the map area.

Lichenometry

Squires (1984) attempted to correlate segments of the Frobisher Bay Moraine System, previously estimated by the radiocarbon method to be 8.2–6.7 ka, by comparative measurements of *Rhizocarpon geographicum* thalli. This proved unsuccessful when the largest thalli were found to be 92 mm diameter, which should be less than 3 ka according to the growth curve constructed by Miller and Andrews (1972) for the climatically slightly harsher Cumberland Peninsula of Baffin Island. Dowdeswell's (1984) study of *R. geographicum* at Watts Bay, 50 km east of the map area, indicated that on surfaces older than late Neoglacial (< 1 ka), lichens coalesced too much to be measured individually.

Weathering zones

The degree of bedrock pitting resulting from removal of grains by weathering processes has been investigated east of the map area on the outer south shore of Frobisher Bay (Muller, 1980; Dowdeswell, 1984; Stravers, 1986). Weathering zones were correlated with terrain known or speculated to be of Neoglacial, Foxe (Wisconsinan), and pre-Foxe age, though studies were confined to areas of a few hundred square kilometres. No rock surface studies were made within the map area, though, as noted above, block fields are not necessarily an indicator of preglacial terrain (except, perhaps, Big Island), and roughness, including tors, does not appear to correlate with age of terrain.

Successive landforms

Several types of deglacial ice-marginal landforms (lateral drainage channels, subaqueous push (De Geer) moraines) are believed to mark annual (summer) periods of erosion or deposition at a retreating ice margin. Hence they record a 'floating' chronology which can be used to indicate the distance and rate of retreat during deglaciation. Lateral drainage channels in some large valleys, particularly the Ramsay River and adjacent rivers, may record hundreds of annual erosional events. Subaqueous moraines in the middle Armshow River valley are spaced at five or six per kilometre in several series; averaged over the total 25 km of valley length in which they occur, this suggests 150 years of retreat is recorded.

QUATERNARY EVENTS

Pre-Late Wisconsin (Foxe) Glaciation

There is no good evidence of the style of early or middle Quaternary glaciations in the map area. Cirques, which include a significant population on the Hudson Strait coast, do not contain cirque deposits and so must have been eroded at initiation of the last glaciation or earlier. A summit weathering zone in the Everett Mountains, 50 km to the east of the map area, was suggested by Dowdeswell (1984) to predate Foxe Glaciation and by Osterman et al. (1985) to have not been inundated by actively eroding ice during most of the Quaternary, but no such old terrain was observed within the map area. The only known preglacial sediments on land are raised shells in glacial marine deposits (possibly in situ) and reworked into last-glacial till along the Hudson Strait coast that indicate ice-free marine conditions 43–30 ka, probably in a Wisconsin Glaciation interstadial (Blake, 1966; Manley, 1995, 1996).

The offshore Quaternary record is more substantial than the terrestrial as shown by profiles and cores from northern Hudson Strait and outer Frobisher Bay (e.g. Osterman and Andrews, 1983; MacLean et al., 1986, 1991a, b, 1994; Manley, 1995; Jennings et al., 1998). At the eastern end of Hudson Strait, MacLean et al. (2001) recorded a 360 m thickness of what they considered to be a sequence of ice-contact sediments deposited by numerous ice streams that flowed through the strait. Much of the central Late Wisconsinan Laurentide Ice Sheet and its precursors drained through Hudson Strait to the Labrador Sea and ultimately the North Atlantic Ocean where they may have significantly contributed to ice-rafted debris (IRD) recording Heinrich (H) events and to detrital-carbonate (DC) layers deposited episodically during at least the last 200 ka (e.g. Hillaire-Marcel et al., 1994; summary *in* Andrews (1998)); however, the location of ice margins and sediments sources, and transport and depositional processes is poorly understood (Andrews et al., 1998). Numerical modelling of the last glaciation suggests that Frobisher Bay (unlike Hudson Strait, and to a lesser degree Cumberland Sound) was not a major ice outlet (Kaplan et al., 1999); this was likely also the case during earlier glaciations. A date of 27 ka for detrital organic matter from the base of a core in outermost Frobisher Bay was correlated with the Loks Land Member of the mid-Foxe (42–35 ka) interstadial by Osterman et al. (1985).

Late Wisconsin (Foxe) Glaciation maximum

Published outlines of the Foxe Ice Dome agree broadly with the ice-flow pattern mapped in this report. Foxe ice is shown radiating from Foxe Basin to western Meta Incognita and Hall peninsulas and the head of Frobisher Bay (i.e. to Hall and Frobisher Bay moraine systems) by Ives and Andrews (1963) and Prest (1969) with local glacierization on the peninsulas. Hudson Strait was occupied by an outlet glacier or ice stream that possibly met Meta Incognita Peninsula (? Foxe Ice Dome) ice at the offshore moraine in North Bay (Manley, 1995) before overlapping southeastern Meta Incognita Peninsula (Prest, 1984). Dyke and Prest (1987c) added to the model the Amadjuak Ice Divide running southeast from Foxe Basin onto Meta Incognita Peninsula (where it is referred to in this report as the Meta Incognita Ice Divide). The Hall Ice Divide branched from the Amadjuak Ice Divide west of the head of Frobisher Bay (Fig. 44). Dyke and Prest (1987c) showed the Hall Ice Divide restricted to the west of that peninsula, whereas the Meta Incognita Ice Divide extended the length of the peninsula, except the Everett Mountains, generating essentially local ice. Stravers (1986) calculated Late Quaternary ice cap and glacier profiles for southeast Baffin Island using weathered zones identified by Mercer (1956), Muller (1980),

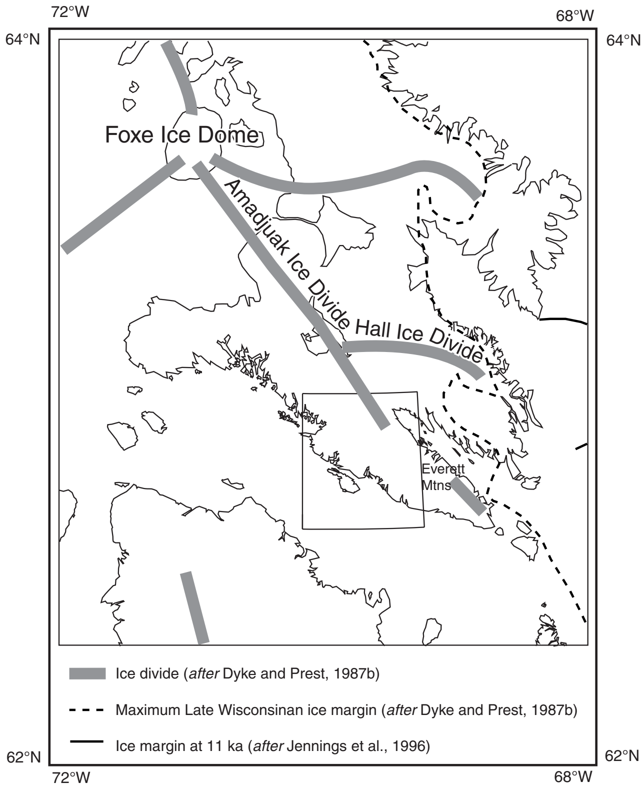

Figure 44. *Foxe Ice Dome, ice divides, and maximum extent of Late Wisconsinan Laurentide Ice Sheet over southeast Baffin Island,* after *Dyke and Prest (1987b); margin* modified from *Jennings et al. (1996).*

and Dowdeswell (1984) on the lower south shore of Frobisher Bay as control points. In one reconstruction, Amadjuak ice and Hudson Strait ice combined to flow southeast over western Meta Incognita Peninsula (unlike the striation record), leaving a local ice divide south of the present topographic height of land. In an alternate model of Stravers'(1986), the Hudson Strait glacier only occupied the western end of the strait, while Labrador ice crossed the strait; this permitted the Meta Incognita Ice Divide to extend the width of the present map area and ice to flow southwest from the ice divide throughout the length of the peninsula (as the record shows). In both models, a glacier filled inner and middle Frobisher Bay. If a low-gradient ice stream is substituted for the Hudson Strait glacier (as shown for Cumberland Sound by Jennings et al. (1998), and suggested for Hudson Strait by MacLean et al. (2001)) then Hudson Strait ice could reach the east end of the strait and the ice divide could contemporaneously extend the length of the peninsula. Duvall (1993) preferred a Meta Incognita Ice Divide extending at least to the Everett Mountains, but no farther than the Grinnell Glacier. These divides, together with a Hudson Strait ice stream or glacier, survived from 18 ka to 8 ka. Kaplan et al. (1999) numerically modelled the late Foxe Dome and ice cover farther north and east, showing a minor Hall Peninsula ice dome mostly draining south to Frobisher Bay. They also succeeded in 'growing' an ice stream through Cumberland Sound in agreement with field evidence of Praeg et al. (1986) and Jennings (1993). Modelling did not produce a similar low-profile glacier in Frobisher Bay, though this area was not the focus of Kaplan et al.'s (1999) study.

Final stages of glaciation and the deglaciation

Previous reconstructions of late-glacial ice flows that affected Meta Incognita Peninsula are summarized in Figure 45. Initial deglaciation of central Hudson Strait, estimated at 10 ka (radiocarbon years) by Stravers (1986) and 9 ka by Dyke and Prest (1987c), is too late according to Gray et al. (1993). Gray (2001) reviewed the question of an early opening and hesitantly continued to support an opening between 11 ka and 10.5 ka. All the critical dates older than 9 ka are from either multivalve (possibly mixed) collections or for *Portlandia arctica*, which is a bottom-feeding mollusc which may yield a radiocarbon age skewed much older than the contemporary surface due to uptake of older subsurface organic carbon or by uptake of inorganic carbon (as noted by Gray (2001)). An early opening (10.5 ka) ice-margin pattern was shown by Andrews et al. (1995) (Fig. 45a), revised to 11.5 ka by MacLean et al. (2001). Meanwhile, the maximum extent of the Frobisher Bay glacier lay at a mid-fiord position according to Osterman et al. (1985) and Duvall (1993).

The Gold Cove advance of Labrador ice across southeasternmost Baffin Island by 9.9 ka filled in or perhaps only blocked an open, central section of the strait (Fig. 45b). Duvall (1993) suggested Gold Cove ice diverted a downstrait glacier across Meta Incognita Peninsula into middle Frobisher Bay; no evidence whatsoever for this was found in the map area. Eastern and central Hudson Strait reopened before 9 ka (Fig. 45c) (Dyke and Prest, 1987c; Andrews et al., 1995) while the Frobisher Bay glacier was restricted to the inner bay. The Noble Inlet advance after 8.9 ka dammed a lake in the central and western strait which drained eastwards between Labrador and Baffin ice across the Meta Incognita Peninsula to the York delta of outer Frobisher Bay (Fig. 45d) (Stravers, 1986; Dyke and Prest, 1987c; Stravers et al., 1992; Manley, 1995, 1996; Andrews et al., 1995). Hudson Strait was finally open by 8.0 ka (Fig. 45e) (Stravers, 1986; Dyke and Prest, 1987c; Stravers et al., 1992; Andrews et al., 1995). For both 8.4 ka and 8 ka, Dyke and Prest (1987c) showed a truncated Meta Incognita Ice Divide on the westernmost part of the peninsula, with ice standing at the Frobisher Bay Moraine System, while for 8 ka Stravers et al. (1992) and Andrews et al. (1995) showed a contiguous independent ice cap covering the central peninsula. By 7 ka (Fig. 45f) the Foxe Ice Dome and the Amadjuak Ice Divide had disintegrated and ice was centred on a divide running up east-central Baffin Island, barely present in the map area (Ives and Andrews, 1963; Dyke and Prest, 1987c).

Ice domains of western Meta Incognita Peninsula

Distribution of landforms, combined with existing radiocarbon dates, led Hodgson (1997) to propose five broad, late-glacial–deglacial domains, each of which represents a phase of similar style and age of ice flow (Fig. 46). Style is determined from major and minor terrestrial landforms such

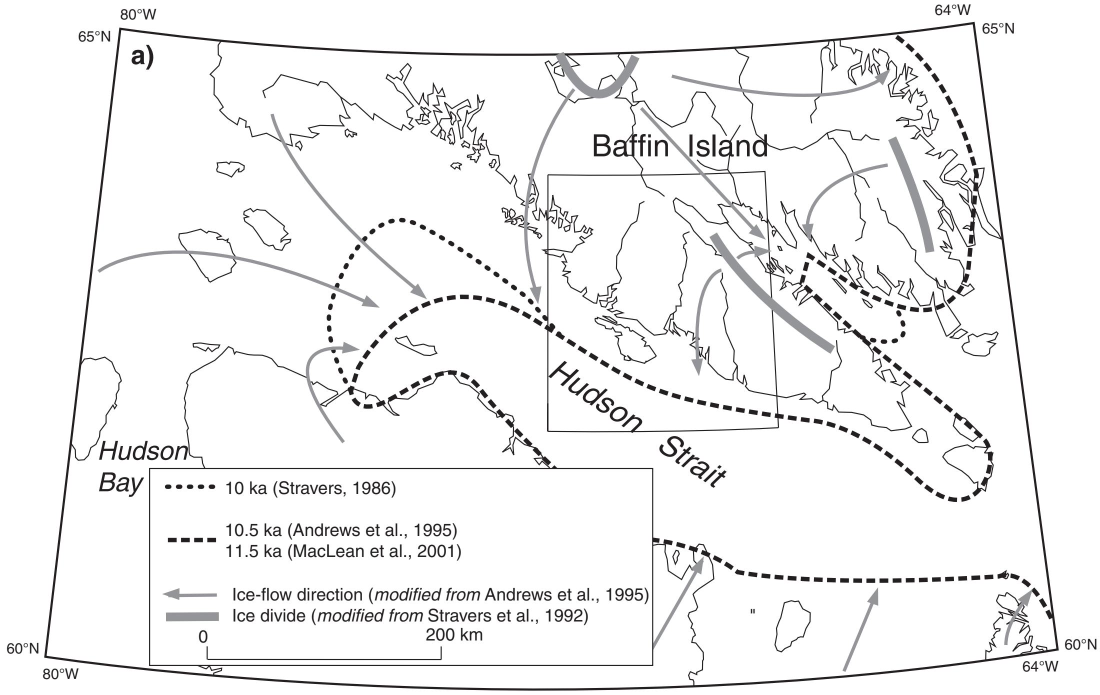

Early deglaciation

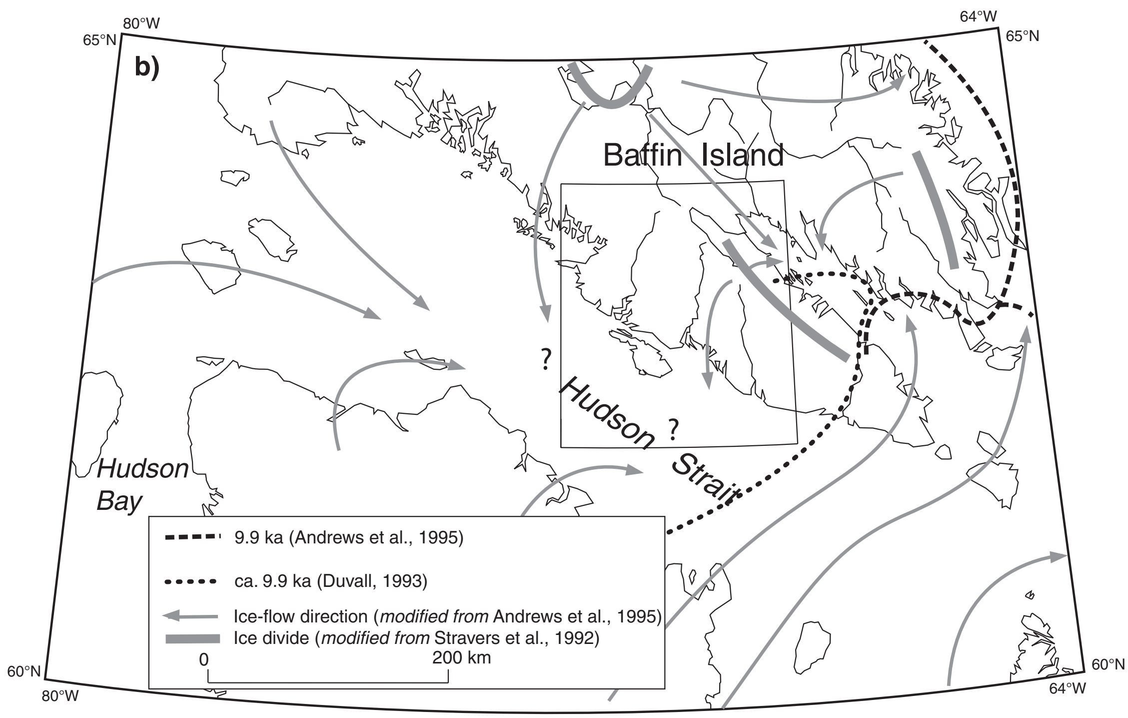

Gold Cove advance

Figure 45. *Reconstructions of deglaciation and readvances over Hudson Strait and southeast Baffin Island; previously published ice limits and flow directions:* ***a****) early deglaciation,* ***b****) Gold Cove advance,* ***c****) early Holocene,* ***d****) Noble Inlet advance,* ***e****) opening of Hudson Strait, and* ***f****) final ice remnants.*

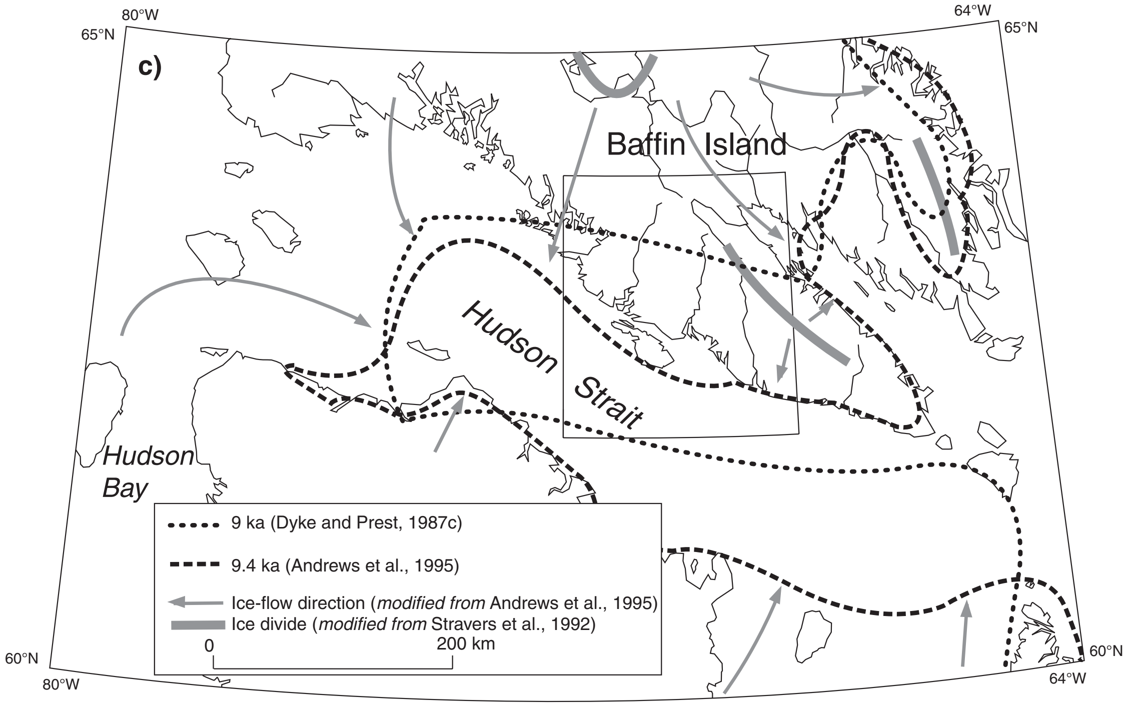

Early Holocene

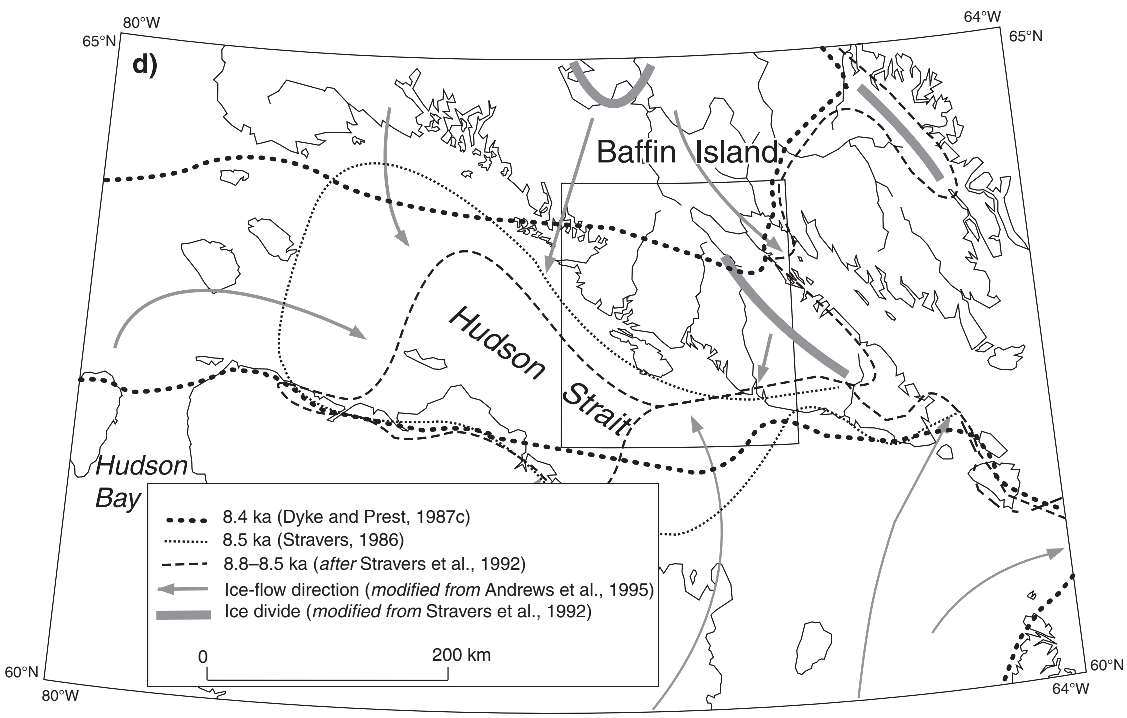

Noble Inlet advance

Figure 45 *(cont.).*

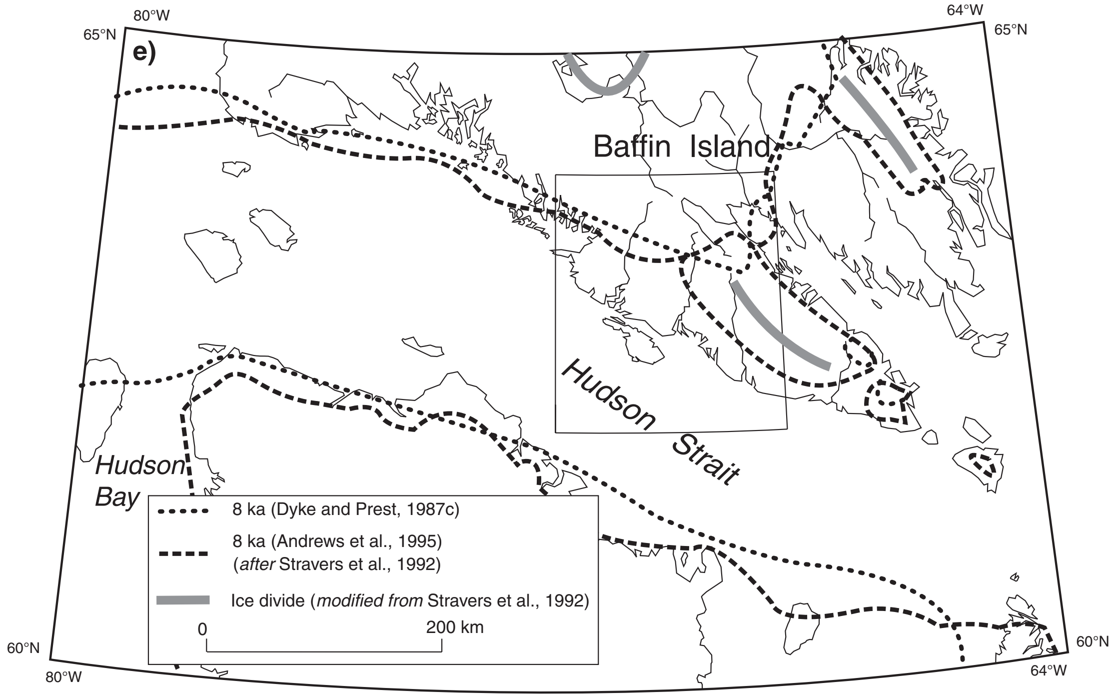

Opening of Hudson Strait

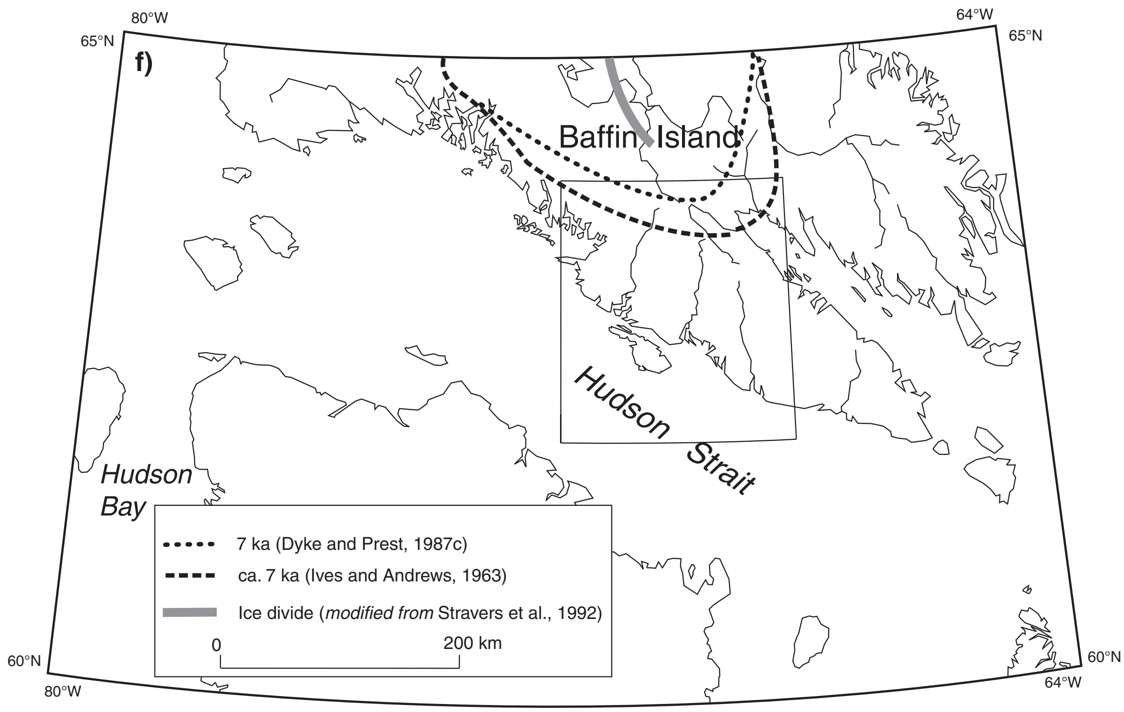

Final ice remnants

Figure 45 *(cont.).*

as drumlins and striations that indicate ice-flow direction, from marginal channels and end moraines that outline former ice margins, and from till composition. Age is based on the pattern of successive landforms and on radiocarbon age determinations of any succeeding marine incursion.

Ice from two sources foreign to Baffin Island overlapped the area: firstly, ice mainly from the central Laurentide Ice Sheet flowing southeast down Hudson Strait (domain 1; Fig. 47) and secondly, Labrador sector (of Laurentide Ice Sheet) ice flowing north (domain 2). Native (Baffin) ice from the Late Foxe Amadjuak Ice Divide and local Meta Incognita and Hall ice divides covered most of the map area (possibly including at times domain 2). Areas encompassed by this maximum glaciation to late-glacial flow and not overlapped by later events compose domain 3, covering more than 60% of the map area. Domain 3 is subdivided into 3a: southwest ice flow between the Meta Incognita Ice Divide and Hudson Strait; 3b: northeast flow from the ice divide to Frobisher Bay; and 3c: south-southeast flow from the Hall Ice Divide to Frobisher Bay. A readvance within domain 3 by the successor ice mass to the glacial maximum Amadjuak Ice Divide formed domain 4 (4a towards Hudson Strait, 4b and 4c to Frobisher Bay). Final drawdown to the head of Frobisher Bay, beheaded domain 4a creating domain 5. Retreat of residual bodies of ice in deeper valleys of both domains 4a and 5 is discussed under domain 6.

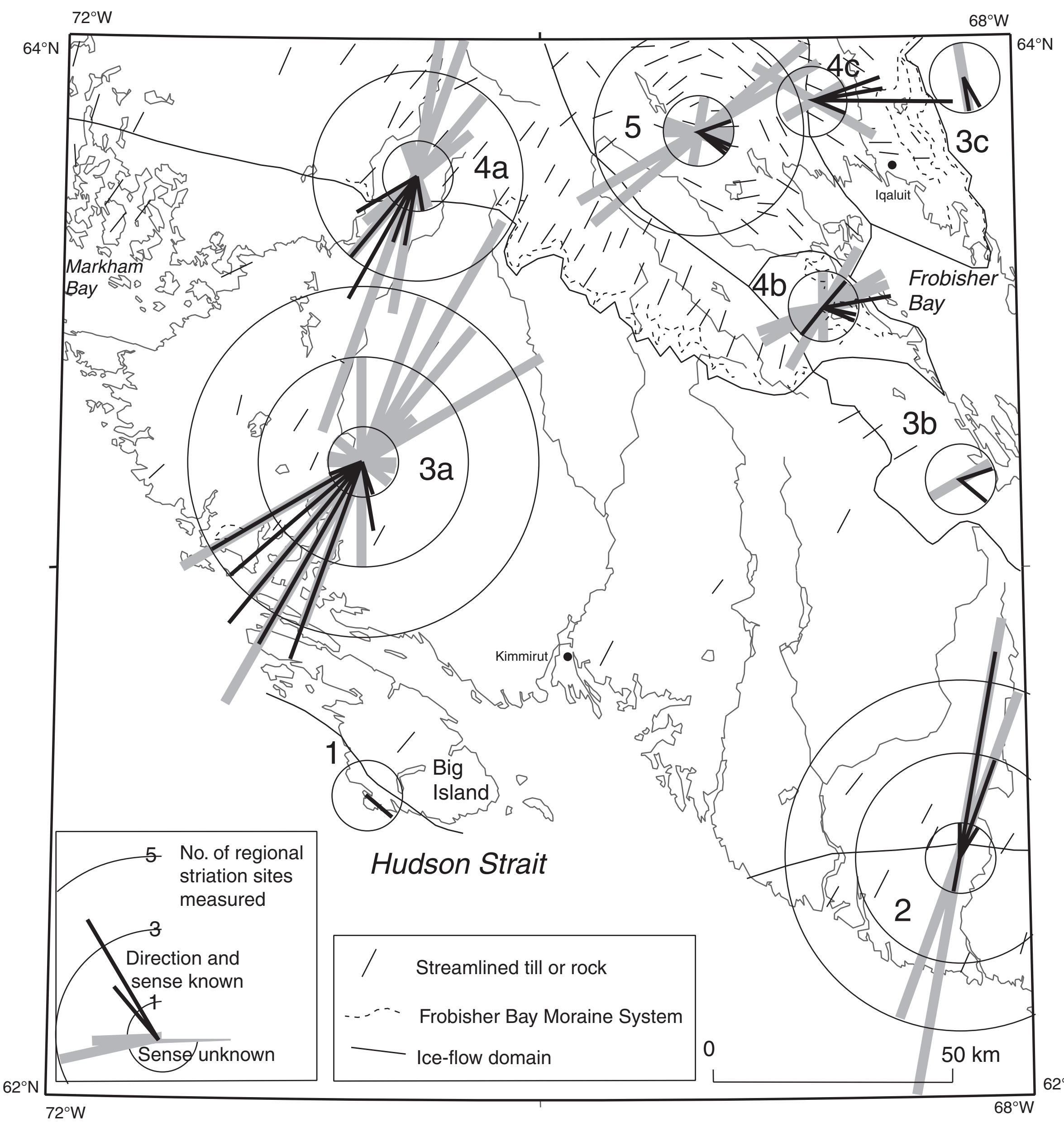

Figure 46. Late-glacial and deglacial ice-flow domains with dominant striation orientation.

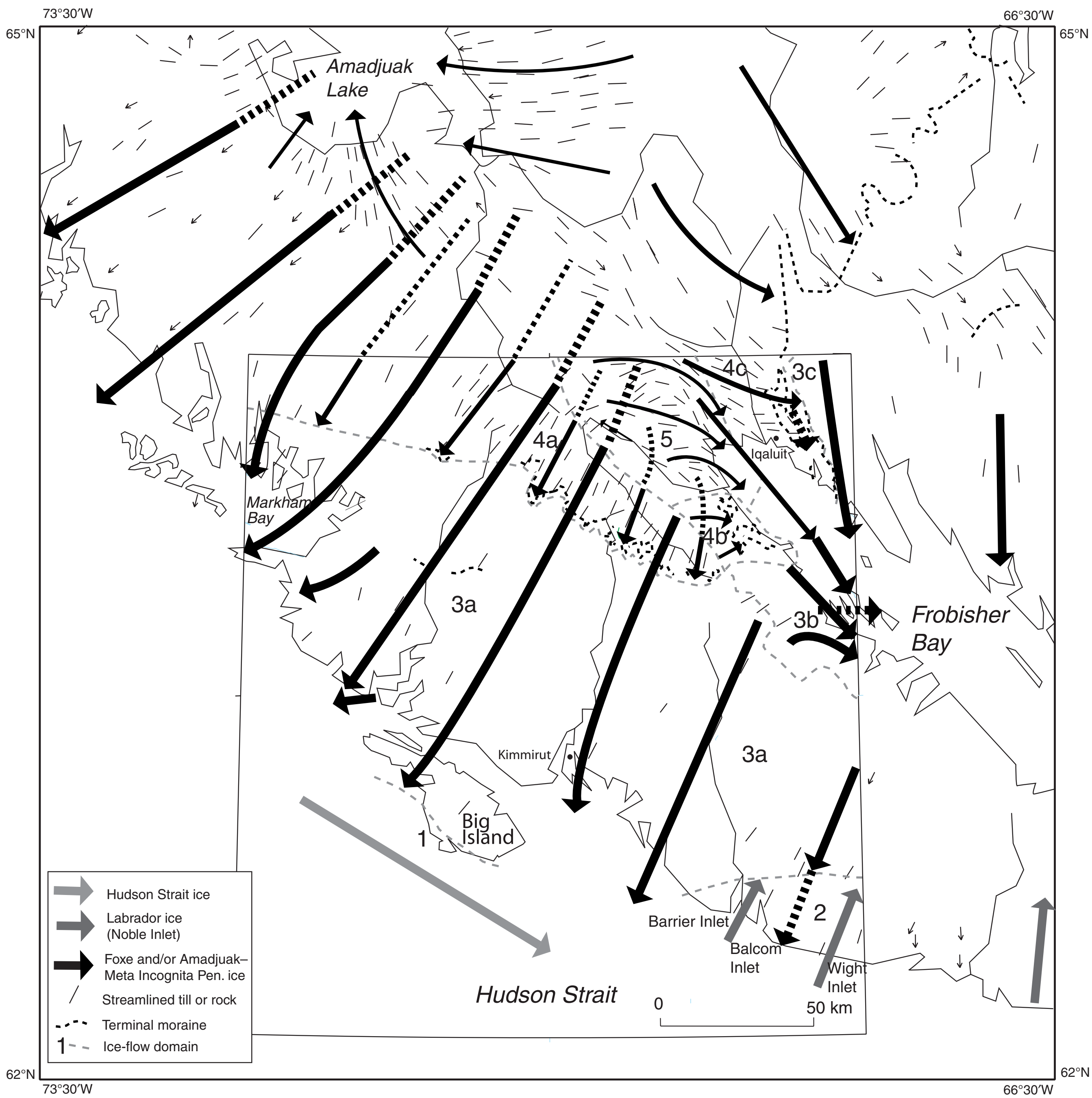

Figure 47. *Generalized ice flow within the last ice cover over Meta Incognita Peninsula. The later the flow, the thinner the arrow. Overrun flows are dashed lines. Streamlined till or rock flows and terminal moraines outside the map area box are* after *Blake (1966).*

Domain 1

A very small, but highly significant domain occupies the southwest tip of Big Island, seaward of Ashe Inlet. From the earliest geological observations in the area (Bell, 1885) it was clear that southeast-trending striations were prominently inscribed here by glacier ice streaming down Hudson Strait. This glacier and later ice rafting in the raised postglacial sea brought in carbonate erratics (bedrock clasts and Pleistocene marine shells) and calcareous till to the Hudson Strait shore here and farther east.

It appears that during the Late Wisconsinan the Hudson Strait glacier was restricted in width to the central area of the strait, for there is no good evidence of it laterally overlapping the present northern shore other than on southwest Big Island (Manley, 1996). This point projects southwestward from the general trend of the south Baffin Island coast halfway to the centre line of the strait, where a bathymetric shoulder is present. Striations and roches moutonnées on other outermost strait islands record flow from Baffin Island to the strait (e.g. Emma Island, off northern Big Island; unnamed island southeast of Hector Island, west of map area off Markham Bay). The disparate striation orientations on Strathcona Islands were ascribed by Manley (1996) to ice flowing from adjacent inlets or the coast. Manley (1996) envisaged an expansion of Baffin Island ice into the strait after retreat of the Hudson Strait glacier, hinging on a set of 160° striations. Nevertheless, there are no landforms indicating the former presence of a glacier margin at the northern boundary of domain 1. Were these eradicated by later Meta Incognita Peninsula ice? (The submerged moraine to the east could be the edge of an ice stream or Meta Incognita Peninsula ice (Manley, 1995; MacLean et al., 2001).) Similar east-trending striations were found on the southern (Ungava) shore of Hudson Strait only where it projects farthest into the strait (Charles Island, Cape de Nouvelle-France, Cape Hopes Advance); however, they were locally over-inscribed by a short-lived offshore flow (summarized by Gray (2001)).

No material from within the domain was dated. An age estimate of 7.98 ka (GSC-425, Table 1) was obtained for molluscs from the postglacial sea collected at 75 m a.s.l. closely adjacent in domain 3a (Fig. 29). Suspect dates (bulk collections from cores) of 8.73 ka (AA-13175) and 8.59 ka (CAMS-22023)(Table 1; *see also* MacLean et al. (2001)) were obtained for molluscs and foraminifers from a core 45 km offshore to the west. A number of studies, summarized by MacLean et al. (2001), raise the possibility that the Hudson Strait glacier had retreated from the eastern and central strait before the three documented advances of Labrador ice filled the eastern end of the strait between 11 ka and 8.4 ka. Hence, Hudson Strait ice could have left southern Big Island before 11 ka. Manley (1996) speculated an ice stream was active at the glacial maximum (18 ka) and the H-1 event (14.5 ka).

Domain 2

The coastal area in the southeast was overrun by north-northeast-flowing ice. The angle between this flow and the axis of Hudson Strait, as well as ice flow in domain 1, is too acute for the Hudson Strait glacier to be the source, hence the flow is assumed to lie on the western flank of one or more of the cross-strait advances of Labrador ice. Manley (1995) showed that the onshore striations were probably left by the final (Noble Inlet) flow after the DC-0/Gold Cove advance was rebuffed by local ice. The Noble Inlet event is well dated to an advance onto Baffin Island ca. 8.9 ka, a maximum extent ca. 8.8 ka, and deglaciation ca. 8.4–8.2 ka (Manley and Miller, 2001).

The limits of the flow within the map area are ill-defined; Manley (1996) showed the western limit at the coast either at Barrier Inlet (the limit of most, though not all, of his onshore striations), or in a minimum model (Manley, 1995) at Wight Inlet, and running inland as much as 30 km at the eastern edge of the map area (68°E). As noted above, in the vicinity of Wight Inlet patches of calcareous silty till with Middle Wisconsinan or older marine shells and carbonate bedrock clasts were observed to 10 km inland. Clear striations and grooves (present to a degree not encountered elsewhere in the map area distal to the Frobisher Bay Moraine System) were found to at least 20 km inland. Incidentally, even though the shells are moderately thick, their commonly whole state is surprising after being overrun by downstrait ice, by at least one cross-strait advance, and possibly by expanded Meta Incognita Peninsula ice. Notwithstanding these distinct deposits and landforms, much of the till, even at the coast, is indistinguishable from till found elsewhere on Meta Incognita Peninsula. Note that a contiguous area of thick shield-derived till extends from close to the coast to more than 50 km inland.

Apparent subglacial–subaerial channels, described above, can be traced from 35 km inland on the eastern margin of the map area, for 50 km eastward to the ‘York gorges’. It is possible that this chain of meltwater landforms marks an interlobate zone between the limit of northward-flowing (domain 2) and southward-flowing Meta Incognita Peninsula ice (domain 3), though, as noted above, deltas of apparently subaerial origin are present. (Note that till sample HCA-97-B112 with 10.7% carbonate is inland from this apparent limit; the anomalously silty till with carbonate content of 17.6% at HCA-97-B120 is even farther inland.) Despite the presence of south-flowing striations in domain 2, Manley (1996) implied a concurrent maximum extent of ice in the two domains. It is probable that the local Meta Incognita Peninsula ice (domain 3) was formerly more extensive, and that onshore-advancing ice reversed the flow direction of a segment of the onland flow. Striations from the two flows are almost exactly reciprocal. The onshore flow was sufficiently strong to cross the 200 m deep Wight Inlet at a shallow oblique angle and not be deflected by the depression.

A moraine ridge at the coast east of Balcom Inlet (identified from airphotos) is similar in form to distinctive interlobate ridges found in domain 3 and may be relict from more expansive domain 3 ice preceding domain 2 onshore ice; however, preservation of a relict landform conflicts with onshore-ice scouring at Wight Inlet. The final decay of ice in domain 2 may have included a reversion to downslope flow to the south. Evidence includes a small end moraine in a valley west of Wight Inlet and a complex of moraines left by south-flowing ice lobes 50 km east of the map area (10–20 km east of Pritzler Harbour). An esker draining eastwards into the middle of Barrier Inlet and a very small esker west of Wight Inlet indicate that disparate deglacial flows also occurred.

The oldest postglacial age determination on the northern Hudson Strait coast, and the oldest date postdating Noble Inlet ice on southeast Baffin Island is from domain 2, 5 km east of Balcom Inlet; a *Portlandia arctica* valve in calcareous, fine-grained glacial marine sediment, dated 8.36 ka (Manley and Jennings, 1996; AA-10645, Table 1). A number of other molluscs from deglacial marine sediments within domain 2 and from west and east of the domain date 8.1 ka to a few hundred years younger (Manley, 1995). This indicates simultaneous deglaciation of the Hudson Strait coasts of both domains 2 and domain 3. It is supported by the uniform east-to-west rise in marine limit measured by Manley (1995, 1996) along the strait — there is no step marking a possible domain 2/3 boundary (Fig. 42). This all favours melding of Noble Inlet and Meta Incognita Peninsula ice rather than retreat of the latter before advance of the former. Note, however, that none of the dated material can be directly related to an ice margin, or even to a marine limit. Marine ice-contact landforms (perched deltas) have only been observed in Barrier Inlet, where they probably formed at final ice disintegration, along with fragmentary eskers.

Domain 3a

Regional ice from the Meta Incognita Ice Divide, or possibly in the northwest of the map area from the Amadjuak divide itself, flowed southwest towards Hudson Strait, undeflected by local topography except at the coast. This flow is indicated by congruent summit striations, scattered roches moutonnées, and rare till lineations and till ramps (Fig. 15, 17). Striations commonly are poorly preserved and much bedrock has rugged unpolished meso- to microrelief (especially on metasedimentary and carbonate rocks). Rocks at lower elevations towards Hudson Strait are more pitted and fractured at a megascale than those found inland. Till is mostly patchy, thin, and rarely streamlined, though a till blanket lies upflow of the coastal upland between Markham and North bays and, in the east, as referred to in domain 2, a substantial body of till covers a major interfluve. Some of the massive interlobate moraines on crests of interfluves tributary to Hudson Strait in the eastern part of the domain may have formed at the maximum flow stage. The westerly component in the ice flow indicates that much of the flow came from a local rather than a continental source. The few unidirectional striations measured at the Meta Incognita Peninsula height of land indicate a zone of reciprocal flow directions 10–20 km wide. This records minor shifts of an ice divide, the location of which mimics the markedly asymmetrical height of land between Frobisher Bay and Hudson Strait. It confounds Straver's (1986) models for eastern Meta Incognita Peninsula which showed an ice divide 20 km southwest of the topographic height of land, producing a symmetrical cross-section ice sheet. The southwest limit of flow may be at the submarine moraine east of Big Island (*see* above). Other possible terminal moraines are present at the coast between Canon and Crooks inlets, wrapping around a summit.

Clark (1985) speculated that over southern Big Island convergence occurred between ice-sheet flow from Meta Incognita Peninsula and an ice stream in Hudson Strait with a consequent sharp eastward bend in Meta Incognita Peninsula flow lines. No evidence of this has been found. Manley (1996) favoured consecutive events: a Hudson Strait flow followed by expansion offshore of Meta Incognita Peninsula ice; he suggested the strait ice stream did not expand onto south-central Big Island, where the predominantly weathered bedrock is indicative of a cold-based, nonerosive ice cover. Stravers' (1986) model for a Labrador ice advance across the strait, but no Hudson Strait glacier, showed a 500 m thickness of ice at the Hudson Strait coast. This ice was buttressed by not only Labrador ice, but ice from northern Ungava extending across most of the width of the strait. No particular support was found for this latter speculation and thus Stravers' (1986) thickness estimate for ice at the coast may have been far too high.

Deglacial landforms are common west of the Soper River. The most prominent are the flights of marginal drainage channels between the upper Ramsay and Soper river valleys, distal to the Frobisher Bay Moraine System of domain 4a (Fig. 37, 47). Channels are sufficiently abundant in places for the pattern of retreating valley ice lobes to be outlined and linked to discontinuous traces of end moraines on uplands (Fig. 29). These indicate a generally northerly retreat within the major consequent valleys, oblique to the southwesterly maximum ice-flow direction. The moraines mark minor stillstands or readvances of the ice margin. As observed above, the lateral channels may have been cut against cold-based ice occupying these valleys during final deglaciation. Eskers are rare landforms; most are west of the Ramsay River valley oriented in the southwest quadrant towards Markham Bay where the southwesterly drawdown of the glacial maximum was apparently maintained during deglaciation. The presence of eskers indicates warm-based ice either coeval with cold basal conditions in deep valleys to the east or dating from a slightly earlier period in deglaciation. Most of the raised marine deltas around Markham Bay and at the head of Crooks Inlet are terminations of the prominent valley trains that head in domain 4a; however, a few are perched and thus contacted domain 3 ice. They accord with other marine limit indicators, but have not yielded any dateable material.

In the east of the map area, deglacial landforms are much scarcer.

Some of the moraines classified as interlobate may be (upper) valley-side recessional moraines. A rare valley-bottom terminal moraine and perched (possibly glaciolacustrine) delta are present below interlobate moraines between the river flowing to the head of Shaftesbury Inlet and west branch of the river that drains to the head of Barrier Inlet. Scattered glaciofluvial terraces along Barrier Inlet and in tributary valleys are remnants of valley trains deposited around residual ice masses. Ice-marginal channels indicate the south side of a wasting ice mass only 10 km southwest of the height of land, in the headwaters of the river flowing to Shaftesbury Inlet. Scattered flights or individual lateral channels were cut by wasting ice bodies in valley bottoms. Marine limit mapped by Manley (1996) rises westward from 70 m at Barrier Inlet to 140 m immediately west of Canon Inlet (Fig. 42). Farther west from Canon Inlet, the elevation of marine limit levels out on the outer coast, but declines northward in Markham Bay registering either a greater ice load in the strait or later deglaciation towards the head of the bay and possibly to the east where marine limit declines by 23 m in less than 20 km in the southeast corner of the bay.

A total of 17 mollusc samples collected by Manley (1996), Blake (1966), and Clark (1985)(Fig. 43; Table 1) on the Hudson Strait coast in domain 3a yielded postglacial ages greater than 7 ka. All but one sample was in or on glacial marine sediments. The oldest in this range dated 8.16 ka (AA-12609) whereas a group of nine samples dated between 8.0 ka and 7.7 ka. The oldest sample on the Hudson Strait coast, as noted above in domain 2, was 8.36 ka (AA-10645). None of the shell samples could be related to an ice margin retreating in domain 3, and in fact most of the glacial marine sediments contain carbonate clasts, presumably dropstones from an offshore (Hudson Strait or Labrador) glacier. Furthermore, no samples could be related to a specific sea level. The sample group as a whole was at only 46% of the elevation of local marine limit, though two samples (7.96 ka, AA-7893; 7.87 ka, QC-1137) were at close to 80% of marine limit elevation. Assuming an emergence half-life of about 1000 years (Dyke and Peltier, 2000), the latter samples were deposited within a few hundred years of deglaciation and establishment of the limit. Hence, Manley (1996) estimated deglaciation of the coast at 8.2 ka — though retreat from the maximum ice limit would have been earlier. The latest date for overlap onto Baffin Island of Noble Inlet ice is 8.2 ka. Peat dated 5.42 ka (GSC-6204) was deposited adjacent to the middle section of the river that drains to the head of Shaftesbury Inlet.

Domain 3b

North of the Meta Incognita Peninsula height of land, rugged terrain dissected by joint-aligned valleys, declines steeply to Frobisher Bay. Striations, roches moutonnées, and (rarely) till lineations indicate ice flow to the northeast, trending east close to Frobisher Bay. Flow was congruent with the orientation of numerous cirques, however, there is no evidence of occupation of these by individual glaciers during or after the last glaciation (Colvill, 1982). Manley and Moore (1995) observed southeast-trending striations on islands in the centre of Frobisher Bay, immediately east of the map area, which they ascribed to the maximum stage of a Frobisher Bay glacier. These were crosscut by younger east-trending striations, which fit with a later dominance of ice from Meta Incognita Peninsula. The terminus of the Late Wisconsinan glacier in Frobisher Bay was modelled by Stravers (1986) to have reached its limit 100 km east of the map area at 10.5 ka, whereas Duvall (1993) placed it only 50 km east. Stravers' (1986) models for a Frobisher Bay glacier showed at least 500 m of ice at the east margin of the map area and 1000 m at the present head of the bay, which would have buttressed Meta Incognita Peninsula ice, explaining how an asymmetrical position for Meta Incognita Ice Divide could be maintained (though Stravers' (1986) model moved the ice divide towards the geographical centre of Meta Incognita Peninsula). Lind (1983) had also calculated that when ice filled the bay to a postulated middle-bay grounding line, it was more than 1000 m thick at the bay head, i.e. sufficient to overrun the height of land at the west end of Meta Incognita Peninsula.

During deglaciation, the Frobisher Bay glacier and Meta Incognita Peninsula ice split into separate ice masses without leaving interlobate landforms. Manley and Moore (1995) observed at Eggleston Bay east-trending striations from assumed preseparation flow crosscut by a younger southeast flow from an assumed Frobisher Bay glacier (i.e. the reverse of the mid-bay record). Retreat to the northwest of the Frobisher Bay glacier is recorded on the shores and up to 5 km inland by glacial marine and glaciolacustrine deltas, by small sandar in valleys parallel to the bay, and by rare lateral moraines and kame terraces. Scattered ice-marginal landforms in valleys transverse to Frobisher Bay indicate either southwest retreat of ice towards the Meta Incognita Peninsula height of land, or simply residual wasting ice in these valleys. The clearest example is 10 km southwest of Cape Rammelsberg, where the right lateral moraine of an ice lobe descending in a scoured valley (probably a minor readvance) blocked a tributary valley resulting in deposition of subaqueous moraines and lacustrine deltas. The age of Meta Incognita Peninsula ice-contact marine deltas in a valley tributary to Jaynes Inlet is noted below.

The marine limit on both sides of Frobisher Bay within the map area east of the Frobisher Bay Moraine System generally lies around 120 m, though measurements have been made up to 10 m higher (Fig. 42). The oldest age determination, on the south shore of Frobisher Bay (9.88 ka, QC-903), was questioned by Miller (*in* Blake, 1988) and rejected by Manley (*in* Manley and Jennings, 1996), leaving thirteen mollusc collections dated 9.06 ka to 7.92 ka (four of them >8.9 ka) from glacial marine sediments between Pike Island and Cape Rammelsberg (Table 1). Thus inner Frobisher Bay, distal to the Frobisher Bay Moraine System was deglaciated by 9 ka. Manley (*in* Manley and Jennings, 1996) also suggested that the terrestrial-based Meta Incognita Peninsula ice front lingered a millennium longer in the valleys transverse to Frobisher Bay. Molluscs within a Meta Incognita Peninsula ice-contact delta, surface 48 m a.s.l., 5 km inland from Jaynes Inlet, provided an age determination of 7.66 ka (AA-15129). Nearby *Portlandia arctica* from distal glacial marine sediments dated 7.76 ka (AA-15128).

Domain 3c

This area is largely bedrock; striations indicate southerly ice flow obliquely towards Frobisher Bay. Lateral drainage channels in shallow valleys show that final retreat of the ice front was northwestward.

Domain 4a

The southwesterly ice flow on the Hudson Strait side of Meta Incognita Peninsula can be traced from Hudson Strait to at least the height of land, but is separated into two domains (3a, 4a) by the prominent Frobisher Bay Moraine System (*see* above). The Frobisher Bay Moraine System glacier forced lobes of ice down south- and southwest-flowing valleys and deposited a belt of thick till up to 15 km wide. Evidence of southwesterly ice flow is preserved in the form of striations and till and rock lineations which have a far greater density than in the down-ice domain 3a, indicative of a strong warm-based flow. The presence of kettles in outwash that issued from the Frobisher Bay Moraine System indicates that the farthest readvance was reached shortly after deglaciation of distal terrain. Following the earlier domain 3a pattern, ice flow in domain 4a did not deviate while crossing several hundred metres of local relief. North of the Armshow River bend indicators of this flow occur as far east as the Hone River, on the northeast-facing slope to the Frobisher Bay lowland, 250 m lower than the height of land. Thus for the northern segment of domain 4a, ice flowed from the Frobisher Bay lowland or farther north, rather than from a Meta Incognita Ice

Divide. At the southern extremity of the Frobisher Bay Moraine System, striations remain normal to the ice margin where it wraps around to the northeast, breaking the concurrence with southwesterly domain 3a flow found everywhere else, and indicating that this was the southeastern extremity of the Meta Incognita Ice Divide at that time. West of the thick till belt and the head of the Ramsay River, a well defined ice front crosses the upper reaches of the river draining into the head of Blandford Bay, while a number of ice-contact deltas at the north end of Markham Bay are probably contemporaneous with the Frobisher Bay Moraine System. The flow pattern in this western sector can be traced north of the map area, again north of the height of land (*see* Blake, 1966). Till in domain 4a is of typical shield composition, even though Paleozoic rocks are exposed in the Amadjuak Lake lowlands 20 km north of the map area. Thus the Amadjuak Ice Divide must have been strongly developed and long-lived, deflecting any tendency for western interior Baffin Island ice to overrun the map area. Deglacial ice margins retreated to the northeast, indicated by sparse lateral channels and eskers, and across the divide and height of land hence damming glacial lakes in the middle Armshow River and tributaries (*see* above and domain 6). The area of hummocky till bearing numerous frost fissure troughs is possibly still underlain by glacier ice.

The few marine limits and ice-contact delta surfaces measured in the field north of Ava Inlet, off Markham Bay, ranged from 60 m a.s.l. to 72 m a.s.l. (topographic maps are of limited use because contours have 200 foot intervals). This is less than half the height of marine limit 40 km to the southwest. Assuming at least as great an ice load over Amadjuak Lake as in Hudson Strait, then at least 70 m of uplift occurred at Ava Inlet while the ice front retreated from outer islands on Hudson Strait, a model which requires the Frobisher Bay Moraine System to be markedly younger than the ca. 8 ka dates from outer coast of domain 3a if those are marine limit dates. The Crooks Inlet delta, at 70 m a.s.l., compared to a 135 m a.s.l. marine limit 30 km to the southwest, was suggested above to be the terminus of a Frobisher Bay Moraine System sandur following the course of the Ramsay River (which requires residual ice to have occupied at least one lake in the domain 3a sandur while the Frobisher Bay Moraine System formed).

Domain 4b

The single ice margin shown crossing the Meta Incognita Peninsula height of land (Fig. 29) expands northeastwards into multiple till ridges intersecting a 30 km length of Frobisher Bay shoreline between Cape Caldwell and Bay of Two Rivers. These are right lateral moraines from a glacier occupying the head of Frobisher Bay. The classic series of landforms includes re-entrant moraines into the orthogonal system of valleys, and a series of kame terraces and deltas, meltwater outlets, and sandar (Fig. 31). Summit sites within 5 km of the coast that are underlain by Cumberland batholith granite are more strongly ice scoured than anywhere else in the map area, showing numerous whalebacks and grooves, as well as striations, all trending southeastward. Several former outlet glaciers draining to the northeast can be traced by end moraines and kames between the Meta Incognita Peninsula height of land and the Frobisher Bay glacier landforms. These end moraines appear to be contemporaneous with a Frobisher glacier margin that lay in the middle of the belt, possibly terminating close to Cape Rammelsberg. The transition from regional flow into Frobisher Bay to a separate Frobisher Bay glacier is unclear, as noted for domain 3b. Most likely a retreat within domain 4 occurred before a readvance of the Meta Incognita Peninsula ice cap and the Frobisher Bay glacier.

A terminal moraine extending into Frobisher Bay, 5 km south of Cape Rammelsberg, is probably not the outermost of the Frobisher Bay Moraine System series in domain 3b, though the bedrock knolls of the Cape Rammelsberg peninsula were a significant pinning point for the Frobisher Bay glacier, anchoring massive glaciofluvial and glacial marine deposits. These sediments were described by Lind (1983) as complexes of silt to sand and gravel, containing less diverse foraminifera than modern sediments, and deposited in close proximity to glacial ice in water that was cooler and less saline than in present inner Frobisher Bay. Shells collected by Manley and Moore (1995) from these sediments yielded ages of 8.96 ka and 8.94 ka (AA-17861, AA-15131, respectively), which are significantly older than the previously believed age of 8.23 ka (GSC-462) for this stage (Blake, 1966). The Cape Rammelsberg sediments are thus only 100 years older than the oldest dates from downfiord domain 3b (AA-15125, AA-15124), and the marine limit at the cape is less than 10 m lower than that at Eggleston Bay, raising the possibility that the Frobisher Bay Moraine System ice extended all the way down the southwest shore of inner Frobisher Bay. The chronology for the map area would be more straightforward if the Cape Rammelsberg glacial marine sediments showed evidence of being overrun by a readvancing Frobisher Bay glacier, but this has not been reported.

Domain 4c

Ice flow north of Frobisher Bay, within the Frobisher Bay Moraine System belt and proximal patches of thick till, is indicated by striations to have been predominantly eastwards. Unlike domain 4a, this flow was discordant with the flow distal to the Frobisher Bay Moraine System, indicating that the Frobisher Bay Moraine System represents a significant readvance. That earlier flow south to southeastwards into Frobisher Bay left few deposits. The flow predating the Frobisher Bay Moraine System was down a regional slope and was most likely rapid and scouring, whereas the Frobisher Bay Moraine System readvance was upslope. The striation trend within the Frobisher Bay Moraine System is orthogonal to the moraines and indicates eastward-fanning ice at the head of Frobisher Bay. Farther west, aligned with the axis of the bay and glacier, rock drumlins trend southeastwards. Rock drumlins, till lineations, and eskers generally parallel striations; however, northeast of Iqaluit, within the moraine system, several clusters of till and rock drumlins are oriented northwest-southeast, paralleling a dominant bedrock structural grain. Rather than a deviant Frobisher Bay Moraine System ice flow, this may be a relic of flow predating the Frobisher Bay Moraine System. A similar phenomena occurs west of the Sylvia Grinnell River, where a south-southeast trend in both hummocky till and till veneer is overprinted by a east-southeast flow. Squires (1984) identified five main moraines and a series of outwash landforms in the Frobisher Bay Moraine System belt marking stillstands or readvances. Four major ice margins can be traced to the shore of Frobisher Bay between Pichi and Laird peninsulas (Fig. 29); other minor moraines include the most proximal, marking an ice lobe that filled Tarr Inlet from Frobisher Bay. Farther north, moraines left by readvances of several kilometres overlap earlier Frobisher Bay Moraine System stillstands.

From the northern limit of the map area, across Hall Peninsula, the Frobisher Bay Moraine System is composed of thick till and one or two moraine ridges in a belt up to 3 km wide, broken by till veneer or bedrock in places. It is only where it flanks Frobisher Bay that the Frobisher Bay Moraine System widens to a belt containing numerous ridges. Two explanations for the widening are that when the glacier terminus lay in deep water in Frobisher Bay 1) buoyancy reduced basal drag thus the glacier was more sensitive to changes in mass balance; or 2) with continuing melting of continental ice, and concomitant rebound, sea level fell, basal friction increased, and the margin retreated. Following from this, there was probably less movement of the Frobisher Bay Moraine System margin in (terrestrial) domain 4a, hence the mostly single margin there. Alternatively, it is possible that a positive change in mass balance late in the Frobisher Bay Moraine System stage, would overrun older moraines of domain 4a, while in a marine-based sector (domain 4c) the order of moraines remained undisturbed. Moraines tend to run off peninsulas into Frobisher Bay because these bathymetric highs (under raised sea level) were local pinning points for the glacier. The terminus of the glacier, within Frobisher Bay, possibly pinned at the shallow neck and islands dividing inner and middle Frobisher Bay (Fig. 29).

Ice-contact deltas at the outermost moraine, at the head of Lewis Bay, yielded molluscs dated 8.45 ka (GX-8159) and 7.95 ka (AA-15123). The delta surfaces, at 42 m a.s.l. and 34 m a.s.l., respectively, mark far lower and presumably younger sea levels than that recorded by an undated 96 m delta and 119 m washing limit (Squires, 1984) 3.5 km farther up the same valley. Manley and Moore (1995) suggested that the calving margin stabilized in inner Frobisher Bay at ca. 8.9 ka and persisted at the outermost domain 4c position for 1000 years. This period is indicated to be closer to 2000 years by the 7.08 ka age (GSC-5903) of molluscs from an apparently ice-contact delta in Porter Inlet, 3 km proximal to the outermost moraine (local marine limit 96 m) (Manley *in* Manley and Jennings, 1996); however, three other mollusc collections from more proximal locations in the moraine system dated between 7.8 ka and 7.34 ka (QC-905, GSC-2771, QC-901). Bulk organic material from a lake core proximal to the outermost moraine dated 8.23 ka (GX-8696), but such a sample may be contaminated by dissolved carbonate and be too old. Molluscs found on the flank of an ice-contact delta at Apex Hill, proximal to the Frobisher Bay Moraine System, dated 6.75 ka (GSC-464). They may be younger than the delta because shells found at Peterhead Inlet, well behind the Frobisher Bay Moraine System yielded an age of 7.08 ka (GX-8160). Iqaluit delta surface sediments, contemporaneous with or younger than meltwater from ice that had retreated north out of the map area, yielded molluscs dated 6.44 ka (GSC-533).

Domain 5

Around the head of Frobisher Bay, between the Meta Incognita Peninsula height of land and the Frobisher Bay Moraine System sector on Hall Peninsula, strong ice flow to the latter Frobisher Bay Moraine System and into the head of the bay is recorded by fields of low, spindle-form drumlins, till and rock lineations, and whalebacks. The flows appear generally concurrent despite directions ranging from northeast to south-southeast divided by local discontinuities. There is a stronger easterly component than might be expected, given the southeast axis of the bay and the former presence of the Amadjuak Ice Divide to the north, and much of the flow seems to head on the north side of the Meta Incognita Peninsula height of land. This implies that any of the southwest flow to Hudson Strait that originated east of the height of land was captured by domain 5 flow. The domain 5 flows were not traced closer than 5–10 km to the height of land and only one crosscutting striation was found. The sense of direction of striations between Hone River and Quasitujuak Lake was not determined. In the absence of other information, a deglacial ice front is assumed to have retreated in a generally northwesterly or westerly direction, and, as noted for domain 4c, left the head of the bay by ca. 7 ka; however, between the Hone River and the height of land, there is clear evidence (lateral channels, minor end moraines, glacial lakes, and striations) of an ice front retreating downslope and east towards the Frobisher Bay lowland, with marginal drainage (and thus an ice gradient) flowing northwest towards Amadjuak Lake.

Domain 6

The last glaciers were confined to deeper valleys on and adjacent to the height of land in domains 4a and 5, and, possibly domain 3a, where they left lateral drainage channels and minor end moraines, glacial-lake shorelines, and spillways. The most consequential of these residual ice bodies occupied the middle and lower reaches of the Armshow River, finally disintegrating 35 km northwest of Bay of Two Rivers. Early in the period during which it retreated 30 km down the valley to this final body, it dammed a glacial lake, eventually 35 km long, against the Meta Incognita Peninsula topographic divide (Fig. 29). The main lake shoreline at 490 m a.s.l. corresponds in elevation with several spillways leading into headwaters of the Livingstone River. When the ice front reached the southeastward turn in the valley, the lake fell in level as it drained to the Hone River and other watercourses east of the divide. The number and spacing of subaqueous moraines formed at the ice-front moraines suggest lakes spanning several hundred years (*see* above). The Jaynes Inlet valley glacier, dated at ca. 7.7 ka (*see* 'Domain 3b'), may be a valley-bottom residual rather than an outlet from an undefined Meta Incognita Peninsula ice cap.

Discussion of deglaciation

Location of ice divides

Erosional landforms (Fig. 15, 17) show that through the Late Wisconsinan a Meta Incognita Ice Divide coincided with the Meta Incognita Peninsula height of land south of the Armshow River. This would have required initiation and maintenance of a local elevation-controlled ice mass on the peninsula, buttressed on the north side by a Frobisher Bay glacier. North of the Armshow River, during the glacial maximum the ice divide departed east of topographically high ground towards the Frobisher Bay lowland, presumably influenced more by the position of the Amadjuak Ice Divide and Foxe Ice Dome than by local topography. The ice dome, or more precisely the fork between Meta Incognita and Hall ice divides (Fig. 44), was the source of the Frobisher Bay glacier. The north end of the Meta Incognita Ice Divide shifted westward and also became topographically controlled when the ice dome and Amadjuak Ice Divide waned. This starved the Frobisher Bay glacier (ca. 8–7 ka). The location of the ice divides glacially isolated the map area from the southeast Arctic Platform, hence little carbonate material was transported into the map area from the north.

Asynchronous deglaciation of Hudson Strait and Frobisher Bay coasts

An outstanding issue in late-glacial history of the map area is the discordance in radiocarbon age between deglaciation of the southwest (Hudson Strait) side of the Meta Incognita Ice Divide and the northeast (Frobisher Bay) side. Given the asymmetry of the Meta Incognita Ice Divide through the Late Wisconsinan as indicated by glacial landforms, it might be expected that deglaciation of the coast of the longer flank (Hudson Strait side) would be at least as early as that of the Frobisher Bay flank. Instead, the reverse appears to be the case, following the usual assumption for a glaciated coastal area that the time of deglaciation is determined from the oldest finite ages of molluscs that migrated into the area during the marine incursion following ice retreat.

For Frobisher Bay, the ten most reliable and oldest dates range between 9.07 ka and 8.59 ka (AA-15125, AA-15124, AA-17861, AA-15131, GSC-5895, AA-15127, GSC-3157, AA-16403, AA-15126, GSC-3666); these were collected from the surface or within mostly glacial marine sediments. All sediments may be older than Frobisher Bay Moraine System (i.e. part of domain 3b), though two samples (AA-17861, AA-15131) could have been contemporaneous with the Frobisher Bay Moraine System or overrun by it. All these shells were collected tens of metres below marine limit; the few within ice-contact deltas may be of similar age to the marine limit, the others may be hundreds of years younger than marine limit. Shell species in this group are varied, though the oldest are all *Macoma* sp. or *Portlandia* sp. (the oldest *Hiatella arctica* is 8.86 ka (GSC-5895)). The oldest shells definitely contemporaneous with the Frobisher Bay Moraine System are 8.45 ka (GX-8159) from the north side of the bay (domain 4c), whereas the ice had retreated from the Frobisher Bay Moraine System by 7.08 ka (GSC-5903).

For Hudson Strait, the oldest postglacial shells are 8.36 ka (AA-10645), collected proximal to the probable limit of the Noble Inlet advance. This is the oldest date from anywhere on southeast Baffin Island postdating the Noble Inlet advance. Noble Inlet ice still overlapped at least part of the area east of the map area ca. 8.6 ka (Manley and Miller, 2001). Shells from Big Island and the Kimmirut area, west of the presumed Noble Inlet overlap, are no older than 8.16 ka (AA-12609). None of these Hudson Strait shells were from ice-contact deposits, and even though most were from glacial marine sediments, the distance to the originating ice front (whether Hudson Strait, Meta Incognita Peninsula, or Noble Inlet glaciers), has not been determined. None of the shells were collected close to the marine-limit elevation, and, as discussed under section ‘Domain 3a’, they could be hundreds of years younger than the marine incursion; however, it would be surprising if an early period with no shells had occurred when there are as many as 21 collections with finite dates greater than 7 ka. The two oldest dates are *Portlandia* sp., but the 8.05 ka sample is *Hiatella arctica*.

In summary, the Frobisher Bay glacier and/or Meta Incognita Peninsula ice had retreated from the southeast shore of Frobisher Bay within the map area (domain 3b) by 9.07 ka. The Frobisher Bay Moraine System distal moraines were deposited by 8.96 ka (Manley and Moore, 1995) or at the latest by 8.45 ka, and ice had retreated from Frobisher Bay Moraine System (domains 4b, 4c) by 7.08 ka. On Hudson Strait, Noble Inlet ice had retreated from the map area by 8.36 ka, but probably no earlier than 8.6 ka. If the marine incursion and assumed coeval deglaciation of Meta Incognita Peninsula ice on the Kimmirut to Big Island coast was ca. 8.4 ka, at the same time ice was active at the Frobisher Bay Moraine System in Frobisher Bay. The western sector of the Frobisher Bay Moraine System lies 75 km inland from the coast at Kimmirut. (The Frobisher Bay Moraine System does intersect the coast at the head of Markham Bay, where no dates have been obtained, but marine limit is half of the elevation on the outer coast.)

Possible causes of the apparently diachronous deglaciation of the limbs of the Meta Incognita Ice Divide include:

1) Differences in the radiocarbon time scale between Frobisher Bay mollusc ages and Hudson Strait ages, due to different reservoir ages between these bodies of water. Both coasts appear to have been inundated by subarctic waters with similarly varied mollusc populations (Dyke et al., 1996a). For ca. 8 ka, Barber et al. (1999) calculated a reservoir correction difference of 225 years between eastern Hudson Strait and southeast Hudson Bay where ^{14}C-free Paleozoic bicarbonate input was probably high, whereas carbonate values for same-age sediments from Frobisher Bay and Hudson Strait are similar. Furthermore, there is no evidence of differences between mollusc populations and ages related to the Noble Inlet or Gold Cove advances on the two coasts where they intersect at the eastern tip of Meta Incognita Peninsula. No coeval terrestrial material has been found to calibrate the mollusc radiocarbon ages.

2) Ice from the Noble Inlet advance grounded in Hudson Strait and depressed the crust resulting in a transgression over the adjacent Hudson Strait coast (i.e. Kimmirut–Big Island). This coast had been deglaciated earlier and inundated by the sea; however, any glacial marine and marine deposits from that time were scoured and replaced by pro-Noble Inlet sediments and a new, higher marine limit. The maximum depression lagged the maximum loading, hence highest sea level occurred after 8.4 ka. An argument for early retreat of Meta Incognita Peninsula ice from coastal areas is the absence of interlobate landforms expected to be deposited if Meta Incognita Peninsula ice contacted Noble Inlet ice. Arguments against a transgression include the preservation of finite age pre-Noble Inlet marine sediments even where overridden by the Noble Inlet advance (at sites outside the map area on southeasternmost Meta Incognita Peninsula (Manley, 1995)), and the uniform westward rise in marine limits along the Hudson Strait shore of Meta Incognita Peninsula, observed by Manley (1996) to be a response to a centre of loading to the west, rather than from cross-strait ice.

3) Transgression-regression took place over a deglaciated coast with a maximum sea level (cusp) reached ca. 8.4 ka, as above; however, crustal loading was the result of an early Holocene increase in snow accumulation over the Meta Incognita and Amadjuak ice divides triggered by the reduction of the ice sheet to the west and increased atmospheric and oceanic circulation in Baffin Bay and the North Atlantic Ocean (cf. Manley, 1996). This resulted in the Meta Incognita Peninsula ice advance to the Frobisher Bay Moraine System. The model implies that rebound increased inland, as should the synchronous marine limit on the deglaciated coast; yet the marine limit declines inland between North Bay and Markham Bay. Manley (1996) suggested the dominant crustal loading was over the Ungava Peninsula or Hudson Bay, explaining the westward or southwestward rise in marine limit; however, the steep decline in marine limit implies a local (Meta Incognita Peninsula) influence rather than a distant load.

4) The assumption of synchroneity of the Frobisher Bay Moraine System in domains 3a, 3b, and 3c is incorrect. The marine-based ice margin in Frobisher Bay retreated rapidly into the map area ca. 9 ka as the northeast flank of the ice divide collapsed, in part due to eustatic sea-level rise. The Frobisher Bay glacier underwent stability-triggered fluctuations in the inner bay until ca. 7 ka. Meanwhile, on the Hudson Strait flank, the margin was firmly land based and stable. In combination with sea-level rise and several surrounding loci of loading, the outer strait shore was deglaciated ca. 8.4 ka. Northeastward retreat through North Bay, Crooks Inlet, and Markham Bay is indicated by declining marine limits, including ice-contact deltas in Markham Bay. Retreat of the margin through domain 3a must have taken at least several hundred years (numerous lateral drainage channels). An otherwise unrecorded climatic event between 8 ka and 7 ka forced a readvance to the domain 4a margin. The continuity in direction of ice-flow landforms from the Meta Incognita Ice Divide to the outer coast through domains 3a and 4a suggests they record retreat of the same ice mass, though the landforms indicate a change from rapid warm-based flow in Frobisher Bay Moraine System to rare striations on Big Island (except domain 1).

None of these hypotheses is convincing to the writer. Key data is needed from Markham Bay to determine if marine limit is synchronous or time transgressive, though it was found to be inexplicably barren of marine molluscs in this survey. A thorough examination of stratigraphy of sediments at Cape Rammelsberg might resolve Frobisher Bay Moraine System ice-front positions with time.

Regional marine limits and relationship to isostatic uplift

Few radiocarbon dates can be related to specific raised sea levels in the map area. Therefore, variations in elevation of marine limit are instead used here as an indicator of regional vertical crustal movement resulting from glacial ice loads. The trend of surfaces connecting marine limit elevations is shown on Figure 42 for the map area and on Figure 48 for all Meta Incognita Peninsula. Surfaces are either synchronous, where the marine limit is the same age and any tilt results from differential uplift (or subsidence), or diachronous, where the age of the marine limit changes, most commonly due to marine incursion against a retreating ice margin. A combination of the two is possible.

The well documented northwest-dipping surface at the head of Frobisher Bay is largely diachronous, resulting from the extended (ca. 2 ka) retreat of the Frobisher Bay glacier. An even steeper marine-limit gradient occurs on the southern flank of the bay, where marine limit falls from 129 m to 48 m in a few kilometres inland from Jaynes Inlet. For middle and outer Frobisher Bay, Duvall (1993) described a synchronous marine limit declining southeastwards, defining a plane which predated the Gold Cove advance (>9.9 ka). This surface is a little higher than the one defined by Manley’s (1995) isolines for southeast Meta Incognita Peninsula, though the latter records a synchronous plane which postdates the Nobel Inlet advance (<8.4 ka). Manley (1995) drew these with increasing elevation inland. For the Big Island–Kimmirut area, Manley (1995, 1996) connected similar marine-limit elevations logically, resulting in a plane paralleling the coast and declining inland. Thus this eastward declining plane intersects the northward rising southeast-coast plane — an untenable circumstance. For Markham Bay, as discussed above, the marine-limit plane declines inland to the northeast, and though there is evidence for the plane being diachronous, especially at the head of the bay (*see* above), an element of synchroneity cannot be ruled out in view of the sparsity of ice-contact features in the outer bay and the complete lack of dated sea levels.

The above patterns are generalized (Fig. 48) into speculative (and due to topography, quite theoretical) marine-limit isolines. These generally parallel the coast, declining inland and over the lowland at the head of Frobisher Bay as might be

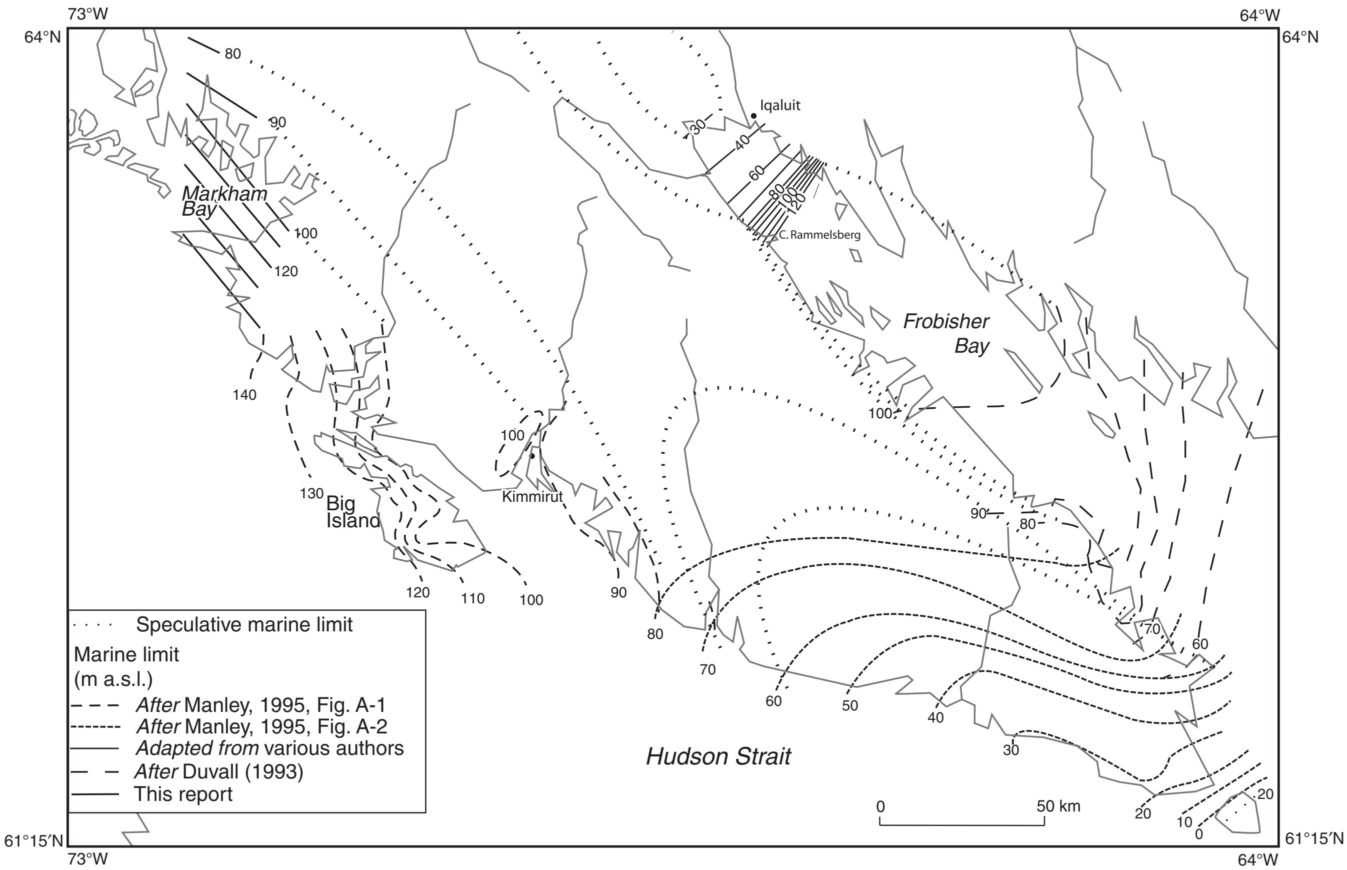

Figure 48. *Regional marine limits and relationship to isostatic uplift.*

expected towards the peninsula ice divide (latest local deglaciation and/or greatest ice load). Marine limit also declines southeastward towards the tip of Meta Incognita Peninsula, where the local ice was presumably thinnest, though deglaciation was late there due to overlap of Noble Inlet ice. Despite the grounding of Noble Inlet ice (MacLean et al., 2001), the load in Hudson Strait is not reflected in the marine-limit surface.

Postglacial sea-level changes

Crustal uplift following decay of glacial ice, together with the concurrent, but lesser (for most of the Canadian Arctic) worldwide sea-level rise, combine in the map area to result in emergence of coasts. Rates of emergence (including the present trend) are of interest in a number of practical and theoretical fields ranging from modern shoreline stability to Earth's structure. Both ends of the two emergence curves (Fig. 49, *see also* Fig. 51) for the map area are reasonably constrained: i.e. the present and the marine limit (the latter is reasonably well dated from marine shells); however, none of the dated molluscs from intermediate elevations and/or ages can be reliably related to a specific sea level. The best that can be done with them is to assume they lie at or below sea level (i.e. the emergence curve). Terrestrial samples constrain the emergence curve from above. For the map area, these are mostly radiocarbon-dated charred fat from archeological sites, or peat from fluvial deposits. Samples used in constructing a curve should have a geographical spread of not more than a few kilometres to avoid errors introduced by deformation of a coeval sea-level plane.

Hudson Strait emergence

Figure 49 shows emergence curves constructed by Clark (1985) and Manley (1996). Clark (1985) used marine mollusc data collected from an area 6 km in width in the vicinity of Kimmirut (Lake Harbour) and terrestrial data spread over 14 km in the Cape Tanfield area, 30 km to the southeast. Manley (1996) used the Cape Tanfield terrestrial data, the Kimmirut data, plus additions which increase the spread, and another 12 km wide cluster of marine samples from eastern Big Island, 40 km southwest of Kimmirut. Error is introduced by the regional tilt of marine limit, shown by Manley (1995, 1996) to have a component of 0.4 m/km along the trend of the southeast coast of Meta Incognita Peninsula. This marine limit is assumed to be synchronous in the southeast, postdating decay of ice from the Noble Inlet advance; however, for both Manley's and Clark's curves it appears that the spread of samples is not significant because the same three critical marine samples controlling each curve are from the Kimmirut cluster, i.e. not more than 6 km apart (QC-1137, QC-1138, GSC-596, Table 1). The curves suggest rapid rebound from a simple ice load, with 75% accomplished in

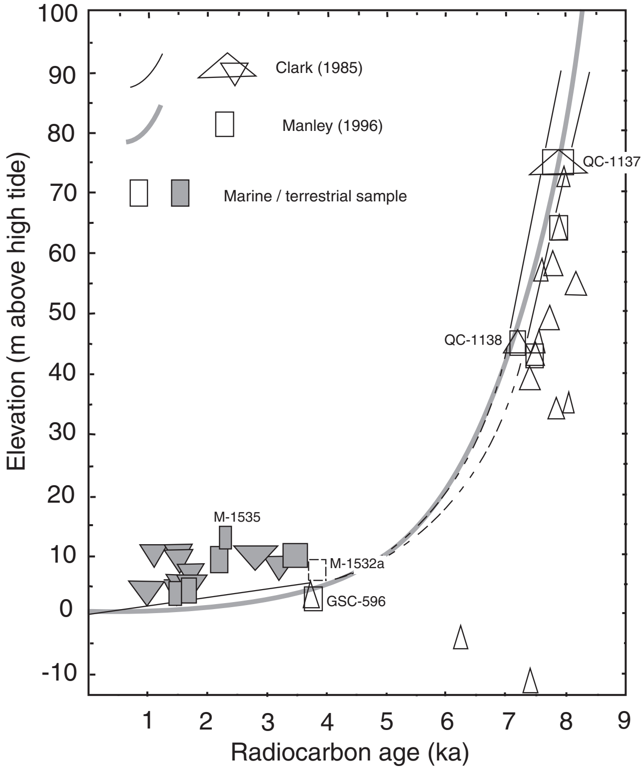

Figure 49.

Emergence of shorelines in Kimmirut–eastern Big Island–Cape Tanfield areas, based on dated marine molluscs and terrestrial (archeological) material; after *Clark (1985, Fig. 3) and Manley (1996, Fig. 7). Sample symbol width is proportional to age error; height of symbol proportional to elevation error (±2 m). All dated material shown is listed in Table 1. None of these dates can be related to a specific sea level. Critical dates (QC-1137, QC-1138, GSC-596) are all from the Kimmirut area. The M-1535 elevation has been corrected to from 7 m to 12 m; M-1532a is contaminated and too old.*

the first 2000 years. They provide no insight into interactions between ice loading Hudson Strait (Laurentide, Noble Inlet) and Foxe or local ice on Meta Incognita Peninsula.

Frobisher Bay emergence

For inner Frobisher Bay, Colvill (1982, Fig. 4.12), Lind (1983, Fig. 6.1), and Squires (1984, Fig. 15) showed diagrammatically how the age and elevation of the marine limit, assumed to be synchronous with deglaciation, declines towards the head of the bay with a big step-down in elevation where the Frobisher Bay Moraine System intersects the coast. There are insufficient samples related to specific sea levels for accurate emergence curves to be drawn, hence Squires (1984) and Jacobs et al. (1985b) drew composite curves embracing all the inner bay. Figure 50 shows a revision incorporating later data summarized in Table 1. The generalized emergence curve shown in Figure 51 approximates emergence for the inner 20 km of the bay where marine limit is around 30 m a.s.l., but is too steep for the zone of inner Frobisher Bay Moraine System where marine limit is 40 m a.s.l., and is drawn to intersect the highest data point for the inner bay beyond 38 km from the head. For the present, McCann et al. (1981) suggested emergence has been replaced by submergence by presenting evidence that the tidal flats of Koojesse Inlet (Iqaluit) are being eroded by a slow sea-level rise.

Postglacial vegetation and climate

Pollen from several buried soil (peat) sections and lake cores from within and immediately adjacent to the map area provides a record of mid- to late Holocene vegetation and, by proxy, paleoclimate (Short and Jacobs, 1982; Jacobs et al., 1985a, b, 1997; Mode and Jacobs, 1985, 1987; Abbott, 1991; Miller, 1992). The general pattern determined from lake cores is the establishment of birch-rich shrub tundra as early as 8 ka, expansion by 5.5 ka, a peak ca. 3 ka, and subsequent decline (Mode and Jacobs, 1985); the shrub tundra is an indicator of a warmer and wetter climate. The terrestrial peat record shows more variation than the lake cores with which it correlates only weakly. Pollen records from niveo-eolian peat sections indicate periods of impoverished grass-dominated vegetation symptomatic of cooler and drier climate phases between 5.5 ka and the present that probably encouraged eolian processes (Mode and Jacobs, 1987). Jacobs et al. (1985b) suggested the peat reflects local effects more strongly. They inferred numerous mid- to late Holocene alternating warm, wet and dry, cool climatic events from peat exposures at Grinnell Bay on eastern Hall Peninsula, at Ward Inlet off Frobisher Bay immediately east of the map area, and at Burton Bay and Peterhead Inlet off inner Frobisher Bay. Because no pronounced cultural changes occurred, Maxwell (1973) suggested climate changes were insufficient to cause major shifts in the ecosystem.

Radiocarbon dates from the base, middle, and top of a 2 m thick exposure of plant material and sand (Fig. 52) found during this study in the valley of the river that drains to

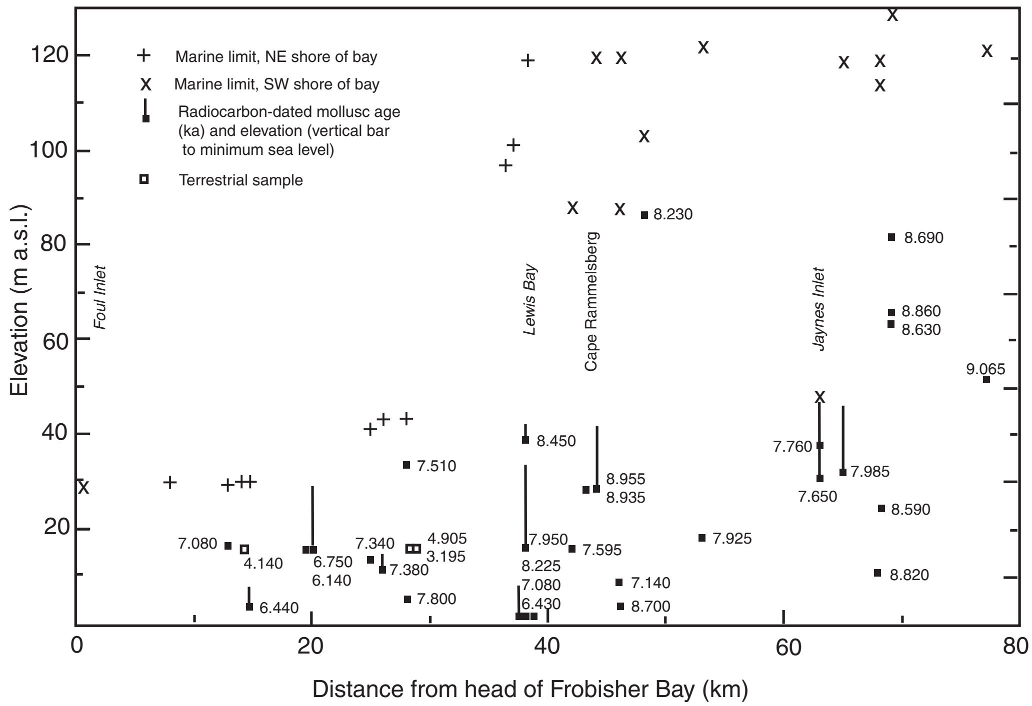

Figure 50. *Location and/or elevation of radiocarbon dated samples plus marine-limit elevations from inner Frobisher Bay. The step down in altitude of marine limit at Cape Rammelsberg (southwest shore of bay) and Lewis Bay (northwest) coincides with the distal limit of the Frobisher Bay Moraine System. Downbay from these locations, oldest ages are ca. 9 ka; no samples bearing on middle Holocene to late Holocene emergence have been collected.*

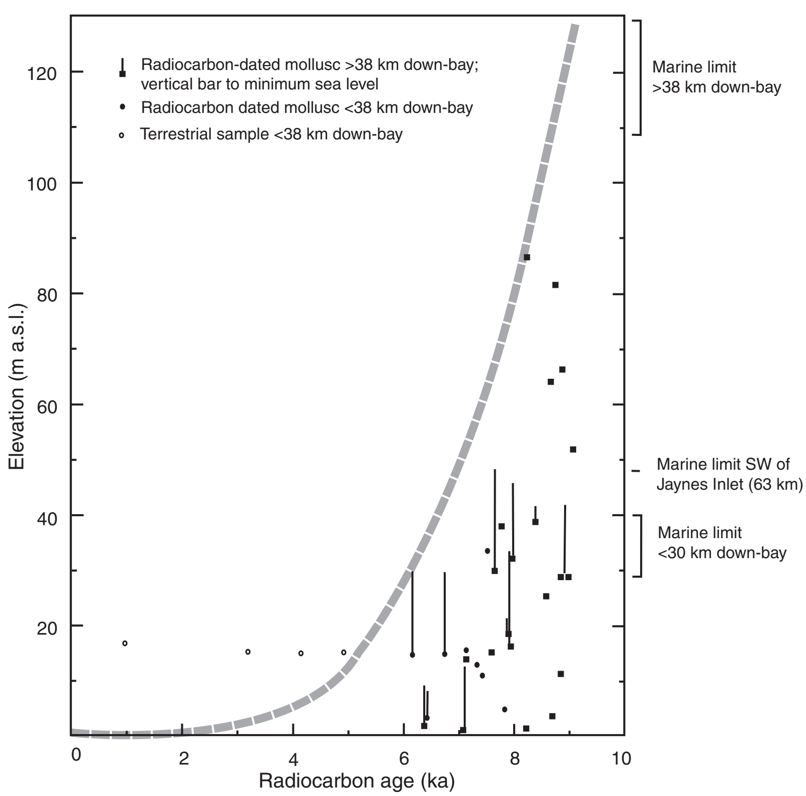

Figure 51.

Emergence of shorelines for all of inner Frobisher Bay (from head to 80 km downbay). Few of the dates can be related to a specific sea level. Marine limit for the area ranges from 129 m to less than 30 m. Hence, the curve is highly generalized.

Figure 52. Niveo-eolian and fluvial sand containing peaty strata; middle area of the river valley that drains to the head of Shaftesbury Inlet. Peat from the top of the 2 m high excavation dated 3.67 ka; from the base, 5.42 ka. Photograph by D.A. Hodgson. GSC 2001-379O

Shaftesbury Inlet suggest continuous accumulation from 5.42 ka (GSC-6204, Table 1), through 4.44 ka (GSC-6208), until at least 3.65 ka (GSC-6226). Similar material continued to accumulate above the uppermost sample, however, it is disturbed by slumping and modern root penetration. At least 1 m of organic-free planar to ripple-bedded sand underlies the basal sample. The interbedded peat and sand, contained in a minor gully, probably has a niveo-eolian origin. The oldest date from this section overlaps that of a basal date from organic-rich partings in fluvial sand at Grinnell Bay, which yielded a date of 5490 ± 180 (QC-683B; Andrews and Short (1983); Jacobs et al. (1985b)); whereas the latter date is from a cryoturbated paleosol marking a transition from a period of soil formation to niveo-eolian conditions, the oldest sample from the river that drains to Shaftesbury Inlet appears part of an undisturbed succession.

ECONOMIC AND ENVIRONMENTAL QUATERNARY GEOLOGY

Aggregate sources and granular materials

Till is the most widespread surficial material, composed of silty sand and granule- to large boulder-size metamorphic clasts in a ratio where clasts are commonly dominant. Small areas of finer grained till occur over limestone, marble, and some of the metasedimentary rocks, and in the southeast coastal margin of the map area where glaciers pushed onshore. Much of the till is well drained and contains only pore ice below the frost table (but *see below*). Fluvially sorted sand and/or gravel deposits occur in largest volume in outwash associated with the Frobisher Bay Moraine System. South of the former position of the Meta Incognita Ice Divide, sand and gravel floors major valleys south of the Frobisher Bay Moraine System; lesser quantities occur in the few eskers, and in raised marine deltas on the shores of Markham Bay. Around Frobisher Bay, sand and gravel outwash is concentrated within the Frobisher Bay Moraine System complex as small to large sandar, valley trains, and glacial marine and glaciolacustrine deltas, and as deposits postdating it (e.g. Sylvia Grinnell River). Deposits are mostly well drained (but *see* below). Modern and raised beaches are rare deposits in the map area. The boulders that stud many intertidal flats are an accessible source of riprap. Weathered metamorphic and igneous rock units are not a directly workable source of aggragate because they fracture to extensive block or boulder fields. Weaker lithologies such as marble disintegrate to finer fragments suitable for ripping.

Natural hazards

No geomorphic processes are known to be hazardous to present land use in the area, but potential hazards exist from two sources.

Permafrost

Excess ground ice will thaw seasonally if the thermal equilibrium of the ground is disturbed by stripping vegetation or thinning the active layer. Though no exposures of visible ground ice were observed, it is assumed that ice wedges are present under the frost-fissure troughs that form polygonal networks over thicker till and some glaciofluvial deposits. As discussed above (*see* 'Till' section above) it is speculated that hummocky till may include a substantial volume of buried glacial ice. Ice lenses may also be present in poorly drained till, especially at the foot of slopes, and in any fine-grained materials including glacial marine blanket and marine veneer deposits.

Slope failures

Rapid failures appear to be active only on a small scale in the form of detachment slides over the frost table on some fine-grained till and glacial marine units. Slow movement is common in the form of creep forming solifluction lobes in till and weathered rock. Rock sags were rarely observed (*see* 'Megascale erosional forms' section, above).

Drift prospecting

With the aim of sampling primary ice-flow patterns, till was collected from regional topographic high points. A low-density sample grid was used (1 sample/218 km^2). Analysis (Table 4, on CD-ROM) showed no anomalously high concentrations of elements nor any especially distinctive distribution patterns.

REFERENCES

Abbott, M.B.
1991: Radiocarbon dating and interpretation of sediments from five lake systems along Frobisher Bay, N.W.T., Canada; M.Sc. thesis, Department of Geological Sciences, University of Colorado, Boulder, Colorado, 237 p.

Allard, M., Baolai, W., and Pilon, J.A.
1995: Recent cooling along the southern shore of Hudson Strait, Quebec, Canada, documented from permafrost temperature measurements; Arctic and Alpine Research, v. 27, p. 157–166.

Ambrose, J.W.
1964: Exhumed paleoplains of the Precambrian Shield of North America; American Journal of Science, v. 22, p. 817–857.

Andrews, J.T.
1998: Abrupt changes (Heinrich events) in late Quaternary North Atlantic marine environments: a history and review of data and concepts; Journal of Quaternary Science, v. 13, p. 3–16.

Andrews, J.T. and Ives, J.D.
1978: "Cockburn" nomenclature and the late Quaternary history of the Canadian Arctic; Arctic and Alpine Research, v. 10, p. 617–633.

Andrews, J.T. and Miller, G.H.
1972: Maps of the present glaciation limit and lowest equilibrium line altitude for north and south Baffin Island; Arctic and Alpine Research, v. 4, p. 45–60.
1984: Quaternary glacial and nonglacial correlations for the eastern Canadian Arctic; *in* Quaternary Stratigraphy of Canada — A Canadian Contribution to IGCP Project 24, (ed.) R.J. Fulton; Geological Survey of Canada, Paper 84-10, p. 102–116.

Andrews, J.T. and Short, S.K.
1983: Radiocarbon Date List V: Baffin Island, N.W.T., Canada, and Radiocarbon Date List II: Labrador and Northern Quebec, Canada; University of Colorado, Institute of Arctic and Alpine Research, Occasional Paper 40, 71 p.

Andrews, J.T., Clark, P., and Stravers, J.A.
1985: The pattern of glacial erosion across the eastern Canadian Arctic; *in* Quaternary Environments: Eastern Canadian Arctic, Baffin Bay and West Greenland, (ed.) J.T. Andrews; Allen & Unwin, Winchester, Massachusetts, p. 69–92.

Andrews, J.T., Kirby, M., Jennings, A.E., and Barber, D.C.
1998: Late Quaternary stratigraphy, chronology, and depositional processes on the slope of S.E. Baffin Island, detrital carbonate and Heinrich events: implications for onshore glacial history; Géographie physique et Quaternaire, v. 52, p. 91–105.

Andrews, J.T., MacLean, B., Kerwin, M., Manley, W., Jennings, A.E., and Hall, F.
1995: Final stages in the collapse of the Laurentide Ice Sheet, Hudson Strait, Canada, NWT: ^{14}C AMS dates, seismic stratigraphy, and magnetic susceptibility logs; Quaternary Science Reviews, v. 14, p. 983–1004.

Barber, D.C., Dyke, A., Hillaire-Marcel, C., Jennings, A.E., Andrews, J.T., Kerwin, M.W., Bilodeau, G., McNeely, R., Southon, J., Morehead, M.D., and Gagnon, J.M.
1999: Forcing of the cold event of 8,200 years ago by catastrophic drainage of Laurentide lakes; Nature, v. 400, no. 6742, p. 344–348.

Barton, G.H.
1899: Evidence of the former extension of glacial action on the west coast of Greenland and in Labrador and Baffin Land; American Geologist, v. 18, p. 379–384.

Bell, R.
1885: Observations on the geology, mineralogy, zoology, and botany of the Labrador coast, Hudson's Strait and Bay; *in* Report of Progress, 1882-83-84, Part DD, VII, Geological and Natural History Survey and Museum of Canada, p. 1–62.
1896: Proofs of the rising of the land around Hudson Bay; American Journal of Science, v. 1, p. 219–228.
1901a: A survey in Baffinland, with a short description of the country; Geographical Journal, v. 18, p. 25–46.
1901b: Report of an exploration on the northern side of Hudson Strait; *in* Annual Report, Volume X1, 1898, Part M, Geological Survey of Canada, p. 1–38.

Benn, D.J. and Evans, D.J.A.
1998: Glaciers & Glaciation; Edward Arnold, London, United Kingdom; Wiley, New York, New York, 734 p.

Bird, J.B.
1958: A report on the physical environment of southern Baffin Island, Northwest Territories, Canada; RAND Memorandum RM-2362-1-PR, The Rand Corporation, Santa Monica, California, 392 p.
1967: The Physiography of Arctic Canada; The Johns Hopkins Press, Baltimore, Maryland, 336 p.

Blackadar, R.G.
1967: Geological reconnaissance, southern Baffin Island, District of Franklin; Geological Survey of Canada, Paper 66-47, 32 p.

Blake, W., Jr.
1966: End moraines and deglaciation chronology in northern Canada with special reference to southern Baffin Island; Geological Survey of Canada, Paper 66-26, 31 p.
1982: Geological Survey of Canada Radiocarbon Dates XXII; Geological Survey of Canada, Paper 82-7, 22 p.
1988: Geological Survey of Canada Radiocarbon Dates XXVII; Geological Survey of Canada, Paper 87-7, 100 p.

Bolton, T.E., Sanford, B.V., Copeland, M.J., Barnes, C.R., and Rigby, J.K.
1976: Geology of Ordovician rocks, Melville Peninsula and region, southeastern District of Franklin; Geological Survey of Canada, Bulletin 269, 137 p.

Bradley, R.S.
1973: Seasonal climatic fluctuations on Baffin Island during the period of instrumental records; Arctic, v. 26, p. 230–243.

Canadian Hydrographic Service
2000: Canadian Tide and Current Tables; v. 4, Arctic and Hudson Bay, Environment Canada, 198 p.

Clark, P.U.
1985: A note on the glacial geology and postglacial emergence of the Lake Harbour region, Baffin Island, N.W.T.; Canadian Journal of Earth Sciences, v. 22, p. 1864–1871.

Colvill, A.
1982: Glacial landforms at the head of Frobisher Bay, Baffin Island, Canada; M.A. thesis, Department of Geography, University of Colorado, Boulder, Colorado, 202 p.

Crane, H.R. and Griffen, J.B.
1966: University of Michigan radiocarbon dates XI; Radiocarbon, v. 8, p. 256–285.

Dale, J.E.
1982: Physical and biological zonation of subarctic tidal flats at Frobisher Bay, southeast Baffin Island; M.Sc. thesis, Department of Geography, McMaster University, Hamilton, Ontario, 284 p.

Davison, W.L.
1958: Geology of Lake Harbour, Baffin Island, District of Franklin, Northwest Territories, sheet 25K/13; Geological Survey of Canada, Map 29-1958, scale 1:63 360.

Dowdeswell, J.A.
1984: Late Quaternary chronology for the Watts Bay area, Frobisher Bay, southern Baffin Island, N.W.T., Canada; Arctic and Alpine Research, v. 16, p. 311–320.

Dredge, L.A.
1992: Breakup of limestone bedrock by frost shattering and chemical weathering, eastern Canadian Arctic; Arctic and Alpine Research, v. 24, p. 314–323.
1995: Quaternary geology of northern Melville Peninsula, District of Franklin, Northwest Territories; Geological Survey of Canada, Bulletin 484, 114 p.
2000a: Age and origin of upland block fields on Melville Peninsula, eastern Canadian Arctic; Geografiska Annaler, v. 82, p. 443–453.
2000b: Carbonate dispersal trains, secondary till plumes, and ice streams in the West Foxe sector, Laurentide Ice Sheet; Boreas, v. 29, p. 144–156.

Duvall, M.L.
1993: Late Foxe glacial geology of the mid-bay area of Frobisher Bay, southeast Baffin Island, Northwest Territories; M.Sc. thesis, Department of Geological Sciences, University of Colorado, Boulder, Colorado, 103 p.

Dyke, A.S.
1993: Landscapes of cold-centred Late Wisconsinan ice caps, Arctic Canada; Progress in Physical Geography, v. 17, p. 223–247.
1999: Last Glacial Maximum and deglaciation of Devon Island, Arctic Canada: support for an Innuitian Ice Sheet; Quaternary Science Reviews, v. 18, p. 393–420.

Dyke, A.S. and Peltier, W.R.
2000: Forms, response times and variability of relative sea-level curves, glaciated North America; Geomorphology, v. 32, p. 315–333.

Dyke, A.S. and Prest, V.K.
1987a: Late Wisconsinan and Holocene history of the Laurentide Ice Sheet; Géographie physique et Quaternaire, v. 41, p. 237–263.
1987b: Late Wisconsinan and Holocene retreat of the Laurentide Ice Sheet; Geological Survey of Canada, Map 1702A, scale 1:5 000 000.
1987c: Paleogeography of northern North America, 18 000-5000 years ago; Geological Survey of Canada, Map 1703A, scale 1:12 500 000.

Dyke, A.S., Dale, J.E., and McNeely, R.N.
1996a: Marine molluscs as indicators of environmental change in glaciated North America and Greenland during the last 18 000 years; Géographie physique et Quaternaire, v. 50, p. 125–184.

Dyke, A.S., McNeely R.N., and Hooper, J.A.
1996b: Marine reservoir corrections for bowhead whale radiocarbon age determinations; Canadian Journal of Earth Sciences, v. 33, p. 1628–1637.

England, J. and Smith, I.R.
1993: Late glacial ice margins and deglacial chronology for southeastern Baffin Island and Hudson Strait, eastern Canadian Arctic: Discussion; Canadian Journal of Earth Sciences, v. 30, p. 1749–1752.

Falconer, G., Ives, J.D., Loken, O.H., and Andrews, J.T.
1965: Major end moraines in eastern and central Arctic Canada; Geographical Bulletin, v. 7, p. 137–153.

Fulton, R.J.
1989: Foreword to the Quaternary Geology of Canada and Greenland; *in* Quaternary Geology of Canada and Greenland, (ed.) R.J. Fulton; Geological Survey of Canada, Geology of Canada, no. 1, p. 1–11 (*also* Geological Society of America, The Geology of North America, v. K-1).

Gray, J.T.
2001: Patterns of ice flow and deglaciation chronology for southern coastal margins of Hudson Strait and Ungava Bay; *in* Marine Geology of Hudson Strait and Ungava Bay: Late Quaternary Sediments, Depositional Environments, and Late Glacial-Deglacial History Derived from Marine and Terrestrial Studies; (ed.) B. MacLean; Geological Survey of Canada, Bulletin 566, p. 31–55.

Gray, J.T., Lauriol, B., Bruneau, D., and Ricard, J.
1993: Postglacial emergence of Ungava Peninsula, and its relationship to glacial history; Canadian Journal of Earth Sciences, v. 30, p. 1676–1696.

Hillaire-Marcel, C., de Vernal, A., Bilodeau, G., and Wu, G.
1994: Isotope stratigraphy, sedimentation rates, deep circulation, and carbonate events in the Labrador Sea during the last ~200 ka; Canadian Journal of Earth Sciences, v. 31, p. 63–89.

Hodgson, D.A.
1997: Last glacial ice flows over western Meta Incognita Peninsula, southern Baffin Island, Northwest Territories; *in* Current Research 1997-C; Geological Survey of Canada, p. 179–184.

Ives, J.D. and Andrews, J.T.
1963: Studies in the physical geography of north-central Baffin Island, N.W.T.; Geographical Bulletin, v. 19, p. 5–48.

Jacobs, J.D. and Stenton, D.R.
1985: Environment, resources, and prehistoric settlement in upper Frobisher Bay, Baffin Island; Arctic Anthropology, v. 22, p. 59–76.

Jacobs, J.D., Headley, A.N., Maus, L.A., Mode, W.N., and Simms, É.L.
1997: Climate and vegetation of the interior lowlands of southern Baffin Island: long-term stability at the low arctic limit; Arctic, v. 50, p. 167–177.

Jacobs, J.D., Mode, W.N., and Dowdeswell, E.K.
1985a: Contemporary pollen deposition and the distribution of *Betula glandulosa* at the limit of low arctic tundra in southern Baffin Island, N.W.T., Canada; Arctic and Alpine Research, v. 17, p. 279–287.

Jacobs, J.D., Mode, W.N, Squires, C.A., and Miller, G.H.
1985b: Holocene environmental change in the Frobisher area, Baffin Island, N.W.T.: deglaciation, emergence, and the sequence of vegetation and climate; Géographie physique et Quaternaire, v. 34, p. 151–162.

Jennings, A.E.
1993: The Quaternary history of Cumberland Sound, southeastern Baffin Island. The evidence; Géographie physique et Quaternaire, v. 47, p. 21–42.

Jennings, A.E., Manley, W.F., MacLean, B., and Andrews, J.T.
1998: Marine evidence for the last glacial advance across eastern Hudson Strait, eastern Canadian Arctic; Journal of Quaternary Science, v. 13, p. 501–514.

Jennings, A.E., Tedesco, K.A., Andrews, J.T., and Kirby, M.E.
1996: Shelf erosion and glacial ice proximity in the Labrador Sea during and after Heinrich events (H-3 or 4 to H-0) as shown by foraminifera; *in* Late Quaternary Paleoceanography of the North Atlantic Margins, (ed.) J.T. Andrews, W.E.N. Astin, H. Bergsten, and A.E. Jennings; Geological Society of London, Special Publication 111, p. 29–49.

Judge, A.S., Taylor, A.E., Burgess, M.M., and Allen, V.S.
1981: Canadian geothermal data collection-northern wells, 1978-80; Geothermal Series Number 12, Earth Physics Branch, Energy, Mines and Resources Canada, 190 p.

Kaplan, M.R., Pfeffer, W.T., Sassolas, C., and Miller, G.H.
1999: Numerical modelling of the Laurentide Ice in the Baffin Island region: the role of a Cumberland Sound ice stream; Canadian Journal of Earth Sciences, v. 36, p. 1315–1326.

Kaufman, D.S. and Williams, K.M.
1992: Radiocarbon Date List VII: Baffin Island, N.W.T., Canada; University of Colorado, Institute of Arctic and Alpine Research, Occasional Paper 48, 82 p.

Kaufman, D.S., Miller, G.H., Gray, J.T., Stravers, J.A., Lauriol, B., Bruneau, D., and Jull, A.J.T.
1992: Chronology and configuration of late-glacial (12-8 ka) fluctuations of the Labrador Dome at the mouth of Hudson Strait; *in* Abstracts, 22nd Arctic Workshop, Institute of Arctic and Alpine Research, University of Colorado, Boulder, Colorado, p. 78–80.

Kaufman, D.S., Miller, G.H., Stravers, J.A., and Andrews, J.T.
1993a: Abrupt early Holocene (9.9-9.6 ka) ice-stream advance at the mouth of Hudson Strait, Arctic Canada; Geology, v. 21, p. 1063–1066.

Kaufman, D.S., Miller, G.H., Stravers, J.A., Manley, W.F., and Duvall, M.
1993b: Late glacial ice margins and deglacial chronology for southeastern Baffin Island and Hudson Strait, eastern Canadian Arctic; Reply; Canadian Journal of Earth Sciences, v. 30, p. 1753–1758.

Keen, C.E. and Beaumont, C.
1990: Geodynamics of rifted continental margins; Chapter 9 *in* Geology of the Continental Margin of Eastern Canada, (ed.) M.J. Keen and G.L. Williams; Geological Survey of Canada, Geology of Canada, no. 2, p. 393–472 (*also* Geological Society of America, The Geology of North America, v. I-1).

Kigoshi, K., Aizawa, H., and Nobuka, S.
1969: Gakushin natural radiocarbon measurements Vll; Radiocarbon, v. 11, p. 295–326.

Kleman, J. and Jansson, K.
1996: Glacial landforms of southern Baffin Island; Department of Physical Geography, Stockholm University; Stockholm, Sweden, scale 1:1:600 000.

Laymon, C.A.
1988: Glacial geology of western Hudson Strait, Canada, with reference to Laurentide Ice Sheet dynamics; Ph.D. thesis, University of Colorado, Boulder, Colorado, 345 p.
1992: Glacial geology of western Hudson Strait, Canada, with reference to Laurentide Ice Sheet dynamics; Geological Society of America, Bulletin 104, p. 1169–1177.

Lind, E.K.
1983: Holocene paleoecology and deglacial history of the Cape Rammelsberg area, southern Baffin Island, N.W.T., Canada; M.Sc. thesis, Department of Geology, University of Colorado, Boulder, Colorado, 219 p.

Lowdon, J.A. and Blake, W., Jr.
1968: Geological Survey of Canada radiocarbon dates VII; Radiocarbon, v. 10, p. 207–245.

Lowden, J.A., Fyles, J.G., and Blake, W., Jr.
1967: Geological Survey of Canada radiocarbon dates VI; Radiocarbon, v. 9, p. 156–197.

Lowdon, J.A., Wilmeth, R., and Blake, W., Jr.
1969: Geological Survey of Canada radiocarbon dates VIII; Radiocarbon, v. 11, p. 22–42.
1970: Geological Survey of Canada radiocarbon dates X; Radiocarbon, v. 12, p. 472–485.
1972: Geological Survey of Canada Radiocarbon Dates XII; Geological Survey of Canada, Paper 72-7, 26 p.

MacLean, B., Andrews, J.T., Gray, J.T., Hall, F.R., Hardy, I., Jennings, A.E., Manley, W.F., Pfeiffer, W.T., and Vilks, G.
2001: Hudson Strait Quaternary sediments, late glacial and deglacial history: a discussion and summary; *in* Marine Geology of Hudson Strait and Ungava Bay: Late Quaternary Sediments, Depositional Environments, and Late Glacial-Deglacial History Derived from Marine and Terrestrial Studies; (ed.) B. MacLean; Geological Survey of Canada, Bulletin 566, p. 181–191.

MacLean, B., Loncarevic, B.D., Hardy, I., Brown, R.G.B., Daigneault, R.A., Day, M., Kerwin, M.W., and Manley, W.F.
1994: Cruise report, CSS Hudson Cruise 93034 - Hudson Strait, Ungava Bay, eastern Canadian Arctic; Geological Survey of Canada, Open File 2818, 157 p.

MacLean, B., Vilks, G., Aitken, A., Allen, V., Briggs, W., Bruneau, D., Doiron, A., Escamilla, M., Hardy, I., Miner, J., Mode, W., Powell, R., Retelle, M., Stravers, J., Taylor, A., and Weiner, N.
1991a: Investigations of the Quaternary geology of Hudson Strait and Ungava Bay, Northwest Territories; *in* Current Research, Part E; Geological Survey of Canada, Paper 91-1E, p. 305–315.

MacLean, B., Vilks, G., Aitken, A., Boudreau, H., Briggs, W., Bruneau, D., Doiron, A., Hardy, I., Miner, J., Mode, W., Powell, R., Retelle, M., Stravers, J., Taylor, A., and Allen, V.
1991b: Cruise report of CSS Hudson cruise 90-023, Marine geological investigations in Hudson Strait, Ungava Bay and Frobisher Bay; Geological Survey of Canada, Open File 2372, 152 p.

MacLean, B., Williams, G.L., Sanford, B.V., Klassen, R.A., Blakeney, C., and Jennings, A.E.
1986: A reconnaissance study of the bedrock and surficial geology of Hudson Strait, N.W.T.; *in* Current Research, Part B; Geological Survey of Canada, Paper 86-1B, p. 617–635.

MacLean, B., Williams, G.L., and Srivastava, S.P.
1990: Geology of the Labrador Shelf, Baffin Bay, and Davis Strait. Part 2: Geology of Baffin Bay and Davis Strait; Chapter 7 *in* Geology of the Continental Margin of Eastern Canada, (ed.) M.J. Keen and G.L. Williams; Geological Survey of Canada, Geology of Canada, no. 2, p. 325–345 (*also* Geological Society of America, The Geology of North America, v. I-1).

Manley, W.F.
1995: Late-glacial record of ice-sheet interactions, Hudson Strait and southern Baffin Island, eastern Canadian Arctic; Ph.D. thesis, Department of Geological Sciences, University of Colorado, Boulder, Colorado, 252 p.
1996: Late-glacial flow patterns, deglaciation, and postglacial emergence of south-central Baffin Island and the north-central coast of Hudson Strait, eastern Canadian Arctic; Canadian Journal of Earth Sciences, v. 33, p. 1499–1510.

Manley, W.F. and Jennings, A.E.
1996: Radiocarbon Date List VIII: Eastern Canadian Arctic, Labrador, Northern Quebec, East Greenland Shelf, Iceland Shelf, and Antarctica; University of Colorado, Institute of Arctic and Alpine Research, Occasional Paper 50, 163 p.

Manley, W.F. and Miller, G.H.
2001: Glacial-geological record on southern Baffin island reflecting late glacial ice-sheet dynamics in the eastern Hudson Strait region; *in* Marine Geology of Hudson Strait and Ungava Bay: Late Quaternary Sediments, Depositional Environments, and Late Glacial-Deglacial History Derived from Marine and Terrestrial Studies; (ed.) B. MacLean; Geological Survey of Canada, Bulletin 566, p. 19–30.

Manley, W.F. and Moore, J.J.
1995: Early Holocene glacial interactions in inner Frobisher Bay, southern Baffin Island, Nunavut; *in* Abstracts, 25th Arctic Workshop, Centre d'Études Nordiques, Université de Laval, Ste Foy, Quebec, p. 123–125.

Manley, W.F., Miller, G.H., Duvall, M.L., and Kaufman, D.S.
1996: Sediment lithology as an indicator of glacial provenance and ice-flow patterns, S. Baffin Island, eastern Canadian Arctic; *in* Programs and Abstracts of 14th Biennial Meeting, American Quaternary Association, p. 105.

Matthews, B.
1967: Late Quaternary marine fossils from Frobisher Bay (Baffin Island, N.W.T., Canada); Paleogeography, Paleoclimatology, Paleoecology, v. 3, p. 243–263.

Maxwell, J.B.
1981: Climatic regions of the Canadian Arctic Islands; Arctic, v. 34, p. 225–240.

Maxwell, M.S.
1973: Archeology of the Lake Harbour District, Baffin Island; Archeological Survey of Canada, Mercury Series, v. 6, 362 p.

McCann, S.B., Dale, J.E., and Hale, P.B.
1981: Subarctic tidal flats in areas of large tidal range, southern Baffin Island, eastern Canada; Géographie physique et Quaternaire, v. 35, p. 183–204.

McNeely, R.
2001: Geological Survey of Canada Radiocarbon Dates XXXIII; Geological Survey of Canada, Current Research 2001-G, 76 p.

Mercer, J.H.
1956: Geomorphology and glacial history of southernmost Baffin Island; Geological Society of America Bulletin, v. 67, p. 553–570.

Miller, G.H.
1980: Late Foxe glaciation of southern Baffin Island, N.W.T., Canada; Geological Society of America Bulletin, v. 91, p. 399–405.
1985: Moraines and proglacial shorelines, Hall Peninsula, Baffin Island; *in* Quaternary Environments: Eastern Canadian Arctic, Baffin Bay and West Greenland, (ed.) J.T. Andrews; Allen and Unwin, Winchester, Massachusetts, p. 546–557.

Miller, G.H. and Andrews, J.T.
1972: Quaternary history of northern Cumberland Peninsula, east Baffin Island, N.W.T., Canada. Part IV: preliminary lichen growth curve for *Rhizocarpon geographicum*; Geological Society of America, v. 83, p. 1133–1138.

Miller, G.H. and Kaufman, D.S.
1990: Rapid fluctuations of the Laurentide Ice at the mouth of Hudson Strait: new evidence for ocean/ice sheet interactions as a control on the Younger Dryas; Paleoceanography, v. 5, p. 907–919.

Miller, G.H., Hearty, J., and Stravers, J.A.
1988: Ice-sheet dynamics and glacial history of southeasternmost Baffin Island and outermost Hudson Strait; Quaternary Research, v. 30, p. 116–136.

Miller, R.J.O.
1992: Late Quaternary lacustrine paleoenvironmental records from south-east Baffin Island, N.W.T., Canada; Ph.D. thesis, Department of Geological Sciences, University of Colorado, Boulder, Colorado, 296 p.

Mode, W.N. and Jacobs, J.D.
1985: Holocene vegetation and climate, southern Baffin Island, N.W.T., Canada; Geological Society of America, Abstracts with Programs, v. 17, p. 319.
1987: Surficial geology and palynology, inner Frobisher Bay; *in* Cumberland Sound and Frobisher Bay, Southeastern Baffin Island, N.W.T., (ed.) J.T. Andrews, R. Gilbert, J.D. Jacobs, G.H. Miller, W.N. Mode, and J.D. Stravers; XIIth International Union for Quaternary Research Congress Field Excursion C-2, Guidebook, p. 53–62.

Muller, D.S.
1980: Glacial geology and Quaternary history of Meta Incognita Peninsula, Baffin Island, Canada; M.Sc. thesis, Department of Geological Sciences, University of Colorado, Boulder, Colorado, 211 p.

Osterman, L.E.
1982: Late Quaternary history of southern Baffin Island, Canada: a study of foraminifera and sediments from Frobisher Bay; Ph.D. thesis, Department of Geological Sciences, University of Colorado, Boulder, Colorado, 380 p.

Osterman, L.E. and Andrews, J.T.
1983: Changes in glacial-marine sedimentation in core HU77-159, Frobisher Bay, Baffin Island, N.W.T.: a record of proximal, distal, and ice-rafting glacial-marine environments; *in* Glacial Marine Sedimentation, (ed.) B.F. Molnia; Pergamon Press, Oxford, United Kingdom, p. 451–493.

Osterman, L.E., Miller, G.H., and Stravers, J.A.
1985: Late and mid-Foxe glaciation of southeast Baffin Island, N.W.T., Canada; *in* Quaternary Environments: Eastern Canadian Arctic, Baffin Bay and West Greenland, (ed.) J.T. Andrews; Allen and Unwin, Winchester, Massachusetts, p. 520–545.

Pfeffer, W.T., Dyurgerov, M., Kaplan, M., Dwyer, J., Sassolas, C., Jennings, A., Raup, B., and Manley, W.
1997: Numerical modeling of late glacial Laurentide advance of ice across Hudson Strait: insights into terrestrial and marine geology, mass balance, and calving flux; Paleoceanography, v. 12, p. 97–110.

Polunin, N.V.
1948: Botany of the Canadian Eastern Arctic, part III, vegetation and ecology, National Museum of Canada, Bulletin 104, Biology Series 32, 304 p.
1951: The real Arctic: suggestions for its delimitation, subdivision and characterization; Journal of Ecology, v. 39, p. 308–315.

Porsild, A.E.
1958: Geographical distribution of some elements in the flora of Canada; Geographical Bulletin, no. 11, p. 57–77.

Porsild, A.E. and Cody, W.J.
1980: Vascular plants of the continental Northwest Territories; National Museum of Canada, Ottawa, Ontario, 667 p.

Praeg, D.B., MacLean, B., Hardy, I.A., and Mudie, P.J.
1986: Quaternary geology of the southeast Baffin Island continental shelf, N.W.T.; Geological Survey of Canada, Paper 85-14, 38 p.

Prest, V.K.
1969: Retreat of Wisconsin and Recent ice in North America; Geological Survey of Canada, Map 1257A, scale 1:5 000 000.
1984: The Late Wisconsinan glacier complex; *in* Quaternary Stratigraphy of Canada - A Canadian Contribution to IGCP Project 24, (ed.) R.J. Fulton; Geological Survey of Canada, Paper 84-10, p. 21–36.

Prest, V.K., Grant, D.R., and Rampton, V.N.
1968: Glacial Map of Canada; Geological Survey of Canada; Map 1253A, scale 1:1:5 000 000.

Rose, A.W., Hawkes, H.E., and Webb, J.S.
1979: Geochemistry in Mineral Exploration; Academic Press, Toronto, Ontario, 657 p.

Sanford, B.V. and Grant, A.C.
2000: Geological framework of the Ordovician system in the southeast Arctic Platform, Nunavut; *in* Geology and Paleontology of the Southeast Arctic Platform and Southern Baffin Island, Nunavut; (ed.) A.D. McCracken and T.E. Bolton; Geological Survey of Canada, Bulletin 557, p. 13–38.

Sebert, L.M. and Munro, M.R.
1972: Dimensions and areas of maps of the National Topographic System; Technical Report No. 72-1, Surveys and Mapping Branch, Energy, Mines and Resources, Canada, 29 p.

Short, S.K. and Jacobs, J.D.
1982: A 1100 year paleoclimatic record from Burton Bay-Tarr Inlet, Baffin Island; Canadian Journal of Earth Sciences, v. 19, p. 398–409.

Soper, J.D.
1936: The Lake Harbour region, Baffin Island; The Geographical Review, v. 26, p. 426–438.

Squires, C.A.
1984: The Late-Foxe deglaciation of the Burton Bay area, southeastern Baffin Island, N.W.T.; M.A. thesis, Department of Geography, University of Windsor, Windsor, Ontario, 115 p.

St-Onge, M.R., Lucas, S.B., Scott, D.J., and Wodicka, N.
1999a: Upper and lower plate juxtaposition, deformation and metamorphism during crustal convergence, Trans-Hudson Orogen (Quebec-Baffin segment), Canada; Precambrian Research, v. 93, p. 27–49.

St-Onge, M.R., Scott, D.J., and Wodicka, N.
1999b: Geology, Frobisher Bay, Nunavut; Geological Survey of Canada, Map 1979A, scale 1:100 000.
1999c: Geology, Hidden Bay, Nunavut; Geological Survey of Canada, Map 1980A, scale 1:100 000.
1999d: Geology, McKellar Bay, Nunavut; Geological Survey of Canada, Map 1981A, scale 1:100 000.
1999e: Geology, Wight Inlet, Nunavut; Geological Survey of Canada, Map 1982A, scale 1:100 000.
1999f: Geology, Blandford Bay, Nunavut; Geological Survey of Canada, Map 1983A, scale 1:100 000.

St-Onge, M.R., Scott, D.J., and Wodicka, N. (cont.)
1999g: Geology, Crooks Inlet, Nunavut; Geological Survey of Canada, Map 1984A, scale 1:100 000.
1999h: Geology, White Strait, Nunavut; Geological Survey of Canada, Map 1985A, scale 1:100 000.

Stravers, J.A.
1986: Glacial geology of outer Meta Incognita Peninsula, southern Baffin Island, Arctic Canada; Ph.D. thesis, Department of Geological Sciences, University of Colorado, Boulder, Colorado, 231 p.

Stravers, J.A., Miller, G.H., and Kaufman, D.S.
1992: Late glacial ice margins and deglacial chronology for southeastern Baffin Island and Hudson Strait, eastern Canadian Arctic; Canadian Journal of Earth Sciences, v. 29, p. 1000–1017.

Stuckenrath, R., Jr., Coe, W.R., and Ralph, E.K.
1966: University of Pennsylvania radiocarbon dates IX; Radiocarbon 8, p. 348–385.

Stuiver, M., Reimer, P.J., Bard, E., Beck, J.W., Burr, G.S., Hughen, K.A., Kromer, B., McCormac, G., Van der Plicht, J., and Spurk, M.
1998: INTCAL 98 radiocarbon age calibration, 24,000-0 cal BP; Radiocarbon, v. 40, p. 1041–1083.

Sugden, D.E.
1978: Glacial erosion by the Laurentide Ice Sheet; Journal of Glaciology, v. 20, p. 367–391.

Sugden, D.E. and John, B.S.
1976: Glaciers and Landscape: a Geomorphological Approach; Edward Arnold, London, United Kingdom, 376 p.

Tarnocai, C. and Kroetsch, D.
1994: Soil landscapes of Canada, Baffin south (east); Centre for Land and Biological Research, Agriculture Canada; scale 1:1 000 000.

Taylor, A.E. and Judge, A.S.
1979: Permafrost studies in northern Québec, Géographie physique et Quaternaire, v. 33, p. 245–251.

Ward, W.H.
1952: A note on the elevated strandlines of Frobisher Bay, Baffin Island; Geographical Revue, v. 42, p. 651.

Watson, T.L.
1897: Evidences of recent elevation of the southern coast of Baffin Land; Journal of Geology, v. 5, p. 17–33.

Wengerd, S.A.
1951: Elevated strandlines of Frobisher Bay, Baffin Island, Canadian Arctic; Geographical Revue, v. 41, p. 622–637.

Williams, L.D. and Bradley, R.S.
1985: Paleoclimatology of the Baffin Bay region; *in* Quaternary Environments: Eastern Canadian Arctic, Baffin Bay and West Greenland, (ed.) J.T. Andrews; Allen and Unwin, Winchester, Massachusetts, p. 741–772.

Wilmeth, R.
1969: Canadian archaeological radiocarbon dates; National Museum of Canada, Bulletin 233, Contributions to Anthropology, VII; Archaeology, p. 68–126.

Young, S.B.
1971: The vascular flora of St. Lawrence Island with special reference to floristic zonation in the arctic regions; Contributions to the Gray Herbarium, v. 201, p. 11–115.

This is a Windows®-based autostart disk. If the autostart is not working, go to the CD-ROM root directory and double-click on the autoplay.exe file. If you read this CD-ROM with a Mac® or UNIX® operating system, the autostart will not work.

PDF files containing the full Bulletin contents are located in the \PDF folder on this CD.

Recommended minimum hardware/software:

PC	-	Pentium® processor with Windows® 95
MAC	-	Mac® OS 7
UNIX	-	SunOS™ 4.1.3
Monitor	-	17" colour monitor, video resolution of 1280 x 1024
RAM	-	16 MB
VRAM	-	2 MB

Adobe® Acrobat® Reader® v. 5.1 is required to view the contents of this CD-ROM. It is included on the CD-ROM in the \APPS directory.

Ceci est un disque à lancement automatique pour les systèmes d'exploitation Windows®. Si le lancement automatique ne fonctionne pas, allez au répertoire principal du CD-ROM et cliquez deux fois sur le fichier autoplay.exe. Si vous lisez ce disque à l'aide d'un système d'exploitation Mac® ou UNIX®, le lancement automatique ne fonctionnera pas.

Des fichiers PDF renfermant le contenu intégral du bulletin sont situés dans le dossier \PDF sur ce disque.

Configuration minimale recommandée :

PC	-	processeur Pentium® avec Windows® 95
MAC	-	Mac® OS 7
UNIX	-	SunOS™ 4.1.3
Moniteur	-	moniteur couleur de 17 po, avec résolution vidéo de 1280 x 1024
RAM	-	16 Mo
VRAM	-	2 Mo

Le logiciel Acrobat® Reader® v. 5.1 d'Adobe® est requis pour visionner le contenu de ce CD-ROM. Il est fourni sur le disque dans le répertoire \APPS.